Clinicopathological Features of the Renal Cell Carcinoma Subtypes Diagnosed According to the 2016 WHO Renal Tumor Classification

Levente Kuthi, MD

PhD Thesis

Szeged, 2020

Clinicopathological Features of the Renal Cell Carcinoma

Subtypes Diagnosed According to the 2016 WHO Renal

Tumor Classification

PhD Thesis

Levente Kuthi, MD

Thesis supervisor: Béla Iványi, MD, Dsc

Department of Pathology, Faculty of Medicine,

University of Szeged,

Szeged, 2020

THIS PHD THESIS IS BASED ON THE FOLLOWING PUBLICATIONS:

Kuthi L, Jenei A, Hajdu A et al. Prognostic factors for renal cell carcinoma subtypes diagnosed according to the 2016 WHO renal tumor classification: a study involving 928 patients. *Pathol Oncol Res.* 2017;23:689-698.

Impact factor: 1.935, independent citations: 25

Somorácz Á, Kuthi L, Micsik T et al. Renal cell carcinoma with clear cell papillary features: perspectives of a differential diagnosis. *Pathol Oncol Res.* 2019. [Epub ahead of print] doi: 10.1007/s12253-019-00757-3.

Impact factor: 2.433, independent citations: 1

Kuthi L, Somorácz Á, Jenei A et al. Xp11.2 renal cell carcinoma: Clinicopathological findings on 28 cases. *Pathol Oncol Res.* 2020. [Epub ahead of print] doi: 10.1007/s12253-019-00792-0.

Impact factor: 2.433

Table of Contents

List of Abbreviations

3p, Short arm of chromosome 3

ABL1, Abelson murine leukemia viral oncogene homolog 1

ACKD, Acquired cystic kidney disease

AJCC, American Joint Committee on Cancer

ALK, Anaplastic lymphoma kinase

AMACR, Alpha-methylacyl Coenzyme A racemase

AML, Angiomyolipoma

ASPL, Alveolar soft part sarcoma chromosomal region candidate gene 1

BAP1, Breast cancer type susceptibility protein (BRCA) associated protein 1

CA9, Carbonic anhydrase 9

CCPRCC, Clear cell papillary renal cell carcinoma

CCRCC, clear cell renal cell carcinoma

CD, Cluster of differentiation

CDC, Collecting duct carcinoma

CDKN2A and B, Cyclin-dependent kinase inhibitor 2A and B

ChRCC, Chromophobe renal cell carcinoma

CLTC, Clathrin heavy chain

c-MET, Tyrosine-protein kinase MET

CNS, Central nervous system

CSS, Cancer-specific survival

CTLA4, Cytotoxic T-lymphocyte-associated protein 4

ESC, Eosinophilic, solid and cystic

ESKD, End-stage kidney disease

FISH, Fluorescent in situ hybridization

FLNC, Folliculin

GI, Gastrointestinal tract

HBB, Hemoglobin beta

HER2, Human epidermal growth factor receptor 2

HIF1α and β, Hypoxia-inducible factor 1 alpha and beta

HLRCC, Hereditary leiomyomatosis and renal cell carcinoma

HMB45, Human melanoma black 45

INI1, Integrase interactor 1

ISUP, International Society of Urological Pathology

KDM5C, Lysine demethylase 5C

MALAT1, Metastasis associated lung adenocarcinoma transcript 1

MiTF, Microphtalmia-associated transcription factor

MRTK, Malignant rhabdoid tumor of the kidney

mTOR, Mammalian target of rapamycin

MTSCC, Mucinous tubular and spindle cell carcinoma

MVI, Microvascular invasion

NF2, Neurofibromin 2

NGS, Next-generation sequencing

NonO, non-POU domain containing octamer binding

PBRM1, Protein polybromo 1

PCR, Polymerase chain reaction

PD1, Programmed death receptor 1

PDGFRA, Platelet-derived growth factor receptor A

PD-L1, Programmed death receptor 1 ligand

PRCC, papillary renal cell carcinoma

PSF, Splicing factor proline and glutamine rich

PTEN, Phosphatase and tensin homolog

RCC, renal cell carcinoma

SDH, Succinate dehydrogenase

SETD2b, Su(var)3-9, Enhancer-of-zeste and Trithorax (SET) domain bifurcated 2

SLC7A11, Solute carrier family 7 member 11

TCEB1, Transcription elongation factor B1

TERT, Telomerase reverse transcriptase

TFE3 and B, Transcription factor E3 and B

TKI, Tyrosine kinase inhibitor

TMA, Tissue microarray

TPRC, Proline rich mitotic checkpoint control factor gene

TSC1 and 2, Tuberous sclerosis complex 1 and 2

UICC, Union for International Cancer Control

VHL, von Hippel-Lindau

WHO, World Health Organization

List of Figures

List of Tables

Introduction

General Features of Renal Cell Carcinoma

Based on the latest incidence and mortality data, renal cell carcinoma (RCC) is the sixth most frequent cancer form in males and tenth in females worldwide and is responsible more than 140 000 cancer-related deaths globally in a year [1, 2], but the incidence shows significant regional differences [3]. The highest rate is registered in Europe and North America, while the lowest is seen in Africa and Oceania [1]. Considering European countries, the Czech Republic and the Baltic States have the highest RCC burden, while Hungary belongs to the middle-risk countries with a 1.03 cumulative risk [1]. RCC affects the elderly; namely, more than 70% of the cases are diagnosed in patients over 60 [4]. RCC rarely occurs under 40, and in such a situation, one should consider a cancer syndrome or a rare RCC subset. RCC is approximately twice frequent in males [5]; however, the reason for this is still not apparent and might be caused by distinct lifestyle and occupational factors [6].

RCCs derive from the kidney tubules. Although the exact causes of sporadic RCC are still debated, there are some risk factors, which surely aggravate the carcinogenetic events in the renal tubules [7]. Smoking is a well-known one, and it was ascertained that it has a dose-dependent effect as well [8]. The RCC risk in smoker men is 50% higher compared to never-smoker ones, and this elevation might be associated with the chronic tissue ischemia induced by cigarette smoking [8]. Obesity turned out to be an RCC risk factor as well, and the risk increases by the body mass index [9], but the data are limited if the body fat distribution influences the RCC risk [10]. Decreased physical activity and RCC risk negatively correlate to each other [11]. Also, several studies conducted that alcohol consumption has a negative effect as well; nevertheless, this effect appears to be dose-dependent, like in the case of smoking [12]. Several occupational carcinogens were investigated, although the conclusions were somewhat conflicting, it was proved that the trichloroethylene exposure was associated with RCC carcinogenesis; and others like cadmium, uranium or radon had no relationship with RCC development [13]. Some medical conditions also increase the RCC risk [7]. One of these is the essential hypertension disease because several studies proved that hypertension elevates the risk of RCC; nevertheless, the reduction of elevated blood pressure by drugs could decrease this risk [14]. Patients with end-stage kidney disease (ESKD) or undergoing hemodialysis have a higher RCC risk [15] because in these damaged kidneys, acquired cystic

kidney disease (ACKD) can develop, and these cysts have a potential for malignant transformation [16]. Of all RCC cases, 2-4% are familial and belong to different kinds of cancer syndromes like von Hippel-Lindau (VHL) syndrome, hereditary leiomyomatosis, and renal cell carcinoma (HLRCC) syndrome, and tuberous sclerosis [16]. These are caused by different kinds of germline mutations in tumor suppressor genes. The most frequent syndrome is the VHL disease, which is resulted by mutations in the *VHL* gene and characterized by renal and pancreatic cysts, central nervous system (CNS) hemangioblastoma, clear cell RCC, pheochromocytoma, endolymphatic sac tumor, and epididymal cystadenoma [17]. The clear cell RCC seen in VHL syndrome is commonly multifocal and bilateral [17]. The average age at the time of the diagnosis is approximately 26 years, but it can vary significantly (from infancy to 70 years) [18]. The genetic alterations of RCC subsets and a summary of hereditary renal tumors are detailed in one of the following chapters.

RCC is not a single disease, but a heterogeneous group of malignant tumors, and the different subtypes have their unique clinical features and morphological patterns [16]. Early classifications were based solely on the histological features of the tumors [19]. Pioneered by Gyula Kovács, the Heidelberg classification, distinguishing conventional, papillary, chromophobe, collecting duct, medullary, and unclassified types, took into account the genetic alterations as well and now is regarded as the forerunner of the modern renal tumor classifications [20]. Later, the 2004 WHO classification relied on the approach [21] and added new entities to the previous subsets. Nine years later, after a consensus conference organized by the International Society of Urological Pathology (ISUP), the Vancouver classification was published [22], which served the basis of the current 2016 WHO classification and defined 14 RCC subtypes [16]. Also, at least seven so-called emerging entities have already been published in the literature (Table 1) [23]. In terms of categorization, the 2016 WHO classification integrated the clinical, histological, immunohistochemical, and genetic features of the tumors [16].

At the same time, a new grading system was created as well, to replace the much-criticized Fuhrman grading system [24]. The Fuhrman grade was based on the size and shape of the nuclei and the presence of the nucleoli (Table 2), hence it was hardly reproducible; furthermore, its prognostic value was debated as well [25, 26]. The proposed, so-called ISUP/WHO grade is influenced solely by the presence of the nucleoli (Figure 1) [24].

RCC subsets accepted in the 2016 WHO Classification [16]

Clear cell carcinoma

Multilocular cystic renal neoplasm of low malignant potential

Papillary carcinoma (type 1, type 2 and not otherwise specified)

Hereditary leiomyomatosis and renal cell carcinoma associated renal cell carcinoma

Chromophobe carcinoma

Collecting duct (of Bellini) carcinoma

Renal medullary carcinoma

Micropthalmia-associated transcription factor family translocation carcinomas

Succinate dehydrogenase deficient carcinoma

Mucinous tubular and spindle cell carcinoma

Tubulocystic carcinoma

Acquired cystic disease-associated carcinoma

Clear cell papillary carcinoma

Renal cell carcinoma, unclassified

RCC subsets not listed in the 2016 WHO Classification [23]

Transcription elongation factor B1 mutated carcinoma

Thyroid-like follicular carcinoma

ALK rearrangement-associated carcinoma

Renal cell carcinoma with prominent smooth muscle stroma

Renal cell carcinoma occurring in patients with prior neuroblastoma

Eosinophilic, solid and cystic carcinoma

Biphasic squamoid papillary carcinoma

Atrophic kidney-like carcinoma

Clear cell carcinoma with giant cells and emperipolesis

Low-grade oncocytic renal tumor [CD117- negative, cytokeratin 7-positive]

High-grade oncocytic renal tumor

Warthin-like papillary carcinoma

Table 1 Renal cell carcinoma subtypes listed and not listed in the 2016 WHO Classification.

Fuhrman grading system [25]			
Grade	Nuclei		Nucleoli
	Size (μm)	Shape	
1	10	Round, uniform	Absent
2	15	Slightly irregular	Observed at x400 magnification
3	20	Obviously irregular	Observed at x100 magnification
4	>20	Bizarre, multilobed	Heavy chromatin clump
ISUP/WHO grading system [24]			
1			Absent at x400 magnification
2			Observed at x400, but not at x100 magnification
3	Not taken into account		Observed at x100 magnification
4			Extreme nuclear pleomorphism and /or presence of giant cells and/or sarcomatoid transformation and/or rhabdoid change

Table 2 Comparison of the Fuhrman and ISUP/WHO grading systems.

However, a major limitation of the ISUP grading system is that it has prognostic value solely in clear cell RCC and papillary RCC tumors [24]. Another conventional prognostic factor is

the TNM staging system [27], which is composed of the local extension of the tumor (T), the involvement of the regional lymph nodes (N), and the presence of systemic dissemination (M). This system is edited, and time-by-time reviewed by the Union for International Cancer Control (UICC), and now the 8th edition is in use [28]. The ISUP investigated other prognostic factors like the presence of microscopic tumor necrosis, rhabdoid change, sarcomatoid transformation, and microvascular invasion (MVI) [24]. Sarcomatoid

Figure 1 The nuclear features seen in grade I (a), II (b), III (c), and IV (d) tumors, respectively. For a better understanding, all images have a magnification factor of 400x.
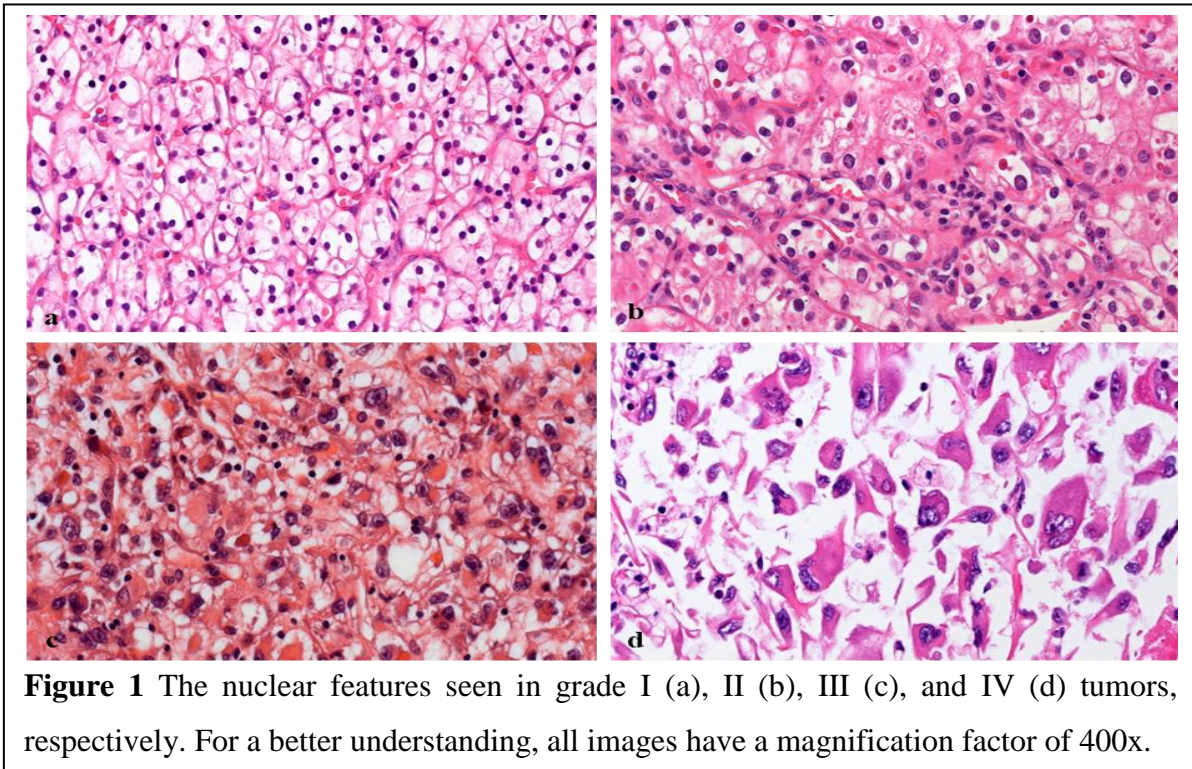
transformation means the presence of fusiform cells with high cytological and nuclear atypia; furthermore, the overall architecture often resembles an undifferentiated pleomorphic sarcoma [29]. This phenomenon can be seen in any of the above-listed RCC entities, and it is most commonly observed in collecting duct RCC [16]. Sarcomatoid transformation is a long known negative prognostic factor with a median survival of 4 to 9 months [30]. However, the sarcomatoid transformation was not proved to be an independent prognostic factor [29], hence according to the consensus decision, the underlying RCC subset must be identified, and the case has to be treated as a grade 4 tumor [24]. The rhabdoid change is another form of dedifferentiation seen in RCC [31]. The typical triad observed in rhabdoid differentiation includes an eosinophilic, paranuclear cytoplasmic inclusion composed of intermediate filaments, an excentric nucleus, and a prominent, cherry red nucleolus [31]. As the sarcomatoid transformation, the rhabdoid change can be noted in any RCC subset [16], and it is associated with a dismal clinical course [32]; hence the histopathological report should state

its presence [24]. It is essential to mention that RCC with a rhabdoid change differs from that of the malignant rhabdoid tumor of the kidney (MRTK) in children [33], namely the *INI1* gene is retained in the former, and a biallelic loss of *INI1* characterizes the MRTK [16]. In RCC, the presence of tumor necrosis is commonly noticed; however, its exact mechanism is still unknown [24]. It was presumed that the necrosis might be caused by the insufficient vascular supply as a result of the tumoral overgrowth of the existing vasculature [34]. Another hypothesis suggested immune mechanism [35], and the vascular immaturity was considered as well [36]; however, a different theory stated that the necrosis was linked to the vascular remodeling observed during the tumor progression [37]. The presence of tumor necrosis inversely correlates with the patient outcome [38], but this seems to be subtype-specific because the studies reported so far did not find any link between the prognosis and the presence of necrosis in case of papillary RCC and chromophobe RCC (ChRCC) [39]. In clear cell RCC, this link between necrosis and an unfavorable clinical course was evident for a long time [40], and Delahunt et al. proposed a grading system that incorporated the presence of tumor necrosis, too [39]. It is accepted that all these negative prognostic features should be reported with a simple yes or no in the pathology report, but it is still debated whether the extension of these parameters has any influence on the prognosis [24]. Also, the minimum area occupied by a sarcomatoid transformation or a rhabdoid change, which exerts an effect on patient outcome, is still not clear. In general, sarcomatoid transformation and rhabdoid change are identified if they fill at least a low-power field; furthermore, their extent must be estimated; however, for the tumor necrosis, both macroscopic and microscopic features should be taken into account [24]. RCC, especially clear cell RCC has an arborized capillary network [16]; hence an MVI is commonly noticed; although the data vary, MVI is seen approximately in 20% of the cases [41]. Also, the accurate relevance of MVI is uncertain because most authors failed to prove a negative link between MVI and survival data in multivariate models [42]; therefore, the description of its presence is not mandatory, and it should be done according to the local guidelines [24].

In terms of clinical presentation and symptoms, RCC has many faces. The classic triad of macroscopic hematuria, costovertebral pain, and palpable renal mass [43] is observed quite rare nowadays because roughly 10% of the patients show these symptoms together [44]. Approximately 60% of the RCC patients are symptomless [45], and their tumors are

diagnosed incidentally by imaging studies performed for other reasons like trauma, follow-up of diabetes or hypertension [46]. Iron-deficient anemia is the consequence of long-term hematuria, and this complication is common when the tumor invaded the renal pelvis [43]. An invasion of the left renal vein might lead to a sudden onset varicocele, while tumor propagation to the inferior vena cava might induce a bilateral swelling of the lower extremities [47]. Hypercalcemia and hyperviscosity syndrome are unusual manifestations in RCC, and these are triggered by increased secretion of parathyroid hormone and erythropoietin, respectively [48]. Also, non-specific symptoms might be observed, including recurrent fever, weight loss, malaise, loss of appetite, and night sweats [44]. About 30% of patients show up with distant metastasis [47], and the most frequent organs are lungs, liver, bones, and brain. Importantly, RCC can give distant metastasis to quite unusual sites like the vagina, testis, or eyelid [43]. Also, in these patients, the first sign of an RCC can be produced by the metastasis like a pathologic bone fracture or a grand mal seizure in case of brain metastasis [44].

Genetic Background of Renal Cell Carcinoma

The first reports on genetic features of sporadic RCC were published in the late 1980s. At that time, Kovács and his co-workers observed by cytogenetic studies that the short arm of chromosome 3 (3p) is frequently lost in clear cell RCC [49]. Later, it turned out that the *VHL* gene located at the 3p25.3 band, is the critical tumor suppressor gene inactivated in clear cell RCC [50]. The inactivation can be happened by chromosomal deletion, gene point mutation, and/or promoter region hypermethylation [18]. The *VHL* gene encodes the VHL protein, which is the member of the VHL-elongin BC complex, and thereby it acts as a substrate of the E3 ubiquitin ligase [18]. The later one degrades the hypoxia-inducible factor 1-alpha (HIF1α) in normoxic circumstances [18]. However, in case of the loss of the VHL protein, the HIF1α remains intact and is relocated to the nucleus where HIF1α is associated with the aryl hydrocarbon receptor nuclear translocator protein, which is also known as the hypoxia-inducible factor 1-beta (HIF1β) [18]. This heterodimeric protein complex formed acts as a transcription factor resulting in angiogenesis, increased cell survival, elevated mitotic activity and enhanced immune evasion (Figure 2) [18]. Additionally, other genes located on the 3p locus, namely *PBRM1*, *BAP1*, *SETD2b*, and *KDM5C*, promote the progression of clear cell RCC [16]. Investigations using high-out sequencing methods revealed a set of clear cell RCC

patients harboring no *VHL*-related anomalies [51]. This so-called *VHL* wild-type subgroup has a dismal clinical outcome, but it is still debated if these cases belong to clear cell RCCs or they have an unidentified genetic change and represent another RCC subset [52].

Figure 2 A schematic illustration of the VHL-elongin BC complex in normoxic (a) and hypoxic conditions. Because of the inactivation of the *VHL* gene, the latter process is observed in clear cell RCC [18].
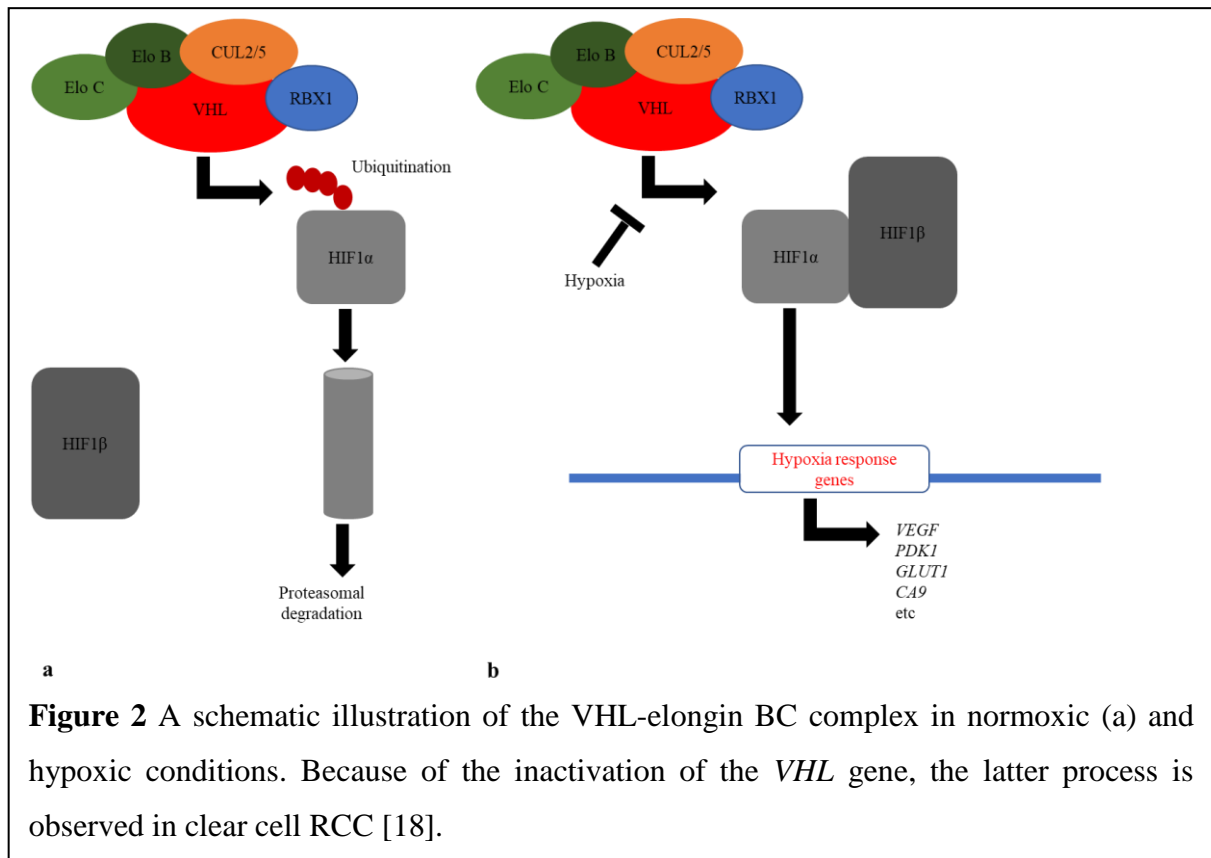
Papillary RCC is rather considered as an umbrella term for those RCCs that have a papillary architecture being characterized by different genetic anomalies [16]. Type 1 papillary RCC harbors activating mutation or amplification of the *c-MET* gene [53], besides the gains of chromosome 3, 7, and 17, along with loss of chromosome Y [54] are observed roughly 80% of the cases. The distinction between type 1 papillary RCC and mucinous tubular and spindle cell carcinoma (MTSCC) might be problematic because they share some histopathological features, but the trisomies of the chromosome discussed above cannot be observed in MTSCC [16]. There is no specific chromosomal alteration for MTSCC, and the tumors investigated were mostly hypoploid with different kinds of chromosomal losses like chromosome 1, 4, 6, 8, 9, 13, 15, and 22 [55]. The genetic changes identified in type 2 papillary RCC are much less consistent that observed in type 1 papillary RCC; namely, the tumor cells frequently have losses and/or gains of chromosome 1, 3, 4, 5, 6, 8, 9, 10, 11, 15, 18 and 22 [56]. A gain of 8q and an allelic imbalance of 9q13 band are associated with worse clinical outcomes [57]; nevertheless, *CDKN2A* and *B*, *TERT*, and *NF2* genes are frequently altered in type 2 papillary

RCCs [53]. In the molecular signature of chromophobe RCC, multiple losses of whole chromosomes, including 1, 2, 6, 10, 13, 17, 21 or Y can be observed, and these alterations are not seen in oncocytoma which is the most important differential diagnosis of chromophobe RCC [58]. According to the current knowledge, clear cell papillary carcinoma (CCPRCC) has no specific genetic anomaly, and more importantly, it harbors no *VHL*-related changes [16, 59]. In terms of translocation carcinoma, the critical genetic alteration detected is a rearrangement of the microphthalmia-associated transcription factors (MiTF), including the *TFE3* and *TFEB* genes [16]. RCCs that are associated with *TFE3* fusions are denominated as Xp11.2 translocation carcinomas, and the partner genes are most frequently the *ASPL*, *NonO*, *TPRC*, *PSF* and, *CLTC* [60-63], but currently next-generation sequencing (NGS) based investigation revealed other partners [64], too. For *TFEB* translocation carcinoma, the partner gene is the *MALAT1*; hence these tumors are regarded as t(6;11) carcinomas [16]. A homozygous loss of the fumarate hydratase gene is typical for HLRCC syndrome associated RCCs [65], and a similar mechanism is observed in succinate dehydrogenase deficient (SDH) RCCs. However, in these tumors, a loss of the SDH subunits encoding genes is the characteristic genetic feature [16, 66]. As regards renal medullary carcinoma, the bilateral loss of the *INI1* gene is the hallmark genomic change [67]. For tubulocystic RCC, targeted NGS-based investigations revealed mutations in 14 genes, and these involved mainly *ABL1* and *PDGFRA* genes [68]. In terms of ACKD RCC, comparative genomic arrays and FISH studies discovered multiple chromosomal losses and gains, including chromosome 3, 7, 16, 17, and sex chromosomes [16]. The later findings help the differentiation between papillary RCC and ACKD RCC because chromosome Y is commonly deleted in papillary RCCs [54]. Collecting duct RCC harbors no consistent genetic change [16], but currently, by using molecular studies, it turned out that *HER2* amplification [69], a homozygous deletion of *CDKN2A* and *SLC7A11* genes are quite frequent in these tumors [70, 71]. Among the emerging entities [23], we discuss here only the *ALK* rearrangement-associated and *TCEB1*-mutated RCC. Although the former is an infrequent entity, its specific genetic change is also a promising therapeutic target, and *ALK* inhibitors are available for years [72]. The *TCEB1* encodes the elongin C protein, which binds exactly the VHL protein to the E3 ubiquitin ligase [18]. The *TCEB1*-mutated RCC harbors the bilateral loss of the *TCEB1* gene, which is resulted by a chromosomal loss of 8q [73] and a nonsense mutation in the gene sequence [74]. So far, two hotspots were identified, and these are as follows Y79C/S/F/N and A100P, which interfere with VHL binding [74]. As we indicated above, a minority of all RCCs have genetic

susceptibilities [16, 17]. Since this thesis does not deal with familial renal cancers, these syndromes are briefly detailed in Table 3.

Therapeutic Options for Renal Cell Carcinoma

For almost one hundred years, the standard treatment of RCC remained unchanged; namely, the surgical removal of the entire tumor is the only option that can cure the patient [44]. The design of the surgery changed a lot because nowadays, the less invasive laparoscopic and nephron-sparing technics are preferred instead of the classic and opened radical nephrectomy [44, 75]. The simultaneous removal of the regional lymph nodes is not obligatory [75]. Unfortunately, imaging technics have no use for preoperative examinations, except for an angiomyolipoma; hence, to avoid unnecessary surgeries, especially for small or uncertain lesions, a core biopsy or a cytological sample should be taken from the tumor [75].

Syndrome	Chromosome Location	Gene	Renal tumor(s) induced	Other organs involved
von Hippel-Lindau	3p25	*VHL*	CCRCC	CNS, pancreas, adrenal
HLRCC	1q42	*FH*	*FH*-deficient RCC	Skin, uterus
Hereditary PRCC	7q31	*c-MET*	PRCC	None
Birt-Hugg-Dubé	17p11	*FLNC*	ChRCC, LOT, HOT	Skin, lung, GI
SDH-associated familial renal cancer	1p36 11q23	*SDHB* *SDHD*	*SDH*-deficient RCC	Ganglia, adrenal, GI
Tuberous sclerosis	9q34 16p13	*TSC1* *TSC2*	ESC RCC, CCRCC, ChRCC, AML	Skin, CNS, lung, heart
Sickle cell trait	11p15	*HBB*	Medullary RCC	None
Cowden	10q22	*PTEN*	PRCC, CCRCC	Skin, breast etc
Translocation of chromosome 3	3p25	*VHL*	CCRCC	Unknown

Table 3 List of hereditary renal tumors syndromes [16, 17].

The treatment of metastatic RCC is still unsolved. A unifocal metastasis can be removed, but in general (the exceptions are not discussed here), there is no meaning of surgical treatment for multiple metastases [75]. Artificial embolization of the renal artery is performed only in inoperable cases having severe bleeding, and the procedure is not used for a preoperative induction of tumor shrinkage anymore [75]. Also, RCC is resistant to conventional chemo- and radiotherapy [44]. In clear cell RCC, the HIF1α overexpression activates many genes and results in increased protein synthesis, but in a therapeutic viewpoint, those genes and proteins are essential, which are responsible for angiogenesis [18]. The angiogenesis induced facilitates the survival of the tumor cells by providing them oxygen and nutrient supply;

nevertheless, these vessels are the main routes of metastatic dissemination, too. The inactivation of the angiogenesis-linked proteins by tyrosine kinase inhibitors (TKIs) results in a tumoral shrinkage and decreases metastatic potential [76]. The sunitinib is the most commonly used first-line drug for metastatic clear cell RCC patients, but others like axitinib or cabozantinib can be prescribed, too [75, 76]. In the case of progression, mTOR inhibition can be used as well [75]. For metastatic papillary RCC, an underlying *c-MET* mutation might be a possible target [77]. Concerning immunotherapy, regardless of the PD-L1 status, a combined PD1 and CTLA4 inhibition are commonly used for metastatic RCC patients [78]. Relying on the literature data, it seems immunotherapy is more effective in those cases that harbors severe genetic abnormalities [78].

Aims

The diagnosis of clear cell RCC, papillary RCC, and chromophobe RCC is straightforward in most of the nephrectomy cases, but tumors with overlapping features can pose diagnostic difficulties. Also, from uncertain renal lesions and inoperable tumors, a biopsy sample is frequently taken. The proper diagnosis of such small and often fragmented material requires in-depth knowledge of histologic and immunohistochemical features of renal tumors to achieve a diagnostic certitude. However, before 2013, the knowledge on immunohistochemical features of RCC subsets was limited on reviews and expert opinions, and no unified recommendations had been published earlier. Besides, the diagnostic experience with the rare entities was minimal at the time of the introduction of the Vancouver classification. Taking into account the above statements, we composed the following aims for this thesis:

To investigate the incidence, clinicopathological, and immunohistochemical characteristics of RCCs according to the 2016 WHO classification to expand our diagnostic expertise.

To test the influence of grade, stage, resection line positivity, and the presence of a rhabdoid/sarcomatoid morphology, giant cells, and microscopic tumor necrosis on patient survival to prompt better patient care.

To analyze the clinicopathological, immunohistochemical, and molecular features of two rare subsets, namely the clear cell papillary RCC and Xp11.2 translocation RCC, and lastly, to harvest data from Hungarian patients and to expand the literature data.

Materials and Methods

General Aspects

Histological Evaluation and Immunohistochemistry

Here, the nephrectomy specimens enrolled were fixed in 10% neutral buffered formalin solution, and then, grossed according to the prevailing grossing protocols. The dissected tumor tissue was embedded in paraffin. Afterward, 4 µm thick sections were cut from the paraffin blocks, and they were stained with hematoxylin and eosin according to in-house protocols. The slides were reviewed, and the histological subtype was identified according to the 2016 WHO classification [16]. Further histological features were assessed, which are discussed below. The pathological stage was evaluated by using macroscopic and microscopic data, and it was amended according to the 8th edition of the AJCC/UICC TNM staging [28]. For immunohistochemistry, tissue microarray (TMA) blocks were created with a TMA Master (3DHISTECH) applying a 2 mm core diameter. One to four representative cores were then punched out from the donor blocks. Immunohistochemical stains together with the source and dilution of the antibodies used are summarized in Table 4. The epitope retrieval was performed for each antibody according to the manufacturer's recommendations. The reactions were conducted using Autostainer (Dako). Afterward, slides were evaluated microscopically by estimating the proportion (%) of immunopositive cells. The scoring was performed in a semiquantitative manner, and staining in over 50% of the tumor cells, in 10 to 50% of tumor cells, or less than 10% of the tumor cells, was interpreted as diffusely or focally positive or negative, respectively. For carbonic anhydrase 9 (CA9), only a membranous, while for TFE3 and TFEB, only nuclear labeling was treated as a positive.

Antibody	Clonality/Source/Clone	Dilution
CA9	rabbit polyclonal, Novus Biologicals	1/2000
CK7	mouse monoclonal, Cell Marque, OV-TL 12/30	1/100
CD10	mouse monoclonal, Biocare Medical, CM129	1/50
AMACR	rabbit polyclonal, Abcam	1/100
MelanA	mouse monoclonal, Labvision, A103	1/200
HMB45	mouse monoclonal, Cell Marque, hmb-45	1/200
TFE3	rabbit monoclonal, Cell Marque, mrq-37	1/100
TFEB	rabbit polyclonal, Bioss USA	1/50
Cathepsin K	mouse monoclonal, Abcam, 3f9	1/100

Table 4 List and specificities of antibodies used.

Molecular Pathological Analysis

Fluorescent in situ Hybridization

FISH assays were carried out to detect either the loss of chromosome 3p and chromosome Y or gain of chromosome 7 and 17; furthermore, to identify a *TFE3* gene rearrangement. Stated briefly, tissue sections were cut from the TMA blocks and deparaffinized. The assays were done using a *VHL*/cen3 probe (ZytoLight® SPEC *VHL*/CEN3 Dual Color Probe, Zytovision), centromeric probes for chromosome 7, 17 and Y (Cytocell) and a *TFE3* probe (ZytoLight® SPEC *TFE3* Dual Color Break-apart FISH Probe, ZytoVision) according to the manufacturer's instructions. The slides were counterstained with 4, 6-diamidino-2-phenylindole (Vysis) and scanned with a Pannoramic Midi slide scanner (3DHISTECH). The reactions were evaluated using a Pannoramic Viewer (3DHISTECH) in the following way. One hundred tumor cells from each case were examined and were compared with the same number of cells of the peritumoral tissue, which served as an internal control. The cutoff values of chromosomal gain and/or loss were set at the mean ±3SD of the corresponding control values, as done in previous studies [79]. The analysis of 3p deletion was also performed based on a published method [80]. The FISH reaction for *TFE3* translocation was considered positive when over 10% of the neoplastic nuclei displayed a rearrangement [81].

VHL Gene Sequence and *VHL* Gene Promoter Region Hypermethylation

Genomic DNA was extracted from tumor tissue using a High Pure PCR Template Preparation Kit (Roche). The *VHL* exons were amplified via specific primer pairs (Table 5). In the case of pathological mutation, the tumor-free renal tissue was analyzed as well. The PCR (25μl final volume) was conducted using 1μl of 10x buffer (Fermentas), 25 mM MgCl2, 2.5 mM dNTP, 0.5 U/ μl Taq DNA polymerase (Fermentas), 10 pmol of each primer, and 50 ng of DNA. The reaction mixture was denatured for 5 min at 95°C and incubated for 39 cycles (denaturing for 20 sec at 95°C, annealing for 30 sec at 59°C and extending for 30 sec at 72°C). The final extension was continued for 5 min at 72°C. The reaction products were checked for size and purity by agarose gel electrophoresis and then utilized for DNA sequencing. The sequencing primers were the same as those above, and a GenomeLAB DTCS - Quick Start Kit (Beckman Coulter) was used for DNA sequencing. The latter was carried out according to the manufacturer's instructions using the GenomeLab GeXP Genetic Analysis System (Beckman Coulter).

VHL	Forward Primer (5'→3')	Reverse Primer (5'→3')
Exon 1a	AGCGCGTTCCATCCTCTAC	CTGCGATTGCAGAAGATGAC
Exon 1b	TACGGCCCTGAAGAAGACGG	GGGCTTCAGACCGTGCTATC
Exon 2	AGGACGGTCTTGATCTC	GATTGGATAACGTGCCTGAC
Exon 3	GTTGGCAAAGCCTCTTGTTC	GAAGGAACCAGTCCTGTATC

Table 5 Primer sequences for three exons of *VHL* used. Exon 1 was split into two parts.

The methylation status of the *VHL* gene promoter region was determined using the methylation-specific PCR method. The extracted genomic DNA was modified using the EpiJET Bisulfite Conversion Kit (Thermo Fischer Scientific) and followed by PCR-based amplification with methylation-specific primer pairs (Table 6). The methylation status (non-methylated or methylated) was determined by gel electrophoresis of the PCR products, as reported previously [82].

VHL	Forward Primer (5'→3')	Reverse Primer (5'→3')
Methylated	TGGAGGATTTTTTTGCGTACGC	GAACCGAACGCCGCGAA
Unmethylated	GTTGGAGGATTTTTTTGTGTATGT	CCCAAACCAAACACAACAAA

Table 6 Primer sequences for the methylation-specific PCR analysis of the *VHL* gene.

Patient Follow-up and Statistical Methods

The accessibility of the patient data was in harmony with ethical standards, and this analysis was conducted with the permission of the Medical Research Council (17489-4/2017/EKU). Demographical and clinical data were collected from the database management systems of Semmelweis University and the University of Szeged. Patient follow-up was based on the available clinical data such as radiological examinations, including ultrasound and computer tomography. The duration of follow-up was calculated from the date of the surgical treatment until the date of death or the last follow-up, and the RCC-related deaths were ascertained. The cancer-specific survival (CSS) was defined as the time from the surgery until death attributable to cancer or disease-related complications. The CSS was analyzed only in patients with clinical M0 disease determined by imaging modalities at the time of the surgery. CSS was estimated by using the Kaplan Meier method and compared among groups using log-rank tests. Deaths from causes other than RCC were censored. Univariate and multivariate Cox proportional hazards regression models were used to estimate the magnitude of the association of the RCC histological subtype with the patient outcome, as shown by the HR and 95% CI. Statistical analysis was performed with the SPSS software package. All p values were two-sided, and $p > 0.05$ was deemed significant. The recurrence-free survival rate was not evaluated in the present study.

Analysis of the Histological Subtypes and Prognostic Factors of RCC According to the 2016 WHO Renal Tumor Classification

Here, a retrospective study was carried out at the Department of Pathology, University of Szeged. Between 1st January 1990 and 31st December 2015, 928 nephrectomies for RCC were evaluated. The ISUP grade, the surgical margin status, presence of necrosis, sarcomatoid differentiation, rhabdoid change, and multinucleated giant tumor cells were assessed. The highest grade occupying at least one low-power field determined the grade of the tumor. Sarcomatoid differentiation was noted if a high-grade spindle cell proliferation was observed (Figure 3a); also, a rhabdoid change was registered if the tumor cells showed the classic triad for rhabdoid cells; namely an excentric nucleus with a vesiculated chromatin structure, a
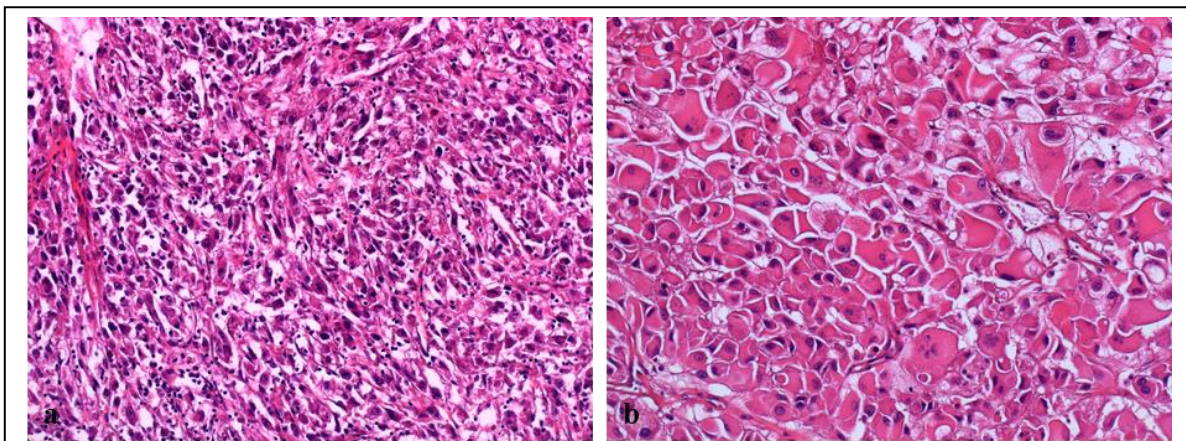
Figure 3 The histological appearance of a sarcomatoid differentiation (a) and a rhabdoid change (b). Both images have a magnification factor of 200x.

prominent (cherry red) nucleolus and a cytoplasmic and eosinophilic inclusion (Figure 3b). The presence of these features was encountered if they occupied at least one low-power field. Additionally, the giant cells were not subcategorized. During the sampling of microscopic tumor necrosis, the extent of necrosis was not given a score.

Analysis of the Clinicopathological, Immunohistochemical and Molecular Features of clear cell papillary RCC

It was a three-institutional retrospective study, in which the Department of Pathology, University of Szeged, the 1st Department of Pathology and Experimental Cancer Research Institute and the 2nd Department of Pathology, Semmelweis University participated. From these departments, 2326 RCC samples were reexamined for clear cell papillary RCC-like

tumors. The inclusion criteria were as follows, low-grade nuclei, the presence of any degree of tubulopapillary growth pattern of tumor cells with clear cytoplasm, linear arrangement of nuclei from the basal membrane, along with the presence of a leiomyomatous stroma. The diagnosis of clear cell papillary RCC was made if the formerly mentioned morphology together with characteristic immunophenotype (CK7- and CA9-positivity, negative CD10 or at most focal CD10-positivity, negative TFE3 and TFEB staining), along with the lack of genetic alterations indicating clear cell RCC (3p deletion, *VHL* mutation, *VHL* promoter hypermethylation), and papillary RCC (7 and 17 trisomy, loss of Y) were detected. Tumors with the same morphology, CK7, and CA9 coexpression, but with diffuse CD10-positivity or with altered *VHL* status were classed as clear cell RCC mimicking clear cell papillary RCC.

Analysis of the Clinicopathological, Immunohistochemical and Molecular Features of Xp11.2 RCC

Lastly, another retrospective study was completed which covered a large part of Hungary, because not just the departments mentioned above participated, but the Pathology Unit, Bács-Kiskun County Teaching Hospital, Pathology Unit, Hetényi Géza County Hospital, Surgical, and Molecular Tumor Pathology Centre, National Institute of Oncology and the Department of Pathology, University of Pécs were involved as well. In total, 2804 RCC samples were reevaluated for translocation RCC. The diagnostic criteria for Xp11.2 RCC were the typical morphological pattern or moderate-to-strong nuclear positivity with TFE3 immunohistochemistry or a positive *TFE3* break-apart FISH analysis.

Results

Histological Subtypes of RCC and Prognostic Factors According to the 2016 WHO Renal Tumor Classification

Based on the light microscopic appearance of the tumor and the results of immunostainings assessed, 83.5% of the samples were classified as clear cell RCC, 6.9% as papillary RCC, 4.5% as chromophobe RCC, 2.3% as RCC unclassified, 1.1% as Xp11.2 translocation RCC, 0.9% as clear cell papillary RCC, 0.4% as collecting duct carcinoma and 0.1% as mucinous tubular and spindle cell RCC. The clinicopathological features of the different subtypes are summarized in Table 7. Apart from chromophobe RCC, all these subsets were more common in men. The series comprised 28 extensively cystic carcinomas. Twenty-five cases were

reclassified as clear cell RCC, two as multilocular cystic clear cell renal cell neoplasm of low malignant potential, and one as clear cell papillary RCC. RCC occurred in 16 patients with end-stage kidney disease. The following morphotypes were encountered: clear cell on eleven occasions, papillary type 1 three times, and clear cell papillary on two occasions. Although the features of ACKD were observed in 9 end-stage kidneys with RCC, the histological evaluation did not lead to the suspicion of ACKD-associated RCC in any of these cases. As for synchronous tumors, clear cell RCC and papillary RCC type 1 in the same kidney were recorded in 2 patients, and clear cell RCC and oncocytoma in 1 patient. Bilateral clear cell RCC occurred in 3 patients, one of whom had end-stage kidney disease.

Clear cell RCC

The tumor was multifocal in 13 samples. Within the 522 (67.3%) low-grade carcinomas, the ISUP grade 2 cases were in the majority, while the ISUP grade 4 cases predominated within the 253 (32.7%) high-grade carcinomas. Among the high-grade carcinomas, the transition of a lower-grade carcinoma to a high-grade carcinoma was commonly observed; purely high-grade "de novo" clear cell RCC was noted in 60 (7.7%) cases. As regards the high-grade features, giant tumor cells were most frequent (13%), followed by rhabdoid morphology (11%) and then sarcomatoid differentiation (6.4%). Four samples exhibited microscopic tumor necrosis in grade 1, 28 in grade 2, 65 in grade 3, and 124 in grade 4 group.

Papillary RCC

Our series consisted of 37 type 1 and 28 type 2 carcinomas, and all cases were unifocal. Type 1 tumors had thin papillae lined usually by a single layer of tumor cells with minimal pale or clear cytoplasm and smaller, round nuclei appearing basophilic upon hematoxylin and eosin staining. In contrast, type 2 tumors displayed thicker papillae lined by tumor cells with abundant eosinophilic cytoplasm and larger, pleomorphic nuclei with a varying degree of nuclear pseudostratification. A combination of features of both histologic subtypes was noted in 5 samples, and these were assigned according to the predominant histological pattern. One type 1 and one type 2 carcinoma was negative for AMACR; however, because of the papillary appearance, the diffuse and strong CK7 reactivity and the TFE3-negativity of the tumor cells, the cases were assigned as papillary RCCs. The CK7 staining was negative in 2 cases of type 1 carcinoma and 14 cases of type 2 carcinomas. Purely high-grade features were noted in 2 cases of type 1 carcinoma and 17 cases of type 2 carcinoma.

Chromophobe RCC

Here, except for a single case, all tumors investigated were unifocal, and they mostly appeared to be low-grade. In 5 cases with marked oncocytic features, the possibility of

oncocytoma was excluded by the diffuse membranous and cytoplasmic CK7 reactivity of the tumor cells. Also, the morphology excluded *SDH*-deficient RCC, LOT along with HOT.

Xp11.2 translocation RCC

Two patients were younger than 45 years, while the eldest one was 72 years. All cases were uniformly negative for CA9 and CK7. The AMACR staining was negative in 7 cases, focally positive in 2 cases, and diffusely positive in 1 case. The labeling for TFE3 protein was diffuse in 8 samples, and focal in 2 samples. The FISH confirmed a *TFE3* rearrangement in all cases.

Clear cell papillary RCC

This subset had the lowest median age. All tumors were in the pT1 stage. Also, two cases developed in end-stage renal disease. On light microscopy, marked angioleiomyomatous stroma was observed in 2 cases. The cup-shaped distribution of CA9 reactivity was seen in 3 samples, box-shaped distribution in 5 samples, and the mixture of the patterns in one sample.

Collecting duct RCC

Four cases met the criteria of this subset. All were highly invasive with an advanced pathological stage. Histologically, high-grade cytological features, tubular or pseudotubular architecture with or without a desmoplastic stroma were observed. The tumor cells were diffusely positive for CK7 and were negative for CA9, AMACR, CD117, and TFE3. The *Ulex europaeus* staining revealed a diffuse positivity in 2 cases, a focal positivity in 1 case, and it was utterly negative in the remaining sample.

Mucinous tubular and spindle RCC

We observed a single case. The tumor was in stage pT1. The patient did not have any evidence of disease recurrence or metastatic dissemination during the follow-up of 7 months.

RCC unclassified

Seventeen out of 22 cases were high-grade carcinomas. One low-grade carcinoma was predominantly tubulopapillary, and the tumor cells had an optically clear cytoplasm. The CK7 staining was negative, the AMACR staining revealed 80% positivity, and the CA9 reactivity appeared to be positive in 70% of the tumor cells. The TFE3 staining was negative. The other low-grade carcinoma resembled type 1 papillary carcinoma; however, the CK7 staining was negative, and the AMACR displayed only 50% reactivity.

		CRCC	PRCC T1	PRCC T2	ChRCC	Unclassified	Xp11.2 RCC	CCPRCC	CDC	MTSCC
Number of cases (%)		775 (83.5)	37 (3.9)	28 (3.0)	42 (4.5)	22 (2.3)	10 (1.1)	9 (0.9)	4 (0.4)	1 (0.1)
Age (years)	Median, range	61, 25-84	62, 12-79	62.5, 39-78	58, 17-74	63, 30-77	55, 15-72	51, 32-78	62, 49-69	68
Male:female ratio		1.5:1	3.1:1	2.1:1	0.82:1	2.6:1	2.3:1	1.25:1	1:1	female
Right:left ratio		1.09:1	0.89:1	1:1	1.21:1	0.69:1	0.25:1	1.25:1	0.33:1	right
Size (mm)	Median, range	55, 10-220	43.5, 10-150	60, 9-170	50, 14-170	86.5, 34-173	90, 25-160	22, 8-65	92, 55-140	40
ISUP grade	G1	158	3	0	18	0	1	8	0	1
	G2	364	29	7	21	5	3	1	0	0
	G3	99	2	15	3	8	0	0	0	0
	G4	154	3	6	0	9	6	0	4	0
Microscopic tumor necrosis		221	11	21	3	19	6	0	3	0
Rhabdoid and/or sarcomatoid		117	3	3	0	9	5	0	2	0
Giant tumor cells		105	3	1	0	2	0	0	0	0
Surgical margin positivity		37	1	2	0	0	2	0	2	0
Postoperative tumor stage	pT1a	216	16	7	13	1	2	8	0	1
	pT1b	147	7	3	9	3	1	1	0	0
	pT2a	49	5	4	6	1	1	0	0	0
	pT2b	18	3	1	8	1	0	0	0	0
	pT3a	297	6	10	6	13	2	0	2	0
	pT3b	16	0	0	0	2	1	0	0	0
	pT3c	9	0	0	0	0	0	0	0	0
	pT4	23	0	3	0	1	3	0	2	0
Lymph node involvement	N1	29	2	5	0	4	2	0	1	0
Distant metastases	M1	39	0	2	0	1	1	0	1	0
TNM stage groupings	I	357	23	10	22	3	3	8	0	1
	II	63	7	5	14	2	1	0	0	0
	III	301	7	9	6	14	3	0	1	0
	IV	54	0	4	0	2	3	0	3	0

Table 7 Clinicopathological features in different types of renal cell carcinoma.

Correlation between the morphotype and CSS

Follow-up data sets were accessible for 804 patients (763 non-metastatic and 41 metastatic diseases at the time of surgery). One hundred thirty-one patients with clear cell RCC, three patients with type 1 papillary RCC, seven patients with type 2 papillary RCC, seven patients with RCC unclassified, six patients with Xp11.2 translocation RCC, and three patients with collecting duct carcinoma had died from an RCC-related cause. The median follow-up of these patients was 29 months (range 1-254 months), whereas the median follow-up for all survivors was 68 months (range 2-313 months). The CSS rates of histological types are shown in Figure 4. The 5-year CSS was significantly different between patients with clear cell RCC and with chromophobe RCC ($p=0.021$) or with RCC unclassified ($p<0.001$) or with Xp11.2 translocation RCC ($p<0.001$), but not between patients with clear cell RCC and those with papillary RCC ($p=0.39$). Although the statistical significance in survival rates could not be calculated
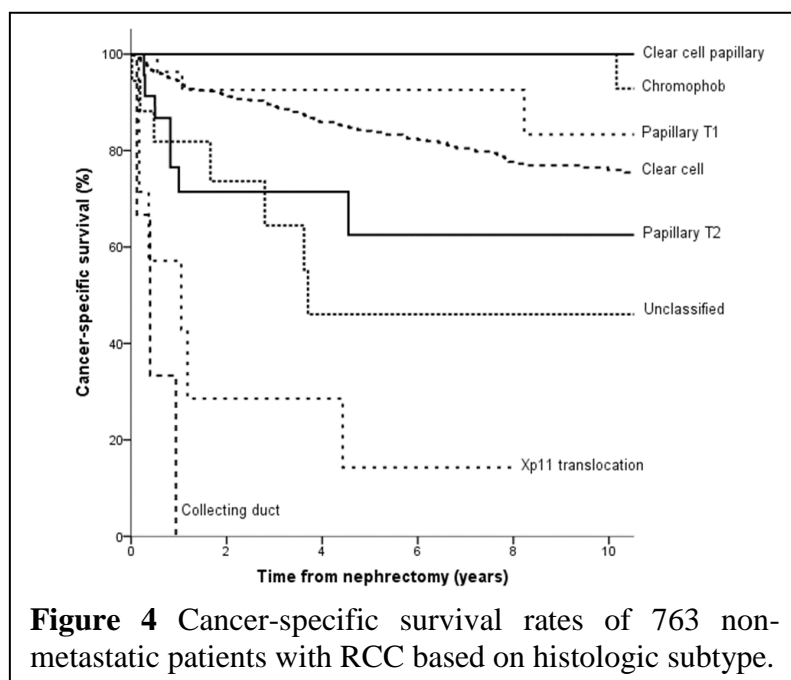
Figure 4 Cancer-specific survival rates of 763 non-metastatic patients with RCC based on histologic subtype.

between clear cell RCC and clear cell papillary RCC or collecting duct carcinoma because of the limited number of cases in the latter entities, the Kaplan Meier curves leave no doubt that these entities represent an entirely different outcome. Among the 90 patients with non-metastatic clear cell RCC at the time of nephrectomy and who died from an RCC-related cause, 18 patients received TKIs. Although the average survival time was longer in the treated group (5.9 years *vs.* 4.5 years), this did not affect CSS significantly ($p=0.271$); hence, the treatment of metastatic disease did not conflict with what the survival data tell us in Figure 4.

Grade and microscopic tumor necrosis in clear cell RCC

CSS rates according to the four-tiered ISUP grade and the two-tiered grade assessment are shown in Figure 5. When CSS according to the presence or absence of microscopic tumor necrosis was analyzed, the necrotic tumors exhibited a significantly poorer outcome than the non-necrotic tumors ($p<0.001$). When the presence or absence of tumor necrosis was tested in

patients with low-grade tumors *vs.* high-grade tumors (Figure 6), necrosis was associated with a significantly poorer outcome only in high-grade tumors. In univariate Cox proportional

Figure 5 Cancer-specific survival in clear cell RCC according to the ISUP grading system. **A**: The Kaplan Meier estimation did not reveal any difference in biological behavior between grade 1 *vs.* grade 2 tumors (*p*=0.550), and grade 3 *vs.* 4 tumors (*p*=0.226). Grade 1 or grade 2 tumors displayed a significantly better survival rate among patients than grade 3 tumors (*p*<0.0001). **B**: When the grade 1 and 2 tumors were lumped together into low-grade carcinomas, and grade 3 and 4 tumors into high-grade carcinomas, the survival analysis revealed a significant difference between the two groups (*p*<0.0001).

hazard analysis, the ISUP grade, TNM stage, tumor necrosis, giant tumor cells, rhabdoid/sarcomatoid change, and positive surgical margins all proved to be negative predictors of CSS. In multivariate Cox proportional hazards analysis, however, only the ISUP grade, TNM stage, and positive surgical margin turned out to be independent prognostic factors (Table 8).

Subtypes and grade in papillary RCC

The 5-year CSS rates in type 1 and type 2 subtypes are shown in Figure 7. When the 5-year CSS was calculated according to the ISUP grade, 100% was observed for grade 1, 94% for grade 2, 74% for grade 3, and

Figure 6 Kaplan Meier estimates in clear cell RCC according to low-grade (ISUP grade 1+2) and high-grade (ISUP grade 3+4) assessment, and the presence or absence of microscopic tumor necrosis. The survival rates tended to be worse when tumor necrosis was present, but a difference attained a level of significance only in the high-grade subtypes (p=0.02).

33% for grade 4 samples, respectively. The 5-year survival rate was significantly better for patients with grade 2 tumors than for those with grade 3 tumors (*p*=0.011). The sample size in grade 1 tumors did not allow a comparison of survival rates between those with grade 1 and grade 3 tumors. However, there was no significant difference in survival rates between cases with grade 1 *vs*. grade 2 (*p*=0.696), and grade 3 *vs*. grade 4 (*p*=0.445); and, therefore, samples with grades 1 and 2, and grades 3 and 4 were merged to low-grade and high-grade categories. The 5-year CSS rates according to the two-tiered grading system exhibited a significant difference (Figure 7). In a Cox proportional hazard analysis, the ISUP grade and TNM stage, but not the morphotype, exerted a significant effect on the patient outcome (Table 9).

| Characteristic		Hazard ratio	CI 95%	*p* value
Univariate				
	ISUP grade	7.50	5.01-11.21	<0.001
	TNM stage	2.54	2.04-3.15	<0.001
	Surgical margin status	2.95	1.57-5.53	<0.001
	Microscopic tumor necrosis	6.74	4.53-10.07	<0.001
	Rhabdoid/sarcomatoid change	5.14	3.39-7.78	<0.001
	Giant tumor cells	3.93	2.51-6.15	<0.001
Multivariate				
	ISUP grade	4.33	2.36-7.95	<0.001
	TNM stage	1.86	1.49-2.33	<0.001
	Surgical margin status	2.61	1.39-5.2	0.003
	Microscopic tumor necrosis	1.69	0.93-3.05	0.081
	Rhabdoid/sarcomatoid change	0.96	0.57-1.61	0.896
	Giant tumor cells	0.67	0.4-1.13	0.139

Table 8 Cox regression analysis for cancer-specific survival rates in non-metastatic CCRCC.

Characteristic		Hazard ratio	CI 95%	*p* value
Univariate				
	ISUP grade	4.12	1.75-9.69	0.001
	TNM stage	2.8	1.36-5.78	0.005
	WHO type	3.64	0.9-14.7	0.039
	Surgical margin status	2.97	0.36-24.1	0.30
	Microscopic tumor necrosis	1.89	0.5-7.15	0.34
	Rhabdoid/sarcomatoid change	3.18	0.63-16.1	0.16
	Giant tumor cells	2.38	0.29-19.4	0.41
Multivariate				
	ISUP grade	2.77	1.01-7.53	0.046
	TNM stage	2.33	103.5.28	0.042
	WHO type	3.15	0.55-17.85	0.19
	Surgical margin status	2.54	0.02-247.3	0.68
	Microscopic tumor necrosis	1.74	0.33-9.16	0.58
	Rhabdoid/sarcomatoid change	5.11	0.25-102.3	0.21
	Giant tumor cells	0.36	0.003-49.1	0.68

Table 9 Cox regression analysis for cancer-specific survival rates in non-metastatic PRCC.
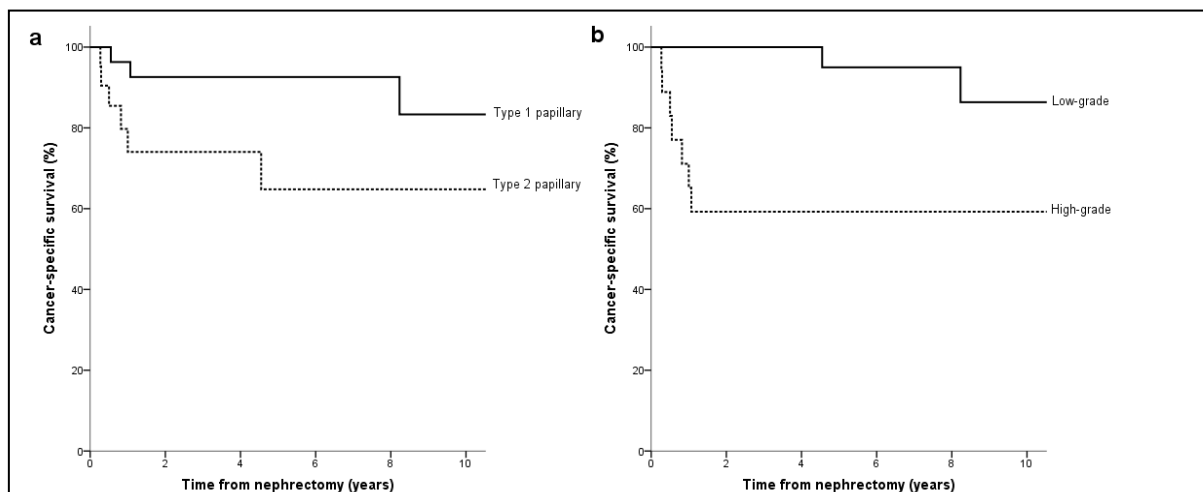
Figure 7 Kaplan Meier estimates in papillary RCC. **A**: The 5-year CSS rates in type 1 and type 2 subtypes were 92% and 65%, respectively (p=0.039). **B**: A significant difference was seen in survival rates between the low-grade (ISUP grade 1 + grade 2) and the high-grade (ISUP grade 3 + grade 4) subtypes (p<0.001).

Clinicopathological, Immunohistochemical and Molecular Features of Clear Cell Papillary RCC

In this retrospective study, using the inclusion criteria, we retrieved 31 samples. All tumors coexpressed CK7 and CA9. The TFE3 and TFEB reactions were uniformly negative, and the CD10 and the AMACR reactions were negative in 27 and 30 cases, respectively. The FISH assays for papillary RCC, available in 27 cases, and deletion of chromosome 3p, available in 29 cases, yielded negative results. The histomorphology, the results for *VHL* mutation and *VHL* methylation testing, and the immunophenotype confirmed 21 cases as clear cell papillary RCC and 10 cases as clear cell RCC. The main characteristics of the subsets are summarized in tables 10 and 11.

General features of clear cell papillary RCCs

Here, 21 tumors were examined, and the specimens were obtained from 12 females and 9 males. The mean age was 60 years. Partial nephrectomy was performed in 4 patients and radical nephrectomy in 17 patients, and one tumor developed in a transplanted kidney. Twenty cases were incidental findings of imaging conducted for non-urological symptoms. All the tumors were solitary, and the mean size was 23 mm (with range 6 to 65 mm).

Microscopic findings on clear cell papillary RCCs

Each tumor was circumscribed, and at least one thin fibrous, or fibromuscular capsule was present, which contained smooth muscle in 13 tumors. A minimal infiltration of renal sinus fat was observed in case #3, but another invasive pattern was not seen at all. The dominant growth pattern was tubulo-acinar, with cyst formation in a continuum from microscopic to

macroscopic cystic spaces in 12 samples. Also, a papillary architecture was observed in 14 tumors and was detected mainly focally, except in one case where it was predominantly seen. Substantial areas with compact cell nests and trabeculae were seen in 11 samples. Foamy macrophages, psammoma bodies, prominent nucleoli, and necrosis were absent. Clear cell phenotype was characteristic that occasionally admixed with an eosinophilic morphology. The linear arrangement of nuclei, together with its orientation away from the basement membrane, was observed in 16 tumors. Stromal smooth muscle was found in 18 cases. For representative images of the features observed, see Figure 8.

Immunohistochemical and molecular findings on clear cell papillary RCCs

All exhibited a strong and diffuse CK7 expression. Immunoreaction for CA9 resulted in diffuse staining in 17 tumor samples and focal staining in 4 tumor samples. The "cup-shaped" pattern was detected in 17 cases, visible mainly in the tubular and cystic areas. CD10 was focally positive in two samples. In addition, weak granular, diffuse AMACR-positivity was noted in case #14. Representative images are in Figure 9. The mutation status of the *VHL* gene was investigated in 11 samples, and in case #12, a single nucleotide polymorphism (SNP) in the untranslated region (UTR) was found. The *VHL* gene methylation status was analyzed in 16 samples, and none of these harbored promoter region hypermethylation.

General features of clear cell RCCs with diffuse CK7-positivity

In this group, we analyzed 10 cases, and the mean age was 51 years, with 5 females and 5 males. Tumor-related symptoms were registered in two patients. In case #23, a clear cell RCC (CA9 and CD10 positive; CK7 negative) was resected from the contralateral kidney two months after the first surgery. Additionally, in case #24, a metastatic perihilar lymph node was removed together with the tumorous kidney. The mean size of the tumors was 29 mm.

Microscopic findings on clear cell RCCs with diffuse CK7-positivity

The predominant growth pattern was a tubulo-acinar, followed by cystic, papillary, and solid. The tumors were composed of clear cytoplasm cells with focal eosinophilic change. Also, an apical linear nuclear arrangement was seen in 6 samples, and 2 cases contained a smooth muscle rich stroma. Infiltration of the renal vein, sinus, and perinephric fat was not observed.

Immunohistochemical and molecular on clear cell RCCs with diffuse CK7-positivity

There was coexpression of CK7 in a diffuse fashion and CA9 in a diffuse (8 cases) or focal fashion (2 cases). The cup-shaped distribution of CA9 was present in 6 cases. Diffuse CD10-positivity was observed in case #23 and #24. The *VHL* gene mutation status was analyzed in 9 samples, and in case #22, #23, and #31 a pathogenic mutation was identified that was not

Clear cell papillary RCC

Case	Sex	Age (y)	ESRD	Tumor-related symptoms	Size (mm)	AJCC Stage	ISUP Grade	Follow-up period (months)	Progression	Comment
1	M	68	No	No	21	T1aNxMx	1	31	No	
2	M	57	No	No	20	T1aNxMx	2	35	No	
3	M	64	No	No	30	T3aNxMx	2	NA	ND	Sinus fat tissue infiltration
4	F	68	No	No	30	T1aNxMx	1	12	No	
5	M	84	ESRD	No	10	T1aNxMx	1	1	No	
6	F	63	No	No	8	T1aNxMx	2	46	No	Ipsilateral oncocytoma
7	F	81	No	No	25	T1aNxMx	1	113	No	
8	F	78	No	No	20	T1aNxMx	1	184	No	
9	M	56	ACKD	No	10	T1aNxMx	1	85	No	
10	M	66	No	No	11	T1aNxMx	1	3	No	
11	F	49	No	No	38	T1aNxMx	1	10	No	
12	M	75	No	No	65	T1bNxMx	2	80	No	
13	F	52	No	No	25	T1aNxMx	2	158	No	
14	M	32	No	No	8	T1aNxMx	1	101	No	
15	F	57	No	No	6	T1aNxMx	1	NA	ND	
16	F	30	ESRD	No	8	T1aNxMx	1	86	No	
17	F	60	No	Abdominal pain	22	T1aNxMx	1	3	No	
18	M	76	No	No	10	T1aN0Mx	1	62	No	Ipsilateral AML and papillary adenomas
19	F	69	No	No	13	T1aNxMx	1	8	No	
20	F	28	ESRD	No	20	T1aNxMx	2	59	No	Tumor in a graft kidney
21	F	56	No	No	30	T1aNxMx	1	NA	ND	

Clear cell RCC with diffuse CK7-positivity

Case	Sex	Age (y)	ESRD	Tumor-related symptoms	Size (mm)	AJCC Stage	ISUP Grade	Follow-up period (months)	Progression	Comment
22	F	41	No	No	20	T1aNxMx	1	26	No	
23	F	44	No	No	50	T1bN1Mx	1	36	No	Lymph node metastasis
24	M	37	No	Hematuria	37	T1aNxMx	1	67	No	Contralateral CCRCC 2 months later
25	M	47	ACKD	No	19	T1aNxMx	1	12	No	
26	F	53	No	No	30	T1aNxMx	1	19	No	
27	F	69	No	No	24	T1aNxMx	2	37	No	
28	M	69	No	Lumbar pain	15	T1aNxMx	1	100	No	Ipsilateral papillary adenoma
29	M	40	No	No	30	T1aNxMx	1	10	No	
30	F	51	No	No	40	T1aNxMx	1	3	No	
31	M	61	No	No	25	T1aNxMx	2	6	No	

M indicates, male; F, female, ESRD, end-stage renal disease; ACKD, acquired cystic kidney disease; NA, not available; ND, no data.

**Table 10** Clinicopathological features of the patients examined.

|	Architecture of tumor volume (%)					Immune profile (%)							Molecular characteristics			
Case	Tubular	Papillary	Cystic	Solid	LiN	CK7	CA9	CA9 cup-shaped	CD10	AMACR	+7	+17	-Y	-3p	*VHL* mut	*VHL* met
Clear cell papillary RCC																
1	90	-	-	10	No	Diff	Diff	Yes	Neg	Neg	-	-	-	-	wt	ua
2	88	2	-	10	Yes	Diff	Diff	Yes	Foc	Neg	-	-	-	-	wt	-
3	95	-	-	5	Yes	Diff	Diff	Yes	Neg	Neg	nd	nd	nd	nd	nd	nd
4	59	1	20	20	Yes	Diff	Diff	Yes	Neg	Neg	-	-	■	-	wt	-
5	100	-	-	-	Yes	Diff	Diff	Yes	Neg	Neg	-	nd	-	-	nd	nd
6	95	5	-	-	Yes	Diff	Diff	Yes	Foc	Neg	-	-	■	-	wt	-
7	44	5	50	1	No	Diff	Diff	Yes	Neg	Neg	-	-	■	-	wt	-
8	50	50	-	-	Yes	Diff	Diff	Yes	Neg	Neg	-	-	■	-	ua	-
9	80	10	-	10	No	Diff	Diff	Yes	Neg	Neg	-	-	-	-	wt	-
10	95	5	-	-	Yes	Diff	Diff	Yes	Neg	Neg	-	-	■	-	wt	-
11	50	40	10	-	Yes	Diff	Diff	Yes	Neg	Neg	-	-	■	-	wt	-
12	50	-	50	-	Yes	Diff	Diff	Yes	Neg	Neg	-	-	-	-	*5'UTR SNP*[#]	-
13	-	80	20	-	No	Diff	Diff	Yes	Neg	Neg	-	-	■	-	ua	-
14	80	10	10	-	Yes	Diff	Diff	Yes	Neg	Poz[§]	-	-	-	-	wt	-
15	-	20	80	-	Yes	Diff	Diff	No	Neg	Neg	-	-	■	-	ua	nd
16	95	-	-	5	Yes	Diff	Diff	No	Neg	Neg	-	-	■	-	ua	nd
17	50	20	30	-	No	Diff	Diff	No	Neg	Neg	-	-	-	-	wt	-
18	90	-	5	5	Yes	Diff	Foc	Yes	Neg	Neg	nd	nd	nd	nd	nd	-
19	45	1	50	4	Yes	Diff	Foc	Yes	Neg	Neg	-	-	■	-	nd	-
20	89	-	1	10	Yes	Diff	Foc	Yes	Neg	Neg	-	-	-	-	ua	-
21	85	1	5	10	Yes	Diff	Foc	No	Neg	Neg	-	-	-	-	ua	-
Clear cell RCC with diffuse CK7-positivity																
22	50	5	35	10	Yes	Diff	Diff	Yes	Neg	Neg	-	-	■	-	*mut*[a]	+
23	50	20	30	-	Yes	Diff	Diff	Yes	Diff	Neg	nd	nd	■	-	*mut*[b]	nd
24	10	50	20	20	No	Diff	Diff	No	Diff	Neg	-	-	-	-	*5'UTR SNP*[¶]	-
25	80	10	10	-	No	Diff	Diff	Yes	Neg	Neg	-	-	-	-	wt	+
26	95	1	-	4	Yes	Diff	Diff	Yes	Neg	Neg	-	-	■	-	wt	+
27	20	10	70	-	Yes	Diff	Diff	Yes	Neg	Neg	-	-	■	-	wt	+
28	40	-	60	-	Yes	Diff	Diff	Yes	Neg	Neg	-	-	-	-	ua	+
29	20	40	40	-	Yes	Diff	Diff	No	Neg	Neg	-	-	-	-	wt	+
30	30	-	20	50	No	Diff	Foc	No	Neg	Neg	-	-	■	-	wt	+
31	90	-	-	10	Yes	Diff	Foc	No	Neg	Neg	-	-	-	-	*mut*[c]	nd

LiN indicates, linear nuclear arrangement from basement membrane; +7 and +17, trisomy of chromosome 7 and 17, respectively; -Y deletion of chromosome Y; -3p, deletion of chromosome 3p; *VHL* mut, von Hippel-Lindau gene mutation status; *VHL* met, von Hippel-Lindau gene methylation status; nd, not determined; wt, wild type; ua: unsuccessful analysis; 5'UTR SNP, single nucleotide polymorphism in 5' untranslated region; diff: diffuse; foc: focal; neg: negative (less than or equal to 10%). [§]: weak granular positivity. [#]: exon 3 could not be amplified; [¶]: exon1b could not be amplified, [a]: c.221T>A/p.V74N; [b]: c.625C>T/p.G209*; [c]: c.354_361delCTTCAGAGinsT.

Table 11 Morphological, immunohistochemical, and molecular characteristics of the tumor cases examined.

present in the tumor-free renal parenchyma. The sequencing revealed an SNP without any clinical significance in case #24. The remaining five tumors analyzed harbored no genetic change. Also, the *VHL* gene promoter hypermethylation was tested in 8 cases, and 7 of them possessed promoter region hypermethylation.
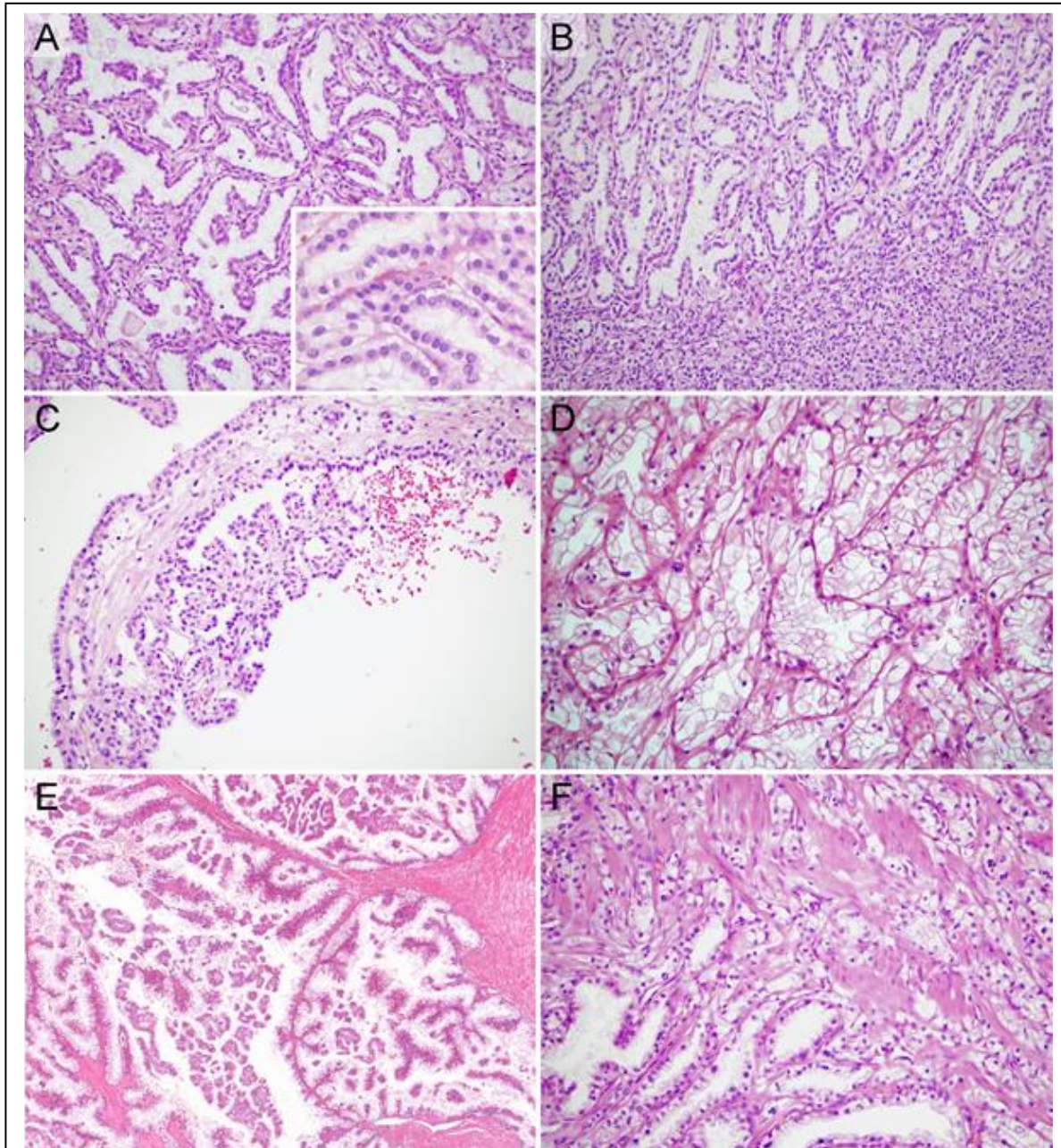
Figure 8 Histological features of the clear cell papillary tumors analyzed. The most characteristic architectural pattern was a branching tubular (a), in which the linear nuclear arrangement could be appreciated (insert in a). Solid areas were also encountered (b). A papillary pattern was frequently represented by papillary projections from cyst walls (c). Some polymorphism was seen, but prominent nucleoli were absent (d). Three tumors had a predominant papillary architecture (e). Myomatous stroma was seen in some cases (f).
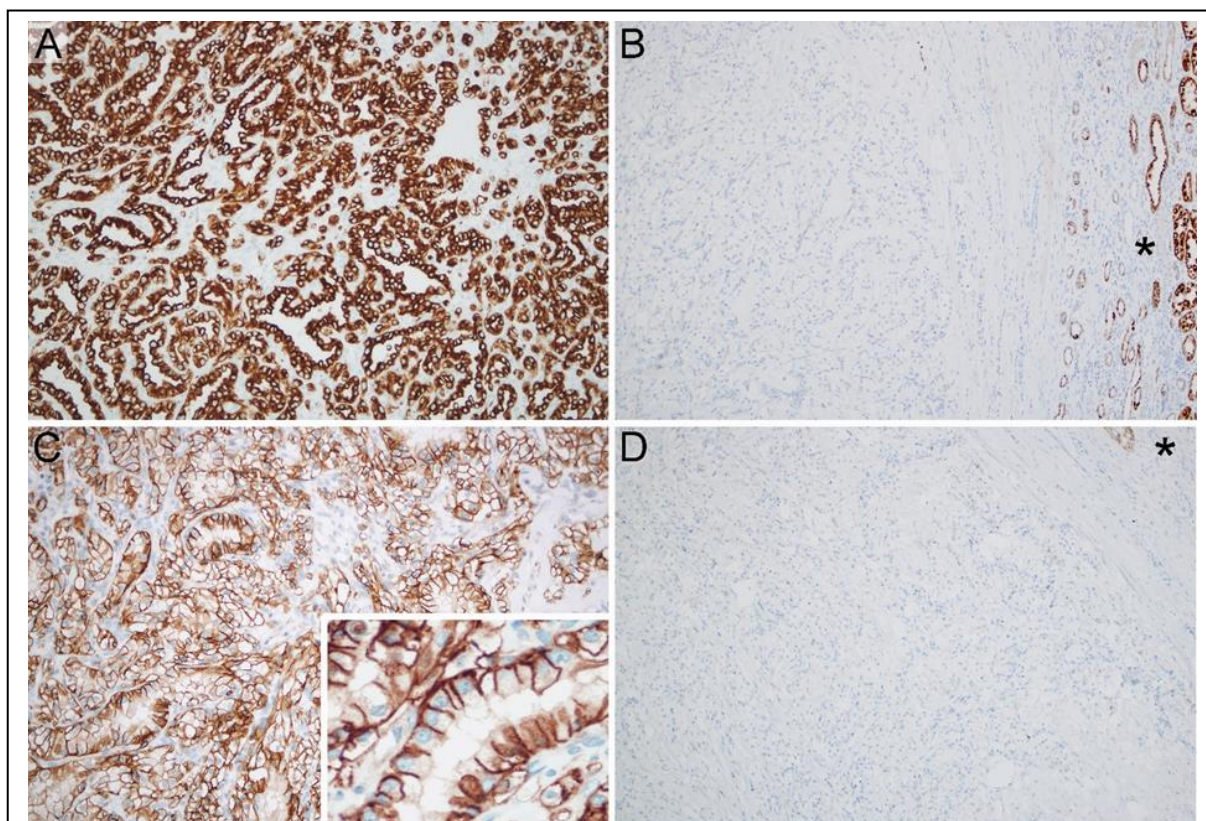
Figure 9 Immunohistochemical characteristics of the clear cell papillary RCC tumors analyzed. All cases displayed a diffuse and strong CK7-positivity (a), whereas CD10 was mainly negative, or only weekly and focally positive (b, asterisk: peritumoral kidney as an internal control). Extensive CA9 staining was also usually seen (c), the "cup-shaped" pattern could be appreciated mainly in the tubular areas (insert in c). AMACR was completely negative in most tumors (d, asterisk: peritumoral kidney as an internal control).

Follow-up data of both patient group

The median time was 52.5 months (with a range of 1 to 184 months) for clear cell papillary RCC patients and 31.6 months (with a range of 3 to 100 months) for clear cell RCC patients. Only three patients had no follow-up data, and two patients died in non-cancer-related causes. No tumor progression and recurrence was documented for the 26 surviving patients.

Clinicopathological, Immunohistochemical and Molecular Features of Xp11.2 Translocation RCC

Twenty-eight tumors proved to be Xp11.2 RCC among 2804 nephrectomies reviewed from the pathology departments listed above (0.99%). The diagnosis was later confirmed by immunohistochemistry in each case and by FISH analysis except for patient #11, #12, and #24.

Clinical and follow-up data

The clinicopathological findings are summarized in Table 12. Thirteen male and fifteen female patients were included in our cohort. The median age was 60 years (with range 8 to 72). Three tumors occurred in children, and Wilms' tumor was suspected in all the cases. The tumor produced symptoms in 9 patients. Also, the tumor was an incidental finding in 7 patients. There were no underlying renal disorders in any patients in the affected kidney, but in patient #12, contralateral kidney agenesis was present. Among our patients, none had received chemotherapy or had had any previous malignant tumors. Nephrectomy was performed in each case except in three patients, who were treated with a partial nephrectomy because of the relatively small tumors (patient #7 and #8), and the absence of the contralateral kidney (patient #12). Follow-up information was accessible in 21 patients, and the mean follow-up time was 14 months (with range 2 months to 321 months). Regional lymph node or distant metastasis developed in 13 patients (9 had been discovered before surgery; 6 distant and 3 regional lymph node metastases). Seven patients died from cancer-related causes, and one patient died from a non-cancer-related cause. In patient #15, a regional lymph node metastasis developed after 12 months, so she was treated with retroperitoneal lymphadenectomy, and in the last follow-up, there were no signs of disease. Sixty months after the nephrectomy, patient #14 had multiple pulmonary, hepatic, and bone metastasis. He received tyrosine kinase and mTOR inhibitors until treatment failure. Also, in patient #27, multifocal vertebral metastasis developed. Currently, she is receiving TKI therapy, and she has stable disease. The remaining 11 patients were alive with no evidence of disease.

Morphological findings on Xp11.2 RCCs

All the tumors that were examined were unilateral and unifocal. The diameter of the tumors ranged from 15 mm to 160 mm, and the average was 78.5 mm. The invasion of the renal vein, sinus, and adipose capsule were observed in 7, 8, 6 cases, respectively. The predominant architectural appearance was a solid pattern, followed by a papillary pattern, while both a solid and papillary pattern was seen in a small proportion of the cases. The tumors were composed mostly of clear cells in 19 cases, mostly of eosinophilic cells in 7 cases, and a mixed eosinophilic and clear cell morphology was seen in two cases. Twenty-two cases had typical architecture with voluminous clear cytoplasm, nested, or papillary growth (Figure 10). The remaining 6 cases had a diverse morphology mimicking clear cell RCC except for patient 5, whose tumor resembled a rhabdoid morphology and patient 6, whose tumor had an anaplastic carcinoma appearance (Figure 11). The presence of foamy cells, intracytoplasmic pigment, cholesterol clefts, psammoma bodies, and

| Patient	Age (y)	Sex	Symptoms†	Side	Size (mm)	pT Stage‖	Node Status§	Metastasis or recurrence*	Follow-up (mo)	Status¶
1	52	M	-	L	70	4	-	-	-	LTF
2	69	M	Incidental finding on CT	L	50	1b	-	-	-	LTF
3	47	M	Hematuria, flank pain	R	100	3b	Neg	Lung, Liver	2	DOD
4	69	F	Hematuria	R	80	3a	-	Bone-U, Local R	53	DOD
5	59	M	Flank pain	L	140	4	Pos	-	-	LTF
6	67	M	Fatigue, subcostal pain	L	160	4	Pos	Liver, LN	2	DOD
7	40	M	-	L	25	1a	-	None	127	NED
8	15	F	Palpable ventral mass	L	55	1b	-	Lung, Vertebrae	14	DOD
9	46	M	Incidental finding	L	100	2a	Neg	Local R	13	DOD
10	72	F	Flank pain	L	140	3a	-	-	4	DOD
11	21	F	-	R	-	3a	-	-	-	LTF
12	14	M	-	L	-	1a	-	None	12	NCRD
13	31	M	Incidental finding on US	L	55	1b	-	None	87	NED
14	57	M	-	L	100	3a	Neg	Lung, Liver, Vertebrae	81	DOD
15	40	F	-	R	110	3a	-	LN	65	NED
16	50	F	-	R	45	1b	-	None	31	NED
17	32	M	Incidental finding	B	15	1a	-	None	24	NED
18	60	F	Incidental finding	-	16	1a	-	-	-	LTF
19	66	F	-	R	60	1b	Pos	Adrenal gland	-	LTF
20	32	M	-	R	20	1a	Pos	Liver	-	LTF
21	17	F	-	R	35	1a	-	None	175	NED
22	36	F	Shoulder pain	R	120	3b	-	Scapula	13	AWD
23	40	F	Incidental finding	R	41	1b	-	None	24	NED
24	8	F	Palpable ventral mass	L	100	2b	-	-	321	NED
25	54	F	-	R	120	3a	Neg	None	10	NED
26	66	M	Abdominal pain	L	110	2b	-	None	4	NED
27	51	F	-	R	65	1b	-	Vertebrae	3	AWD
28	46	F	Incidental finding	L	110	3a	Pos	None	7	NED

†Symptoms: including any tumor-related symptoms; incidental finding indicates a symptomless tumor; -, no data. ‖pT Stage: classification by AJCC 2016 TNM Staging System. §Node Status: nodal status at time of surgery; -, no lymph node was removed; Neg, negative; Pos, positive. A lymph node metastasis that developed during the follow-up period is listed in the "Metastasis" column. *Metastasis: either found earlier or at the same time with the primary renal tumor, or during the follow-up period; Bone-U, bone, exact location is unknown; -, no data; R, recurrence; LN, lymph node. ¶Status: DOD, died of disease; LTF, patient is deceased, but lost to follow-up; NED, no evidence of disease; NCRD, not a cancer-related death; AWD, alive with disease; -, no data.

Table 12 Clinicopathological features of the patients analyzed with Xp11.2 RCC.

necrosis was observed in 7, 4, 1, 11, and 17 cases, respectively. Most of the tumors had high-grade features. A detailed summary of these microscopic findings can be found in Table 13.

Immunohistochemical findings on Xp11.2 RCCs

The results of the immunohistochemistry are summarized in Table 14. Three cases displayed positivity with CA9, although two of these were necrotic tumors. All the cases investigated were negative with CK7, while CD10 was strongly positive in 17 cases. AMACR was negative in 14 tumors, and a diffuse-to-focal positivity was seen in the remaining 14 cases. The diagnostic TFE3 reaction strongly labeled the nuclei in 26/28 cases, but Cathepsin K displayed positivity only in 6 tumors. MelanA was positive only in four cases, and HMB45 showed a weak-to-diffuse positivity in three patients.
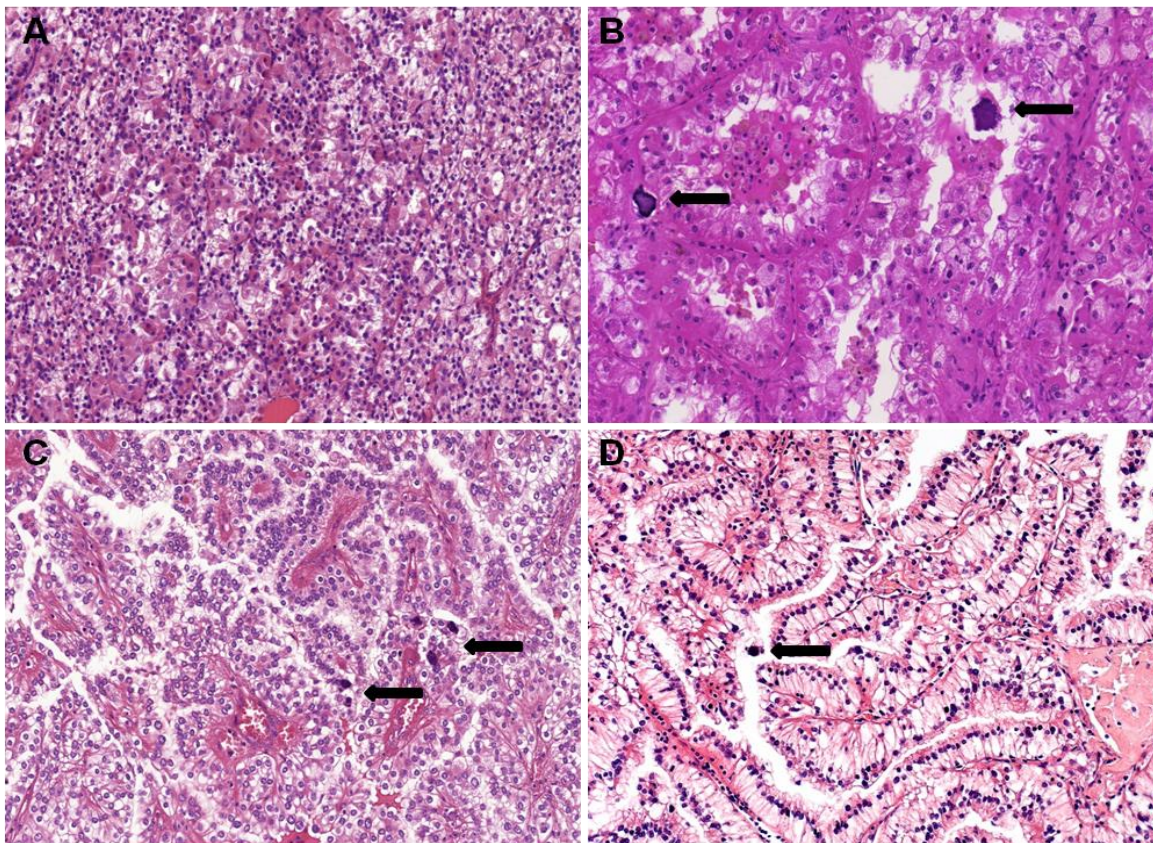
Figure 10 Representative images of typical morphological features of Xp11.2 renal cell carcinomas. (a) A solid-nested pattern with an admixture of eosinophilic and clear cells. (b) An alveolar pattern populated by eosinophilic cells. Psammoma bodies are also present. (c) Papillary pattern with voluminous clear cells and psammoma bodies. (d) Occasionally the nuclei are near the apical surface of the cells, and they mimic clear cell papillary renal cell carcinoma. The arrows indicate the psammoma bodies. All the images have a magnification factor of 200x.

FISH findings on Xp11.2 RCCs

The FISH reaction was performed in 25 cases because in patient #11, #12, and #24, the quality of the tumor tissue was not sufficient for a proper analysis. In 21 tumors, typical split signals were seen, while in patient #9 and #10, mostly a truncated signal pattern was observed. In patient #14, the signals were separated, but they were unusually close to each other. In patient #23 (a female), an entire break-point region was utterly absent. Hence, in this case, only one signal pair was detected in the nuclei of the tumor cells, while in the surrounding renal parenchyma, two unaffected signal pairs were present. In this case, the immunophenotype and histomorphology led us to classify the case as Xp11.2 RCC.

Patient	PP (%)	SP (%)	CCs (%)	ECs (%)	Foamy cells	IP	ChC	PB	Necrosis	ISUP grade
1	5	95	50	50	-	-	-	-	+	4
2	40	60	30	70	+	+	-	-	-	2
3	1	99	20	80	-	-	-	-	+	4
4	50	50	90	10	-	-	-	-	+	2
5	-	100	10	90	-	-	-	-	+	4
6	-	100	5	95	-	-	-	-	+	4
7	-	100	100	-	-	-	-	-	-	1
8	90	10	80	20	-	-	-	-	-	2
9	50	50	70	30	-	-	-	-	+	4
10	80	20	75	25	-	-	-	-	+	4
11	95	5	90	10	+	-	-	-	-	3
12	50	50	80	20	-	-	-	+	+	3
13	100	-	100	-	+	-	+	+	+	2
14	10	90	60	40	-	+	-	+	-	2
15	80	20	70	30	-	+	-	-	+	3
16	90	10	75	25	+	-	-	+	-	3
17	100	-	100	-	-	-	-	+	-	2
18	5	95	30	70	+	-	-	+	-	3
19	10	90	80	20	-	-	-	+	+	2
20	-	100	95	5	-	-	-	+	+	4
21	-	100	30	70	-	-	-	+	-	2
22	50	50	90	10	-	-	-	-	+	3
23	-	100	80	20	+	-	-	-	+	3
24	-	100	60	40	-	-	-	-	-	3
25	80	20	30	70	+	-	-	+	+	3
26	95	5	90	10	-	+	-	-	+	3
27	100	-	50	50	-	-	-	+	-	3
28	90	10	80	20	-	-	-	-	+	3

PP, indicates papillary pattern; SP, solid pattern; CCs, clear cells; ECs, eosinophilic cells; IP, intracytoplasmic pigment; ChC, cholesterol clefts; PB, psammoma bodies; +, present; -, absent.

Table 13 Histological findings of the Xp11.2 RCC tumors investigated

Pati-ent	CA9	CK7	CD10	AMACR	MelanA	HMB45	Cathepsin K	TFE3 IHC	*TFE3* FISH
1	N	N	D	N	N	N	N	D	+
2	N	N	D	N	N	N	N	D	+
3	N	N	N	N	N	N	N	D	+
4	N	N	D	D	N	N	D	D	+
5	N	N	D	N	N	N	N	D	+
6	N	N	N	N	N	N	N	D	+
7	N	N	D	F	N	N	N	D	+
8	N	N	D	D	N	N	N	D	+
9	N	N	N	N	N	N	N	D	+
10	N	N	D	N	D	N	N	D	+
11	N	N	D	F	N	N	F	F	NA
12	N	N	D	D	N	N	N	D	NA
13	N	N	D	D	N	D	N	D	+
14	N	N	D	D	N	F	D	D	+
15	N	N	N	N	D	N	N	D	+
16	N	N	D	D	N	N	N	D	+
17	N	N	D	F	N	N	N	D	+
18	N	N	F	D	N	N	N	F	+
19	N	N	F	N	N	N	N	D	+
20	F	N	N	N	N	N	N	N	+
21	N	N	D	N	N	D	D	D	+
22	N	N	F	D	N	N	F	D	+
23	N	N	N	N	N	N	N	D	+
24	N	N	N	N	D	N	N	F	NA
25	N	N	D	D	N	N	N	F	+
26	N	N	D	D	F	N	F	F	+
27	F	N	D	N	N	N	N	N	+
28	F	N	F	F	N	N	N	D	+

N, indicates negative; F, focally positive; D, diffusely positive; NA, data not available.

Table 14 Immunohistochemical results of the Xp11.2 translocation RCCs analyzed.
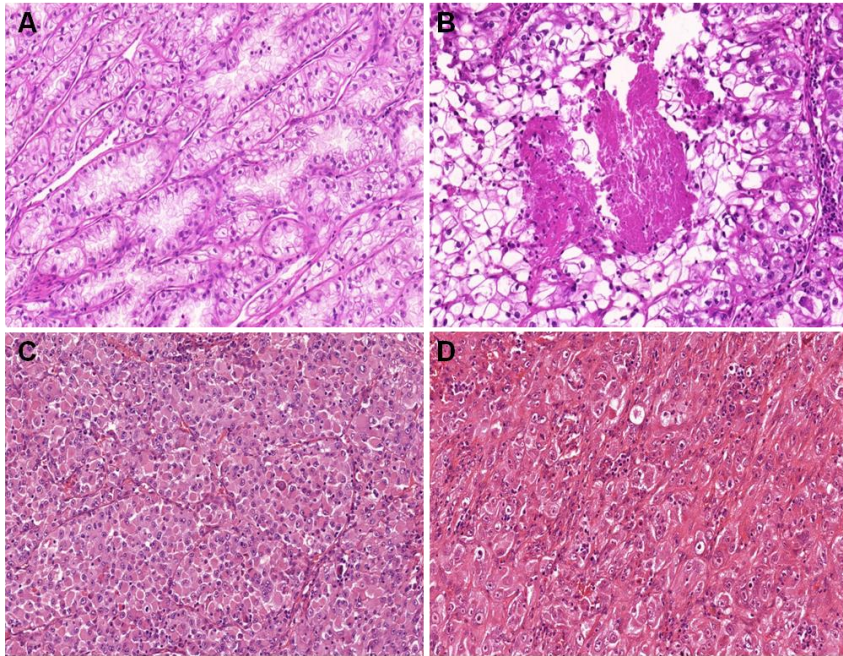
Figure 11 Representative images of Xp11.2 renal cell carcinomas with unusual morphological features. (a) A tubular pattern resembling a low-grade clear cell carcinoma. (b) A solid pattern with foci of comedo-like necrosis. (c) A rhabdoid tumor-like pattern. (d) It has an anaplastic carcinoma appearance. All the images have a magnification factor of 200x.
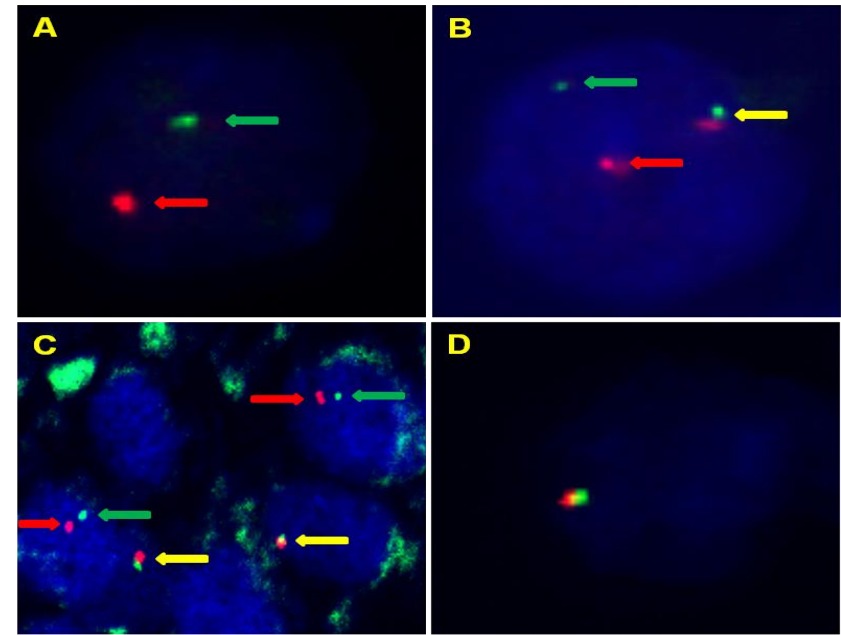
Figure 12 Representative images of the signal patterns seen in the tumors analyzed. (a) We see a pair of split signals (red and green arrows) in a male patient. (b) We see a pair of split signals (red and green arrows) in a female patient. Both images have a magnification factor 2000x. (c) The signals are separated (red and green arrows) but are unusually close to each other and normal fused (yellow arrows) signals are present in lymphocytes (patient 14). (d) The loss of an entire break-point region that was observed in patient #23.

Discussion

Histological Subtypes and Prognostic Factors of RCC According to the 2016 WHO Renal Tumor Classification

Here, our investigation provided three new observations that complement or contradict the corresponding epidemiologic data of RCC. First, our series was characterized by a relatively low incidence of papillary RCC (6.9%). A literature survey on the incidence of RCC in European countries reveals a uniform occurrence rate of approximately 80% for clear cell RCC and a geographical variation for the occurrence of papillary RCC. In the series of 2333 RCCs from Austria, 82.8% were clear cell, 10.9% papillary, 3% chromophobe, 0.3% collecting duct, and 3% unclassified [83]. In the study of 2197 small RCCs (≤ 4 cm) from Germany, the occurrence of clear cell, papillary, chromophobe, and unclassified histology was 84.4%, 10.3%, 4.5%, and 0.8%, respectively [84]. Also, a papillary RCC occurrence rate of 11% was observed in both Italy and Switzerland [85, 86]. In a recent publication from Denmark that focused on incidental renal neoplasms, 16% of the cases were diagnosed with papillary RCC [87]. The reason for the relatively low prevalence of papillary RCC in the Carpathian Basin remains unclear at present. Second, as regards the occurrence of the uncommon subtypes, clear cell papillary and Xp11.2 translocation RCC had a 0.9% and 1.1% prevalence, respectively. Our observation disagrees with those obtained in a much smaller series from the USA, claiming that clear cell papillary RCC should be the fourth most common (4.1%) RCC morphotype [88]. Regrettably, that study did not investigate the race of their patients, and hence a possible racial difference in the occurrence rate of clear cell papillary RCC should not be concluded. Collecting duct RCC or mucinous tubular and spindle cell RCC are very rare subtypes worldwide, and accordingly, these were the rarest in the present series. Third, a surprising finding was the lack of ACKD-associated RCC, which was said to be the most common RCC subtype in end-stage kidneys [89]. In our series, the most frequent subtype was clear cell RCC. In the evaluation of 43 RCCs in the native kidneys of patients who received kidney transplants in Budapest, Hungary, the predominant histological type was clear cell RCC [90]. In a multi-institutional study from Italy and Spain that analyzed the outcomes of RCC in patients with end-stage renal disease, clear cell RCC was similarly the most frequent subtype; and ACKD-associated RCC was not identified at all

[91]. Taken together, these findings do not support at all the statement that ACKD-associated RCC is the most common RCC subtype in end-stage renal disease [16].

Prognostic value of histologic subtypes of RCC

Previous large sample sized studies focusing on the prognostic impact of clear cell, papillary, and chromophobe RCCs provided contradictory results. In the study of Patard et al. [92] on 4063 RCC cases, the 5-year survival rates for localized clear cell, papillary, and chromophobe RCC were around 73.2% (in our cohort 83.4%), 79.4% (in our cohort 81%), and 87.9% (in our cohort 100%), respectively, but the histologic subtypes did not prove to be an independent prognosticator. By contrast, in the study of Leibovich et al. with 3062 RCCs, clear cell RCC subtype remained a significant predictor of cancer-specific death after adjustment for tumor size, stage, and grade [93]. In two studies examining 16957 patients together, the histologic subtype remained an independent prognostic factor in a multivariate model [94, 95].

In the present study, the Kaplan Meier curves explored three, prognostically different groups. The first group, associated with an excellent prognosis, was formed by chromophobe RCC and clear cell papillary RCC. Chromophobe RCC has been described as usually a low-grade neoplasm with little tendency to progress and metastasize, and the reported 5-year survival rates range from 78% to 100% [96, 97]. Regarding clear cell papillary RCC, all our cases were kidney-limited and low-grade tumors, with no evidence of recurrence or metastatic disease in the follow-up period. Clear cell papillary RCC is discussed in more detail below.

The second prognostic group, displaying a fair outcome (5-year survival rate around 80%), comprised papillary RCC and clear cell RCC. Type 1 tumors exhibited a pretty good, 92% 5-year survival rate; these cancers were usually ISUP grade 1 or grade 2 tumors and not outgrown the kidney. In contrast, in type 2 tumors, the 5-year survival rate was just 65%; these cancers were predominantly present with ISUP grade 3 or grade 4 atypia and with locally advanced disease. The third group, displaying a bad prognosis, was observed with cases of unclassified RCCs, Xp11.2 translocation RCCs and collecting duct RCCs. More than half of our cases with unclassified RCC exhibited rhabdoid or sarcomatoid change or giant tumor cells, and the majority spread beyond the kidney; these features are predictors of a dismal prognosis. Xp11.2 translocation and collecting duct RCC have the worst prognosis reportedly, and our corresponding survival data was in accordance with this finding.

Grade and microscopic tumor necrosis as prognostic parameters in clear cell RCC

The survival analysis according to the ISUP grade provided two, statistically different subgroups, namely ISUP 1 plus 2 tumors, characterized by an excellent 5-year survival rate (96%) and ISUP 3 plus 4 tumors, characterized by a much worse survival rate (63%).

Delahunt et al. recently regraded 3017 clear cell RCCs from the Mayo Clinic according to the ISUP grades [39]. The difference in the survival rate between grade 1 and grade 2 groups did not attain a level of significance, and a similar situation was observed in our series. In contrast to our results, however, the survival rates of grade 3 *vs.* grade 4 cancers were significantly different. The reason for the different survival rates in the Szeged and the Mayo series appears to be the difference in the rates of grades: 21.5% and 9% for grade 1, 48.5% and 42% for grade 2, 12.2% and 40% for grade 3, and 17.6% and 9% for grade 4, respectively. The differences in the cases of the grade 1 and grade 3 cancers are significant, with many more grade 1 tumors in Szeged, and many more grade 3 tumors in Rochester. In our cohort, there was no significant difference in the survival rates between cases with grade 1 *vs.* grade 2, and grade 3 *vs.* grade 4 atypia and, therefore, samples with grades 1 and 2, and grades 3 and 4 could be merged to low-grade and high-grade categories. Treating microscopic tumor necrosis as a prognostic parameter multivariate analyses yielded contradictory results [39, 98]. In our study, the multivariate model excluded microscopic tumor necrosis as an independent predictor of survival.

Morphotype and grade as prognostic parameters in papillary RCC

In our series, type 1 tumors exhibited a pretty good, 92% 5-year CSS rate. By contrast, the 5-year CSS rate in type 2 tumors was only 65%. In a multivariate analysis, however, the ISUP grade and stage, but not the morphotype, affected patient outcome. Warrick et al. obtained similar results investigating correlations between tumor grade and histologic characteristics with clinical outcomes in 154 papillary RCCs [99]. In this study, no significant difference was found in survival rates between cases with grade 1 *vs.* grade 2, and grade 3 *vs.* grade 4 atypia, while the 5-year CSS rates in terms of the to the two-tiered grading system revealed a significant difference between the low-grade (95%) and high-grade cases (59%).

Two-tiered grading for clear cell and papillary RCCs

Since in clear cell RCC and papillary RCC there were no difference in survival in ISUP grade 1 and grade 2, and ISUP grade 3 and grade 4 tumors, we have decided to start reporting these subsets as either "low-grade" (ISUP 1 or 2) or "high-grade" (ISUP 3 or 4). Our findings are supported by a recent report published by urologists, who simplified the four-tiered Fuhrman grading system into a low-grade/high-grade scheme, and the prognostic accuracy of the two schemes agreed perfectly in 2415 cases with clear cell RCC [100].

Clinicopathological, Immunohistochemical and Molecular Features of Clear Cell Papillary RCC

In this study, we focused on the discrimination of clear cell papillary RCC from other subtypes by applying the well-known immunohistochemical markers supplemented with molecular analysis that seeks to find chromosomal aberrations and *VHL* abnormalities. We made a formal diagnosis of clear cell papillary RCC when both the immunohistochemical and the genetic tests were in complete accordance with the histology. All the RCC subtypes with clear cell phenotype (e.g., *TFE3* or *TFEB* translocation RCCs [16, 81], *TCEB1*-mutated RCC [73], RCC with 8p monosomy [101], RCC with prominent smooth muscle stroma (RCCSMS) [102-107] and RCC associated with von Hippel-Lindau syndrome) can exhibit a CCPRCC-like morphology [108, 109], but clear cell RCC cases pose the most significant difficulty because this tumor is the most common and it also has some morphological similarities. We performed our case selection based on histological features suggestive of clear cell papillary RCC, and in all cases, the immunophenotype was in full harmony with this diagnosis except in two tumors displaying a CD10-positivity. In terms of genetics, 10 cases harbored a *VHL*-related anomaly, so these were not treated as clear cell papillary RCCs. We accepted the view of Hes et al., who recommended not classifying cases with any *VHL* gene abnormality as clear cell papillary RCC [59]. Based on their approach, our tumors with altered *VHL* status were classified as clear cell RCC. After performing an immunohistochemical and molecular analysis, our selected cases were subdivided into two groups. These are clear cell papillary RCCs (21 cases), and clear cell RCCs with diffuse CK7-positivity (10 cases).

Features of clear cell papillary RCC cases

Here, the characteristic pattern was branching tubulo-acinar that was commonly accompanied by cyst formation, and the papillary pattern was a minor component. A similar observation was obtained by Aydin et al. [79] and Williamson et al. [110], hence the appellation "tubulopapillary" would perhaps be more apt, as was suggested by Aydin [79]. Linear nuclear arrangement away from the basement membrane is regarded as characteristic for clear cell papillary RCC [88]. We observed this phenomenon in 16 clear cell papillary RCCs and 7 clear cell RCCs with diffuse CK7-positivity. Dhakal et al. examined 37 tumors with a morphologic overlap between clear cell papillary RCC and clear cell RCC features, and the linear nuclear arrangement was not seen exclusively in clear cell papillary RCC cases [111]. In another series of clear cell papillary RCCs, Williamson et al. noticed linear nuclear arrangement only in 24/55 cases [112]; therefore, it seems that linear nuclear arrangement is

an overemphasized phenomenon. Another finding considered specific for clear cell papillary RCC is the cup-shaped expression of CA9. We had four tumors with mostly a boxed-shaped staining pattern. Upon reviewing the literature, a cup-shaped expression involving 50% of tumor cells was reported by Rohan et al. in 3/9 cases [113]; and Dhakal et al. noted this pattern in 74% of their cases [111]; but Aydin et al. did not mention this feature at all in their 36 cases [79]. Regarding the immunophenotype of our clear cell papillary RCCs, all tumors showed coexpression of CA9 and CK7. A focal CD10 and AMACR staining was encountered in 2 and 1 case, respectively. The former one raised the possibility of renal angiomyomatous tumor, which is currently considered as a morphologic variant of clear cell papillary RCC. Our clear cell papillary RCC group comprised 19 pT1a, 1 pT1b, and 1 pT3a cases, respectively. To best of our knowledge, this is the first reported case with infiltration outside of the kidney parenchyma. Also, in case #20, the tumor developed in a transplanted kidney. In a recently published review, RCCs arising in kidney grafts were summarized, but among the 48 tumors described, not one was clear cell papillary RCC [114]. All our clear cell papillary RCC cases had an excellent clinical outcome, reinforcing the view that the carcinoma designation might be exaggerated [115].

Features of clear cell RCCs with diffuse CK7-positivity

A series of clear cell RCC with diffuse CK7-positivity was published a decade ago by Mai et al. [116]. Similar to our experiences, these samples were small-sized, and a non-metastatic course was recorded over a mean of a 3-year follow-up; and diffuse CK7-positivity was viewed as the indicator of indolent behavior [117]. Our results provide further clinicopathologic data on this rare subset of clear cell RCC. Accordingly, neither 3p deletion nor other chromosomal anomalies were present. The *VHL* gene sequence analysis revealed pathologic mutations in cases #22, #23, and #31. Since *VHL* mutations were not identified in the non-tumorous renal tissue, the possibility of VHL-disease-associated clear cell RCC was excluded. In seven samples, the histological and immunphenotypic data favored the diagnosis of clear cell papillary RCC; however, the presence of the *VHL* gene promoter hypermethylation abnormality led us to place these samples into the clear cell RCC group (in case #22 a coexisting *VHL* gene mutation was seen, too). After a search for methylation data, only two tumors analyzed were found in the literature out of 400 or so clear cell papillary RCCs [79, 118]. Methylation analyses performed by others in the future may validate our assumption that a *VHL* promoter hypermethylation is definitely not compatible with the diagnosis of clear cell papillary RCC. Every case was in pT1 stage, and there was no progression or recurrence.

Clinicopathological, Immunohistochemical and Molecular Features of Xp11.2 RCC

Here, we reviewed 2804 nephrectomy cases and identified 28 Xp11.2 translocation RCCs. The incidence was low, and in our cohort, it was even lower than the literature data (0.99 vs. 1-4%) [119]. We think that due to the relatively large number of patients studied, the analysis represents the exact frequency of Xp11.2 RCC in Hungary. These tumors were once regarded as childhood malignancies, but because of the significant overlapping features with clear cell and papillary RCC along with the limited cytogenetic data, some authors suggested that the exact frequency is underestimated in adults [120]. In our experience, 12 tumors occurred in less than 40 years, only four tumors affected children, and the oldest patient examined was 72 years old. The previous use of chemotherapy and the association of translocation RCC was reported [121], but in our study, there was no patient with a prior history of malignancy. Discriminating Xp11.2 RCC from other subtypes of RCC is crucial for prognostic and predictive reasons. Recently, it was suggested that patients with Xp11.2 RCC might benefit from mTOR inhibitors [76]. The diagnosis relies on the morphological features, immunohistochemical findings, and molecular pathological analysis, but the latter is the most important because the detection of a *TFE3* rearrangement is essential for a diagnosis of such a tumor. Xp11.2 RCC is usually diagnosed as a sizeable mass in the kidney. The mean size of our tumors (78.5 mm) was larger than that reported in earlier series [60, 120]. In our previous experience, only RCC unclassified and collecting duct carcinoma were larger than Xp11.2 RCC. An invasion of the renal vein or the sinus is quite frequent; we noticed at least one of these in 12 patients. Metastatic spread to the regional lymph nodes or distant organs was observed in 32% cases; seven patients had the nephrectomy at the pM1 stage. Our observations on the rate of pT3/pT4 stage and the occurrence of metastasis are in accordance with the literature data [120]. This late-stage discovery might partly explain the generally poor outcome in Xp11.2 RCC. Microscopically, the predominant growth pattern is papillary, tubular, nested, and mixed, and a striking histological finding is the presence of the psammoma bodies [63, 122]. We saw a different distribution because the most frequent pattern was the solid one, followed by papillary and mixed architecture. Tumors were composed of mainly clear cells in 19 and eosinophilic cells in 7 cases. Also, the simultaneous presence of both cell types was noted in two cases. Psammoma bodies were observed only in 11 cases. Cases with atypical architecture can cause serious diagnostic difficulties; namely, the morphologic spectrum of Xp11.2 RCC is quite broad, and even urothelial cell carcinoma

mimicking translocation RCC was reported as well [81]. In our collection, we had a case mimicking anaplastic carcinoma and another with rhabdoid morphology. Some authors suggested that the specific translocation influences the histological appearance [123]. Xp11.2 RCC is negative with CA9, CK7, and positive with CD10 and AMACR [16]. In our series, both CA9 and CK7 were entirely negative in almost every case except for CA9 in three samples. However, two of these tumors were extensively necrotic, and this is why we concluded that the staining was related to hypoxia of the tumor tissue. Diffuse CD10 labeling was noted in 60% of the cases, while AMACR-positivity was observed only in 50% of the tumors. The expression of MelanA and HMB45 is frequent in *TFEB* translocation RCC, but rare in Xp11.2 translocation RCC [63]. We saw a similar proportion; namely, MelanA and HMB45 were positive only in 4 and 3 tumors, respectively. For the diagnosis of Xp11.2 RCC, the TFE3 immunostaining is the most frequently used method. Earlier, the specificity and sensitivity of the immunohistochemistry were found to be 99.6%, and 97.5% [124], but in some cases, false-negative and false-positive results can be detected as well [125]. Argani et al. suspected that the shorter incubation time with the automated detection system made the TFE3 IHC more sensitive, while the specificity of the reaction decreased. For the false-negative results, some authors showed that this might be caused by preanalytic factors (e.g., fixation time) or by the different analytical methodologies applied (e.g., poor-quality antibodies and inappropriate antigen retrieval) [81, 126]. There were only three tumors (patient #20, #24, and #27) with a TFE3-negativity, and the remaining cases displayed a diffuse and robust nuclear positivity. This is why, in our analysis, the sensitivity of the TFE3 immunohistochemistry correlates with data in the earlier reports [124]. The cysteine protease Cathepsin K is a novel immunohistochemical marker for Xp11.2 RCC, although the expression depends on the fusion partner of the *TFE3* gene, and this explains why it is expressed only in approximately 60% of Xp11.2 RCC [127, 128]. We had only six cases with Cathepsin K-positivity, which is slightly under the reported rate in the literature [81]. This difference might be related to different translocation partners.

A *TFE3* rearrangement can be identified by various methods, namely reverse transcription PCR, cytogenetic karyotyping, FISH analysis, and NGS. In the routine pathology service, the FISH test is the most commonly carried out technic [81, 129], but nowadays, NGS is more and more often used. NGS has a significant advantage because it can also detect the partner gene [130]; although, the influence on the prognosis of the fusion partner is unclear [125]. The *TFE3* break-apart FISH probe was introduced in 2011, and it has since become an indispensable diagnostic tool for Xp11.2 RCC [81, 131]. However, the FISH analysis has its

limitations as well, because poor fixation, inappropriate hybridization, and/or extensive contamination with normal stromal cells can lead to negative results, but an optimized *TFE3* FISH is extremely useful in routine diagnosis and pathology consultation [129]. In our study, the diagnosis was supported by the *TFE3* break-apart FISH analysis in 25 cases. The classic break-apart pattern was observed in 19 tumors, and a truncated signal pattern was noted in 2 cases. In patient #14, the signals were unusually close to each other, and this phenomenon is indicative of intrachromosomal inversion, resulting in *NonO-TFE3* gene fusion [62]. In a female patient, an entire break-point region was utterly missing from the cells due to an atypical translocation. In this case, the histomorphology and immunophenotype were concordant with Xp11.2 RCC. To our knowledge, this is the first report of such a signal pattern in Xp11.2 RCC.

Some authors previously reported that Xp11.2 RCC had an indolent course [132-135]. Camparo et al. calculated a mortality rate of 13.6% for Xp11.2 RCC from their analysis and literature data, although the follow-up period was quite short [120]. In our cohort, the mean follow-up time was 14 months, and, in the meantime, 33% of the patients died from a cancer-related cause. This indicates that Xp11.2 RCC has the same mortality rate as that calculated overall for RCC patients [92].

Conclusions

In our first study, the distribution and prognostic features of RCC subtypes in 928 Hungarian Caucasian patients were analyzed. A relatively low incidence of papillary RCC was observed. Also, Xp11.2 RCC and clear cell papillary RCC exhibited frequencies of 1.1% and 0.9%, respectively. ACKD-associated RCC did not occur in a cohort of 16 end-stage kidney disease with RCC. Immunohistochemistry provides better subtyping of the cases, and in our hands, the panel of CA9, CK7, CD10, AMACR, and TFE3 is quite useful for the daily diagnostic service. For clear cell RCCs and papillary RCCs, low-grade (ISUP grade 1 plus 2) and high-grade groups (ISUP grade 3 and 4) were assigned, and these groups were associated with different survival rates. Lastly, among the pathological prognostic factors in clear cell RCC, microscopic tumor necrosis did not prove to be an independent predictor of outcome.

In the subsequent paper of ours, the immunophenotype and the genetic profile of 31 RCCs composed of clear cells, low-grade nuclei, and a tubulopapillary architecture were investigated. Twenty-one cases were classified as clear cell papillary RCC, and 10 as clear

cell RCC with diffuse CK7-positivity, and the following conclusions were drawn. First, clear cell papillary RCCs rarely exhibit a predominant papillary architecture, hence their name is misleading. Second, a linear nuclear arrangement away from the basement membrane and cup-like CA9-positivity is not essential feature. Third, the evidence for their malignant potential is still lacking. Fourth, RCCs with clear cell papillary RCC morphology, diffuse CK7-positivity, and with an altered *VHL* status do exist; and these tumors can be interpreted as clear cell RCC with diffuse CK7-positivity, and they can be differentiated from clear cell papillary RCCs only by carrying out molecular tests for the *VHL* status. Last but not least, the biological behavior of both clear cell papillary RCCs and clear cell RCCs with diffuse CK7-positivity seems to be indolent with a favorable clinical outcome.

Lastly, we studied 28 Xp11.2 RCC cases by descriptive light-microscopy, a panel of immunohistochemistry, and FISH tests. We had two tumors with a reasonably unusual morphology, one with an anaplastic carcinoma appearance and another with rhabdoid morphology. We observed a unique FISH pattern with the complete loss of the labeled break-point region. The clinical follow-up was not complete for all the patients, but the mean follow-up period was more than 4 years, and it turned out that the prognosis of Xp11.2 RCC in adults is rather poor.

To sum up, we gathered diagnostic experience in both common and rare RCC subsets. This knowledge makes us able to deal with in-house and consultation cases with certainty regardless of the specimen type. By analyzing the validated survival data, we identified prognostic groups according to the histological subsets, and we believe this will facilitate a better patient follow-up and treatment. The investigation of the patient outcomes in clear cell RCC led us to merge the ISUP grade 1 and 2 cases into low-grade and the ISUP grade 3 and 4 cases into high-grade categories. We studied the clear cell papillary and Xp11.2 RCCs firstly in detail in Hungary. We estimated their incidence rate and provided clinicopathological, immunohistochemical as well as genetic data. Regarding the latter two, in our eyes, immunohistochemistry, along with the genetic tests, have an essential rule to discriminate against the overlapping and doubtful entities. Based on our experience, we created a summary table on the RCC subsets.

	CCRCC	PRCC T1	PRCC T2	ChRCC	CCPRCC	Xp11.2 RCC	CDC	MTSCC
Dominant cell type	Clear	Basophilic	Eosinophilic	Eosinophilic	Clear	Clear or eosinophilic	Eosinophilic	Basophilic
Typical architecture	Solid	Papillary, rarely solid	Papillary	Solid	Papillary	Papillary	Tubular or solid	Tubular
Other HE feature(s)	Rich capillary network	Foam cells, low-grade	Foam cells, high-grade	Perinuclear halos	Leiomyomatous stroma	Psammoma bodies	Desmoplasia, inflammatory cells	Mucin
CA9	++	-	-	-	+ (cup-shaped)	+/-	+/-	-
CK7	+/-	++	+/-	++	++	-	++	++
CD10	++	+	+/-	-	-	++	-	+
AMACR	+/-	++	+	-	+/-	+	+	++
Other IHC(s)	Vimentin +	Vimentin +	Vimentin +	CD117 + Vimentin -	Ø	TFE3 +, MelanA +, HMB45 +, Cathepsin K +	p63 -, CK20 -, GATA3 -, *U. europeus* +	Vimentin +
Genetics	-3p, *VHL* mutation and hypermethylation	*c-MET* mutation +7, +17, -Y	Ø specific	Chromosomal losses and gains	No *VHL*-related anomaly	*TFE3* rearrangement	Ø specific	Ø specific, but no +7, +17, -Y

If the histological appearance, immunohistochemistry, and genetic test are inconclusive, but the tumor is positive for PAX8, furthermore, urothelial carcinoma along with metastasis was excluded, the case can be treated as an unclassified RCC.

Table 15 A brief summary of the histological, immunohistochemical and genetic features of the RCC subsets experienced.

Acknowledgments

Firstly, I wish to express special thanks to my supervisor, Béla Iványi for his support and scientific guidance of my work.

Secondly, I am grateful to my closest colleagues Alex Jenei, Áron Somorácz, Boglárka Pósfai, and Adrienn Hajdu. Without their support and help, this thesis would never have been completed.

Thirdly, I am grateful for everyone who contributed my work by sharing their cases, namely Tamás Micsik, Dávid Semjén, Katalin Kóczián, Dániel Imre, Janina Kulka, Zoltán Sápi, and István Sejben.

Finally, I appreciate all the support and love of my family and friends.

References

1.   Capitanio U, Bensalah K, Bex A et al (2019) Epidemiology of Renal Cell Carcinoma. Eur Urol 75:74-84

2.   Tarabeia J, Kaluski DN, Barchana M et al (2010) Renal cell cancer in Israel: sex and ethnic differences in incidence and mortality, 1980-2004. Cancer Epidemiol 34:226–231

3.   Lipworth L, Morgans AK, Edwards TL et al (2016) Renal cell cancer histologic subtype distribution differs by race and sex. BJU Int 117:260–265

4.   Siegel RL, Miller KD, Jemal A (2018) Cancer statistics, 2018. CA Cancer J Clin, 68:7-30

5.   Saad AM, Gad MM, Al-Husseini MJ et al (2019) Trends in Renal-Cell Carcinoma Incidence and Mortality in the United States in the Last 2 Decades: A SEER-Based Study. Clin Genitourin Cancer 17:46-57

6.   Hew MN, Zonneveld R, Kümmerlin IP et al (2012) Age and gender related differences in renal cell carcinoma in a European cohort. J Urol 188:33-38

7.   Kabaria R, Klaassen Z, Terris MK (2016) Renal cell carcinoma: links and risks. Int J Nephrol Renovasc Dis 9:45-52

8.   Hunt JD, van der Hel OL, McMillan GP et al (2005) Renal cell carcinoma in relation to cigarette smoking: meta-analysis of 24 studies. Int J Cancer 114:101-108

9.   Choi Y, Park B, Jeong BC et al (2013) Body mass index and survival in patients with renal cell carcinoma: a clinical-based cohort and meta-analysis Int J Cancer 132:625-634

10.   Pischon T, Lahmann PH, Boeing H et al (2006) Body size and risk of renal cell carcinoma in the European Prospective Investigation into Cancer and Nutrition (EPIC). Int J Cancer 118:728-38

11.   Behrens G, Leitzmann MF (2013) The association between physical activity and renal cancer: systematic review and meta-analysis. Br J Cancer 108:798–811

12.   Lew JQ, Chow WH, Hollenbeck AR et al (2011) Alcohol consumption and risk of renal cell cancer: the NIH-AARP diet and health study. Br J Cancer 104:537–541

13.   Chow WH, Dong LM, Devesa SS (2010) Epidemiology and risk factors for kidney cancer. Nat Rev Urol 7: 245–257

14.   Colt JS, Schwartz K, Graubard BI et al (2011) Hypertension and risk of renal cell carcinoma among white and black americans. Epidemiology 22:797–804

15.   Stewart JH, Vajdic CM, van Leeuwen MT et al (2009) The pattern of excess cancer in dialysis and transplantation. Nephrol Dial Transplant 24:3225-3231

16. Moch H, Humphrey PA, Ulbright TM, Reuter V (2016) WHO Classification of Tumours of the Urinary System and Male Genital Organs. International Agency for Research on Cancer, Lyon

17. Maher ER (2018) Hereditary renal cell carcinoma syndromes: diagnosis, surveillance and management. World J Urol 36:1891–1898

18. Gossage L, Eisen T, Maher ER (2015) VHL, the story of a tumour suppressor gene. Nat Rev Cancer 15:55-64

19. Delahunt B, Srigley JR (2015) The evolving classification of renal cell neoplasia. Semin Diagn Pathol 32:90-102

20. Kovacs G, Akhtar M, Beckwith JB et al (1997) The Heidelberg classification of renal cell tumours. J Pathol 183:131–133

21. Eble JN, Sauter G, Epstein JI, Sesterhenn IA (2004) Pathology and genetics of tumors of the urinary system and male genital organs. International Agency for Research on Cancer, Lyon

22. Srigley JR, Delahunt B, Eble JN et al (2013) The International Society of Urological Pathology (ISUP) Vancouver Classification of Renal Neoplasia. Am J Surg Pathol 37:1469-1489

23. Trpkov K, Hes O (2019) New and emerging renal entities: a perspective post-WHO 2016 classification. Histopathology 74:31-59

24. Delahunt B, Cheville JC, Martignoni G et al (2013) The International Society of Urological Pathology (ISUP) Grading System for Renal Cell Carcinoma and Other Prognostic Parameters. Am J Surg Pathol 37:1490-1540

25. Fuhrman SA, Lasky LC, Limas C (1982) Prognostic significance of morphologic parameters in renal cell carcinoma. Am J Surg Pathol 6:655–663

26. Delahunt B (2009) Advances and controversies in grading and staging of renal cell carcinoma. Mod Pathol 22 Suppl 2:S24–S36

27. Trpkov K, Grignon DJ, Bonsib SM et al (2013) Handling and staging of renal cell carcinoma: the International Society of Urological Pathology Consensus (ISUP) conference recommendations. Am J Surg Pathol 37:1505-1517

28. Brierley JD, Gospodarowicz MK, Wittekind C (2017) TNM Classification of Malignant Tumours, 8th Edition. Wiley-Blackwell, Oxford

29. de Peralta-Venturina M, Moch H, Amin M et al (2001) Sarcomatoid differentiation in renal cell carcinoma. A study of 101 cases. Am J Surg Pathol 25:275–284

30. Shuch B, Bratslavsky G, Linehan WM et al (2012) Sarcomatoid renal cell carcinoma: a comprehensive review of the biology and current treatment strategies. Oncologist 17:46–54

31. Gokden N, Nappi O, Swanson PE et al (2000) Renal cell carcinoma with rhabdoid features. Am J Surg Pathol 24:1329–1338

32. Leroy X, Zini L, Buob L et al (2007) Renal cell carcinoma with rhabdoid features: an aggressive neoplasm with overexpression of p53. Arch Pathol Lab Med 31:102–106

33. Humphrey PA (2011) Renal cell carcinoma with rhabdoid features. J Urol 186:675–676

34. Brinker DA, Amin MB, de Peralta-Venturina M et al (200) Extensively necrotic cystic renal cell carcinoma: a clinicopathologic study with comparison to other cystic and necrotic renal cancers. Am J Surg Pathol 24:988–995

35. Faria V, Surendra T, Poller DN (2005) Prognostic relevance of extensive necrosis in renal cell carcinoma. J Clin Pathol 58:39–43

36. Hemmerlein B, Kugler A, Ozisik R et al (2001) Vascular endothelial growth factor expression, angiogenesis, and necrosis in renal cell carcinomas. Virchows Arch 439:645–652

37. Delahunt B, Bethwaite PB, Thornton A (1997) Prognostic significance of microscopic vascularity for clear cell renal cell carcinoma. Br J Urol 80:401–404

38. Cheville JC, Lohse CM, Zincke H et al (2003) Comparisons of outcomes and prognostic feature among histological subtypes of renal cell carcinoma. Am J Surg Pathol 27:612–624

39. Delahunt B, McKenney JK, Lohse CM et al (2013) A novel grading system for clear cell renal cell carcinoma incorporating tumor necrosis. Am J Surg Pathol 37:311–322

40. Amtrup F, Hansen JB, Thybo E (1974) Prognosis in renal carcinoma evaluated from histological criteria. Scand J Urol Nephrol 8:198–202

41. Kroeger N, Rampersand EN, Patard JJ et al (2012) Prognostic value of microvascular invasion in predicting cancer specific survival and risk of metastatic disease in renal cell carcinoma: a multicenter investigation. J Urol 187:418–423

42. Cho HJ, Kim SJ, Ha US, et al (2009) Prognostic value of capsular invasion for localized clear-cell renal cell carcinoma. Eur Urol 56:1006–1012

43. Ritchie AWS, Chisholm GD (1983) The natural history of renal carcinoma. Semin Oncol 10:390-400

44. Cohen HT, McGorvern FJ (2005) Renal-Cell Carcinoma N Engl J Med 353:2477-2490

45.   Ljungberg B, Hanbury DC, Kuczyk MA et al (2007) Renal cell carcinoma guideline. Eur Urol 51:1502-1510

46.   Niewiadomski D, Acuna CL, Eduardo Morgenfeld EL et al (2017) Incidental vs. clinical diagnosis of renal cell carcinoma (RCC): Population, treatment and outcome in a cohort of 828 patients followed at Instituto Oncológico Henry Moore (IOHM). J Clin Oncology DOI: 10.1200/JCO.2017.35.15_suppl.e16075

47.   Motzer RJ, Bander NH, Nanus DM. (1996) Renal-Cell Carcinoma. N Engl J Med 335: 865–875

48.   Palapattu GS, Kristo B, Rajfer J (2002) Paraneoplastic syndromes in urologic malignancy: the many faces of renal cell carcinoma. Rev Urol 4:163-170

49.   Kovacs G, Erlandsson R, Boldog F et al. (1988) Consistent chromosome 3p deletion and loss of heterozygosity in renal cell carcinoma. Proc Natl Acad Sci USA 85:1571-1575

50.   Latif F, Tory K, Gnarra J and et al (1993) Identification of the von Hippel-Lindau disease tumor suppressor gene. Science 260:1317-20

51.   de Cubas AA, Rathmell WK (2018) Epigenetic modifiers: activities in renal cell carcinoma. Nature Reviews Urology 15:599–614

52.   Batavia AA, Schraml P, Moch H (2019) Clear cell renal cell carcinoma with wild-type von Hippel-Lindau gene: a non-existent or new tumour entity? Histopathology 74:60-67

53.   Pal SK, Ali SM, Yakirevich E et al (2018) Characterization of Clinical Cases of Advanced Papillary Renal Cell Carcinoma via Comprehensive Genomic Profiling. Eur Urol 73:71-78.

54.   Hughson MD, Johnson LD, Silva FG, Kovacs G (1993) Nonpapillary and papillary renal cell carcinoma: a cytogenetic and phenotypic study. Mod Pathol 6:449-456

55.   Peckova K, Martinek P, Sperga M et al (2015) Mucinous spindle and tubular renal cell carcinoma: analysis of chromosomal aberration pattern of low-grade, high-grade, and overlapping morphologic variant with papillary renal cell carcinoma. Ann Diagn Pathol 19:226-231

56.   Saleeb RM, Brimo F, Farag M et al (2017) Toward biological subtyping of papillary renal cell carcinoma with clinical implications through histologic, immunohistochemical, and molecular analysis. Am J Surg Pathol 41:1618-1629

57.   Schraml P, Müller D, Bednar R et al (2000) Allelic loss at the D9S171 locus on chromosome 9p13 is associated with progression of papillary renal cell carcinoma. J Pathol 190:457-461

58.	Brunelli M, Eble JN, Zhang S et al (2005) Eosinophilic and classic chromophobe renal cell carcinomas have similar frequent losses of multiple chromosomes from among chromosomes 1, 2, 6, 10, and 17, and this pattern of genetic abnormality is not present in renal oncocytoma. Mod Pathol 18:161-169

59.	Hes O, Compérat EM, Rioux-Leclercq N (2016) Clear cell papillary renal cell carcinoma, renal angiomyoadenomatous tumor, and renal cell carcinoma with leiomyomatous stroma relationship of 3 types of renal tumors: a review. Ann Diagn Pathol 21:59-64

60.	Argani P, Antonescu CR, Illei PB, Lui MY, Timmons CF et al. (2001) Primary renal neoplasms with the ASPL-TFE3 gene fusion of alveolar soft part sarcoma: a distinctive tumor entity previously included among renal cell carcinomas of children and adolescents. Am J Pathol 159:179–192

61.	Sidhar SK, Clark J, Gill S, Hamoudi R, Crew AJ et al. (1996) The t(X;1)(p11.2;q21.2) translocation in papillary renal cell carcinoma fuses a novel gene PRCC to the TFE3 transcription factor gene. Hum Mol Genet 5:1333–1338

62.	Clark J, Lu YJ, Sidhar SK, Parker C, Gill S et al. (1997) Fusion of splicing factor genes PSF and NonO (p54nrb) to the TFE3 gene in papillary renal cell carcinoma. Oncogene 15:2233–2239

63.	Argani P, Lui MY, Couturier J, Bouvier R, Fournet JC et al. (2003) A novel CLTC-TFE3 gene fusion in pediatric renal adenocarcinoma with t(X;17)(p11.2;q23). Oncogene 22:5374–5378

64.	Pei J, Cooper H, Flieder DB et al. (2019) NEAT1-TFE3 and KAT6A-TFE3 renal cell carcinomas, new members of MiT family translocation renal cell carcinoma. Mod Pathol 32:710-716

65.	Trpkov K, Hes O, Agaimy A et al (2016) Fumarate hydratase-deficient renal cell carcinoma is strongly correlated with fumarate hydratase mutation and hereditary leiomyomatosis and renal cell carcinoma syndrome. Am J Surg Pathol 40:865-875

66.	Gill AJ, Pachter NS, Clarkson A et al (2011) Renal tumors and hereditary pheochromocytoma-paraganglioma syndrome type 4. N Engl J Med 364:885-886

67.	Beckermann KE, Sharma D1, Chaturvedi S et al (2017) Renal Medullary Carcinoma: Establishing Standards in Practice. J Oncol Pract 13:414-421

68.	Lawrie CH, Armesto M, Fernandez-Mercado M et al (2018) Noncoding RNA Expression and Targeted Next-Generation Sequencing Distinguish Tubulocystic Renal Cell Carcinoma (TC-RCC) from Other Renal Neoplasms. J Mol Diagn. 20:34-45

69. Selli C, Amorosi A, Vona G et al (1997) Retrospective evaluation of c-erbB-2 oncogene amplification using competitive PCR in collecting duct carcinoma of the kidney. J Urol 158:245-247

70. Pal SK, Choueiri TK, Wang K et al (2016) Characterization of Clinical Cases of Collecting Duct Carcinoma of the Kidney Assessed by Comprehensive Genomic Profiling. Eur Urol 70:516-521

71. Wang J, Papanicolau-Sengos A, Chintala S et al (2016) Collecting duct carcinoma of the kidney is associated with CDKN2A deletion and SLC family gene up-regulation. Oncotarget 7:29901-29915

72. Kusano H, Togashi Y, Akiba J et al (2016) Two cases of renal cell carcinoma harboring a novel STRN-ALK fusion gene. Am J Surg Pathol 40:761-769

73. Hakimi AA, Tickoo SK, Jacobsen A et al (2015) TCEB1-mutated renal cell carcinoma: a distinct genomic and morphological subtype. Mod Pathol 28:845-853

74. Sato Y, Yoshizato T, Shiraishi Y et al (2013) Integrated molecular analysis of clear-cell renal cell carcinoma. Nat Genet 45:860-867

75. Ljungberg B, Albiges L, Abu-Ghanem Y et al (2019) European Association of Urology Guidelines on Renal Cell Carcinoma: The 2019 Update. Eur Urol 75:799-810

76. Powles T, Albiges L, Staehler M et al (2018) Updated European Association of Urology guidelines recommendations for the treatment of first-line metastatic clear cell renal cancer Eur Urol 73:311-315

77. Giubellino A, Linehan WM, Bottaro DP (2009) Targeting the Met signaling pathway in renal cancer. Expert Rev Anticancer Ther 9:785-793

78. Motzer RJ, Tannir NM, McDermott DF et al (2018) Nivolumab plus ipilimumab versus sunitinib in advanced renal-cell carcinoma N Engl J Med 378:1277-1290

79. Aydin H, Chen L, Cheng L et al (2010) Clear cell tubulopapillary renal cell carcinoma: a study of 36 distinctive low-grade epithelial tumors of the kidney. Am J Surg Pathol 34:1608-1621

80. Fallon KB, Palmer CA, Roth KA et al (2004) Prognostic value of 1p, 19q, 9p, 10q, and EGFR-FISH analyses in recurrent oligodendrogliomas. J Neuropathol Exp Neurol 63:314-322

81. Rao Q, Williamson SR, Zhang S et al. (2013) TFE3 break-apart FISH has a higher sensitivity for Xp11.2 translocation-associated renal cell carcinoma compared with TFE3 or cathepsin K immunohistochemical staining alone: expanding the morphologic spectrum. Am J Surg Pathol 37:804-815

82.   Herman JG, Graff JR, Myohanen S et al (1996) Methylation-specific PCR: a novel PCR assay for methylation status of CpG islands. Proc Natl Acad Sci USA 93:9821–9826

83.   Pichler M, Hutterer GC, Chromecki TF et al (2012) Renal cell carcinoma stage migration in a single European centre over 25 years: effects on 5- and 10-year metastasis-free survival. Int Urol Nephrol 44:997-1004

84.   Steffens S, Junker K, Roos FC et al (2014) Small renal cell carcinomas--how dangerous are they really? Results of a large multicenter study. Eur J Cancer 50:739-745

85.   Novara G, Ficarra V, Antonelli A et al (2010) Validation of the 2009 TNM version in a large multi-institutional cohort of patients treated for renal cell carcinoma: are further improvements needed? Eur Urol 58:588-595

86.   Moch H, Gasser T, Amin MB, Torhorst J et al (2000) Prognostic utility of the recently recommended histologic classification and revised TNM staging system of renal cell carcinoma: a Swiss experience with 588 tumors. Cancer 89:604-61

87.   Rabjerg M, Mikkelsen MN, Walter S et al (2014) Incidental renal neoplasms: is there a need for routine screening? A Danish single-center epidemiological study. APMIS 122:708-14

88.   Zhou H, Zheng S, Truong LD et al (2014) Clear cell papillary renal cell carcinoma is the fourth most common histologic type of renal cell carcinoma in 290 consecutive nephrectomies for renal cell carcinoma. Hum Pathol 45:59-64

89.   Tickoo SK, dePeralta-Venturina MN, Harik LR et al (2006) Spectrum of epithelial neoplasms in end-stage renal disease: an experience from 66 tumor-bearing kidneys with emphasis on histologic patterns distinct from those in sporadic adult renal neoplasia. Am J Surg Pathol 30:141-153

90.   Végső G, Toronyi E, Hajdu M et al (2011) Renal cell carcinoma of the native kidney: a frequent tumor after kidney transplantation with favorable prognosis in case of early diagnosis. Transplant Proc 43:1261-1264.

91.   Breda A, Luccarelli G, Rodriguez-Faba O et al (2015) Clinical and pathological outcomes of renal cell carcinoma (RCC) in native kidneys of patients with end-stage renal disease: a long-term comparative retrospective study with RCC diagnosed in the general population. World J Urol 33:1-7

92.   Patard JJ, Leray E, Rioux-Leclercq N, Cindolo L et al (2005) Prognostic value of histologic subtypes in renal cell carcinoma: a multicenter experience. J Clin Oncol 23:2763-2771

93.   Leibovich BC, Lohse CM, Crispen PL, Boorjian SA, Thompson RH, Blute ML, Cheville JC (2010) Histological subtype is an independent predictor of outcome for patients with renal cell carcinoma. J Urol 183:1309-1315

94.   Capitanio U, Cloutier V, Zini L et al (2009) A critical assessment of the prognostic value of clear cell, papillary and chromophobe histological subtypes in renal cell carcinoma: a population-based study. BJUI 103:1496-1500

95.   Novara G, Ficarra V, Antonelli A et al (2010) Validation of the 2009 TNM version in a large multi-institutional cohort of patients treated for renal cell carcinoma: are further improvements needed? Eur Urol 58:588-595

96.   Volpe A, Novara G, Antonelli A et al (2012) Chromophobe renal cell carcinoma (RCC): oncological outcomes and prognostic factors in a large multicentre series. BJU Int 110:76-83

97.   Frees S, Kamal MM, Knoechlein L et al (2016) Differences in overall and cancer-specific survival of patients presenting with chromophobe versus clear cell renal cell carcinoma: a propensity score matched analysis. Urology 98:81-87

98.   Frank I, Blute ML, Cheville JC et al (2002) An outcome prediction model for patients with clear cell renal cell carcinoma treated with radical nephrectomy based on tumor stage, size, grade and necrosis: the SSIGN score. J Urol 168:2395-2400

99.   Warrick JI, Tsodikov A, Kunju LP et al (2012) Papillary renal cell carcinoma revisited: a comprehensive histomorphologic study with outcome correlations. Hum Pathol. 45:1139-1146

100.   Becker A, Hickmann D, Hansen J et al (2016) Critical analysis of a simplified Fuhrman grading scheme for prediction of cancer specific mortality in patients with clear cell renal cell carcinoma--Impact on prognosis. Eur J Surg Oncol 42:419-425.

101.   Lan TT, Keller-Ramey J, Fitzpatrick C et al (2016) Unclassified renal cell carcinoma with tubulopapillary architecture, clear cell phenotype, and chromosome 8 monosomy: a new kid on the block. Virchows Arch 469:81-91

102.   Canzonieri V, Volpe R, Gloghini A et al (1993) Mixed renal tumor with carcinomatous and fibroleiomyomatous components, associated with angiomyolipoma in the same kidney. Pathol Res Pract 189:951-956

103.   Martignoni G, Brunelli M, Segala D et al (2014) Renal cell carcinoma with smooth muscle stroma lacks chromosome 3p and VHL alterations. Mod Pathol 27:765–774

104.   Petersson F, Branzovsky J, Martinek P et al (2014) The leiomyomatous stroma in renal cell carcinomas is polyclonal and not part of the neoplastic process. Virchows Arch 465:89–96

105.   Kuhn E, De Anda J, Manoni S et al (2006) Renal cell carcinoma associated with prominent angioleiomyoma-like proliferation: Report of 5 cases and review of the literature. Am J Surg Pathol 30:1372-1381

106.   Shannon BA, Cohen RJ, Segal A et al (2009) Clear cell renal cell carcinoma with smooth muscle stroma. Hum Pathol 40:425-429

107.   Petersson F, Martinek P, Vanecek T et al (2018) Renal cell carcinoma with leiomyomatous stroma: a group of tumors with indistinguishable histopathologic features, but 2 distinct genetic profiles: next-generation sequencing analysis of 6 cases negative for aberrations related to the VHL gene. Appl Immunohistochem Mol Morphol 26:192-197

108.   Williamson SR, Zhang S, Eble JN et al (2013) Clear cell papillary renal cell carcinoma–like tumors in patients with von Hippel-Lindau disease are unrelated to sporadic clear cell papillary renal cell carcinoma. Am J Surg Pathol 37:1131-1139

109.   Rao P, Monzon F, Jonasch E et al (2014) Clear cell papillary renal cell carcinoma in patients with von Hippel-Lindau syndrome--clinicopathological features and comparative genomic analysis of 3 cases. Hum Pathol 45:1966-1972

110.   Williamson SR, Eble JN, Cheng L et al (2013) Clear cell papillary renal cell carcinoma: differential diagnosis and extended immunohistochemical profile. Mod Pathol 26:697-708

111.   Dhakal HP, McKenney JK, Khor LY et al (2016) Renal neoplasms with overlapping features of clear cell renal cell carcinoma and clear cell papillary renal cell carcinoma: a clinicopathologic study of 37 cases from a single institution. Am J Surg Pathol 40:141-154

112.   Williamson SR, Gupta NS, Eble JN et al (2015) Clear cell renal cell carcinoma with borderline features of clear cell papillary renal cell carcinoma: combined morphologic, immunohistochemical, and cytogenetic analysis. Am J Surg Pathol 39:1502-1510

113.   Rohan SM, Xiao Y, Liang Y et al (2011) Clear-cell papillary renal cell carcinoma: molecular and immunohistochemical analysis with emphasis on the von Hippel-Lindau gene and hypoxia-inducible factor pathway-related proteins. Mod Pathol 24:1207-1220

114.   Dhakal P, Giri S, Siwakoti K et al (2017) Renal cancer in recipients of kidney transplant. rare tumors 9:6550

115.   Massari F, Ciccarese C, Hes O et al (2018) The tumor entity denominated "clear cell-papillary renal cell carcinoma" according to the WHO 2016 new classification, have the

clinical characters of a renal cell adenoma as does harbor a benign outcome. Pathol Oncol Res 24:447-456

116.   Mai KT, Kohler DM, Belanger EC et al (2008) Sporadic clear cell renal cell carcinoma with diffuse cytokeratin 7 immunoreactivity. Pathology 40:481-486

117.   Mertz KD, Demichelis F, Sboner A et al (2008) Association of cytokeratin 7 and 19 expression with genomic stability and favorable prognosis in clear cell renal cell cancer. Int J Cancer 123:569-576

118.   Diolombi ML, Cheng L, Argani P et al (2015) Do Clear Cell Papillary Renal Cell Carcinomas Have Malignant Potential? Am J Surg Pathol 39:1621-1634

119.   Komai Y, Fujiwara M, Fujii Y et al (2009) Adult Xp11 translocation renal cell carcinoma diagnosed by cytogenetics and immunohistochemistry. Clin Cancer Res 15:1170-1176

120.   Camparo P, Vasiliu V, Molinie V et al (2008) Renal translocation carcinomas: clinicopathologic, immunohistochemical, and gene expression profiling analysis of 31 cases with a review of the literature. Am J Surg Pathol 32:656-670

121.   Argani P, Laé M, Ballard ET, Amin M, Manivel C et al (2006) Translocation carcinomas of the kidney after chemotherapy in childhood. J Clin Oncol 24:1529-1534

122.   Argani P, Antonescu CR, Couturier J et al (2002) PRCC-TFE3 renal carcinomas: morphologic, immunohistochemical, ultrastructural, and molecular analysis of an entity associated with the t(X;1)(p11.2;q21). Am J Surg Pathol 26:1553-1566

123.   Argani P, Ladanyi M (2005) Translocation carcinomas of the kidney. Clin Lab Med 25:363-378

124.   Argani P, Lal P, Hutchinson B et al (2003) Aberrant nuclear immunoreactivity for TFE3 in neoplasms with TFE3 gene fusions: a sensitive and specific immunohistochemical assay. Am J Surg Pathol 27:750-761

125.   Ellis CL, Eble JN, Subhawong AP et al (2014) Clinical heterogeneity of Xp11 translocation renal cell carcinoma: impact of fusion subtype, age, and stage. Mod Pathol 27:875-886

126.   Argani P, Aulmann S, Illei PB et al (2010) A distinctive subset of PEComas harbors TFE3 gene fusions. Am J Surg Pathol 34:1395-1406

127.   Martignoni G Gobbo S, Camparo P et al (2011) Differential expression of cathepsin K in neoplasms harboring TFE3 gene fusions. Mod Pathol 24:1313-1319

128. Martignoni G, Pea M, Gobbo S et al (2009) Cathepsin-K immunoreactivity distinguishes MiTF/TFE family renal translocation carcinomas from other renal carcinomas. Mod Pathol 22:1016-1022

129. Green WM, Yonescu R, Morsberger L et al (2013) Utilization of a TFE3 break-apart FISH assay in a renal tumor consultation service. Am J Surg Pathol 37:1150-1163

130. Pei J, Cooper H, Flieder DB et al (2019) NEAT1-TFE3 and KAT6A-TFE3 renal cell carcinomas, new members of MiT family translocation renal cell carcinoma. Mod Pathol 32:710-716

131. Mosquera JM, Dal Cin P, Mertz KD et al (2011) Validation of a TFE3 break-apart FISH assay for Xp11.2 translocation renal cell carcinomas. Diagn Mol Pathol 20:129-137

132. Argani P, Ladanyi M (2003) Distinctive neoplasms characterised by specific chromosomal translocations comprise a significant proportion of the paediatric renal carcinomas. Pathology 35:492-498

133. Dal Cin P, Stas M, Sciot R et al (1998) Translocation (X;1) reveals metastasis 31 years after renal cell carcinoma. Cancer Genet Cytogenet 101:58-61

134. Perot C, Bougaran J, Boccon-Gibod L et al (1999) Two new cases of papillary renal cell carcinoma with t(X;1)(p11;q21) in females. Cancer Genet Cytogenet 110:54-56

135. Rais-Bahrami S, Drabick JJ, De Marzo AM et al (2007) Xp11 translocation renal cell carcinoma: delayed but massive and lethal metastases of a chemotherapy-associated secondary malignancy. Urology 70:178e3-e6

Prognostic Factors for Renal Cell Carcinoma Subtypes Diagnosed According to the 2016 WHO Renal Tumor Classification: a Study Involving 928 Patients

Levente Kuthi[1] · Alex Jenei[1] · Adrienn Hajdu[1] · István Németh[2] · Zoltán Varga[3] ·
Zoltán Bajory[4] · László Pajor[4] · Béla Iványi[1]

Abstract The morphotype and grade of renal cell carcinoma (RCC) in 928 nephrectomies were reclassified according to the 2016 WHO classification in order to analyze the distribution and outcomes of RCC subtypes in Hungary, to assess whether microscopic tumor necrosis is an independent prognostic factor in clear cell RCC, and to study whether a two-tiered grading (low/high) for clear cell and papillary RCC provides similar prognostic information to that of the four-tiered ISUP grading system. 83.4% of the cohort were clear cell, 6.9% papillary, 4.5% chromophobe, 2.3% unclassified, 1.1% Xp11 translocation, 1.1% clear cell papillary, 0.3% collecting duct and 0.1% mucinous tubular and spindle cell RCCs. RCC occurred in 16 patients with end-stage kidney disease and none of them displayed features of acquired cystic kidney disease-associated RCC. The 5-year survival rates were as follows: chromophobe 100%, clear cell papillary 100%, clear cell low-grade 96%, papillary type 1 92%, clear cell high-grade 63%, papillary type 2 65%, unclassified 46%, Xp11 translocation 20%, and collecting duct 0%. The 5-year survival rates in low-grade and high-grade papillary RCC were 95% and 59%, respectively. In clear cell RCC, only the grade, the stage and the positive surgical margin proved to be

independent prognostic factors statistically. Overall, papillary RCC occurred relatively infrequently; microscopic tumor necrosis in clear cell RCC did not predict the outcome independently of the tumor grading; and the assignment of clear cell and papillary RCCs into low-grade or high-grade tumors was in terms of survival no worse than the ISUP grading.

Keywords Renal cell carcinoma · ISUP grading ·
Microscopic tumor necrosis · Survival rates · Prognostic factors

Introduction

The diagnostic categories of the 2016 WHO Renal Tumor Classification was largely elaborated by the International Society of Urological Pathology (ISUP) consensus conference held in Vancouver, Canada in 2012 [1, 2]. The conference made recommendations on classification, prognostic factors, staging, and immunohistochemical and molecular evaluation of renal cell carcinoma (RCC) [2–4]. 5 new entities were recognized. A new grading system was formulated with the intention of replacing the Fuhrman's grading system, which has problems with the interpretation, validation and reproducibility [3, 5]. The incorporation of microscopic tumor necrosis in clear cell RCC as a grading parameter was also proposed, but it was agreed that further confirmatory studies were required [6].

In the present study, the distribution and outcomes of RCC morphotypes were analyzed in a set of Hungarian patients in accordance with the 2016 WHO Renal Tumor Classification in order to obtain reference data for the prevalence and cancer-specific survival (CSS) of the traditional and new entities in the south-eastern, non-industrialized region of Hungary, populated entirely by Caucasians. Since the prognostic

✉ Levente Kuthi
  kuthi.levente@med.u-szeged.hu

[1] Department of Pathology, University of Szeged, Állomás Street 1, Szeged H-6725, Hungary

[2] Department of Dermatology and Allergology, University of Szeged, Korányi Alley 6, Szeged H-6720, Hungary

[3] Department of Oncotherapy, University of Szeged, Korányi Alley 12, Szeged H-6720, Hungary

[4] Department of Urology, University of Szeged, Kálvária Lane 57, Szeged H-6725, Hungary

significance of microscopic tumor necrosis in clear cell RCC has not yet been resolved, its presence relative to sarcomatoid/rhabdoid differentiation, tumor grade, TNM stage and surgical margin involvement was investigated using statistical methods in order to see whether it has an independent impact on CSS. Furthermore, the prognostic ability of a two-tiered grading system for clear cell RCC and papillary RCC was tested in order to conclude whether the simplification of the four-tiered ISUP grading system to a two-tiered grading system can be used in reporting RCCs.

Material and Methods

Review Process

Between 1st January 1990 and 31th December 2015, 843 radical and 85 partial nephrectomies for RCC were evaluated in our department. The pathology reports and the hematoxylin and eosin-stained slides were reviewed. Later the cases were regraded according to the recommendations of the consensus conference, and samples requiring immunostainings were selected [4].

Immunohistochemical Support for the Diagnosis

Carbonic anhydrase IX, cytokeratin 7 (CK7), alpha-methylacyl-CoA racemase, CD117, transcription factor E3 (TFE3), HMB-45 and *Ulex europaeus* agglutinin 1 immunostainings were applied in panels on tissue microarray slides of samples taken (2 cores/case) from 474 cases with overlapping light microscopical features. The histomorphology and the typical immunoprofile of the tumor served to clarify the diagnosis [2, 4, 7–9]. If the light microscopical appearance and the immunoprofile of the tumor did not allow the case to be assigned to the recognized categories, unclassified RCC was diagnosed.

Fluorescence in Situ Hybridization (FISH) Assays

The histological diagnosis of Xp11 translocation RCC was confirmed by Zyto*Light*® SPEC TFE3 Dual Color Break Apart Probe [4], considered positive if more than 10% of the tumor cells displayed a split signal. The diagnosis of clear cell papillary RCCs was supported by the lack of chromosome 3p loss (characteristic for clear cell RCCs), and the lack of trisomy of chromosomes 7 and 17 and Y chromosome loss (feature of papillary RCCs), looked for with appropriate probes (Cytocell Chromosome 7, 17 and Y Alpha Satellite Probes, Zyto*Light*® SPEC VHL/CEN3 Dual Color Probe) [10].

Pathological Features Evaluated

The ISUP nucleolar grade, the TNM stage amended according to the seventh edition, the surgical margin status, and features of nuclear pleiomorphism (i.e. sarcomatoid differentiation, rhabdoid change, and multinucleated giant tumor cells) were assessed [3, 11]. The highest grade occupying at least 1 high-power field determined the grade of the tumor. During the sampling of microscopic tumor necrosis in clear cell RCC, the extent of necrosis was not given a score.

Estimation of CSS

The duration of follow-up was calculated from the date of the surgical treatment to the date of death or the last follow-up. The CSS was analyzed only in patients with clinical M0 disease determined by imaging modalities at the time of the surgery. CSS was estimated by using the Kaplan-Meier method, and compared among groups via log rank tests. Deaths from causes other than RCC were censored. Univariate and multivariate Cox proportional hazard regression models served to estimate the degree of the association of the RCC histological subtype with the patient outcome, as shown by the HR and 95% CI. The statistical analyses were performed using the SPSS software package ($p > 0.05$).

Results

The clinicopathological features of the different subtypes are summarized in Table 1. The series comprised 28 extensively cystic carcinomas. 25 cases were reclassified as clear cell RCC, 2 as multilocular cystic clear cell renal cell neoplasm of low malignant potential, and 1 as clear cell papillary RCC. RCC occurred in 16 patients with end-stage kidney disease. The following morphotypes were encountered: clear cell on 11 occasions, papillary type 1 on 3 occasions and clear cell papillary on 2 occasions. Although the features of acquired cystic kidney disease (ACKD) were observed in 9 end-stage kidneys with RCC, the histological evaluation did not lead to the suspicion of ACKD-associated RCC in any of these cases. As for synchronous tumors, clear cell RCC and papillary RCC type 1 in the same kidney were recorded in 2 patients, and clear cell RCC and oncocytoma in 1 patient. Bilateral clear cell RCC occurred in 3 patients, one of whom had end-stage kidney disease.

Clear Cell RCC

Among the 253 (27%) high-grade carcinomas, the transition of low-grade tumor cells to high-grade tumor cells was commonly observed; and purely high-grade clear cell RCC was noted in 60 (7.7%) cases. 4 samples exhibited microscopic

Table 1 Clinicopathological features in different subtypes of renal cell carcinoma

		Clear cell	Papillary T1	Papillary T2	Chromophobe	Unclassified	Xp11 translocation	Clear cell papillary	Collecting duct	Mucinous tubular
Number of cases (%)		774 (83.4)	37 (3.9)	28 (3.0)	42 (4.5)	22 (2.3)	10 (1.1)	10 (1.1)	4 (0.4)	1 (0.1)
Age (years)	Median, range	61, 25–84	62, 12–79	62.5, 39–78	58, 17–74	63, 30–77	55, 15–72	50, 32–78	62, 49–69	68
Male:female ratio		1.5:1	3.1:1	2.1:1	0.82:1	2.6:1	2.3:1	1.5:1	1:1	female
Right:left ratio		1.09:1	0.89:1	1:1	1.21:1	0.69:1	0.25:1	1:1	0.33:1	right
Size (mm)	Median, range	55, 10–220	43.5, 10–150	60, 9–170	50, 14–170	86.5, 34–173	90, 25–160	30, 10–65	92, 55–140	40
ISUP grade	G1	157	3	0	not graded	0	1	9	0	1
	G2	364	29	7	not graded	5	3	1	0	0
	G3	99	2	15	not graded	8	0	0	0	0
	G4	154	3	6	not graded	9	6	0	4	0
Microscopic tumor necrosis		221	11	21	3	19	6	0	3	0
Rhabdoid and/or sarcomatoid		117	3	3	0	9	5	0	2	0
Giant tumor cells		105	3	1	0	2	0	0	0	0
Surgical margin positivity		37	1	2	0	0	2	0	2	0
Postoperative tumor stage	pT1a	215	16	7	13	1	2	9	0	1
	pT1b	147	7	3	9	3	1	1	0	0
	pT2a	49	5	4	6	1	1	0	0	0
	pT2b	18	3	1	8	1	0	0	0	0
	pT3a	297	6	10	6	13	2	0	2	0
	pT3b	16	0	0	0	2	1	0	0	0
	pT3c	9	0	0	0	0	0	0	0	0
	pT4	23	0	3	0	1	3	0	2	0
Lymph node involvement	N1	29	2	5	0	4	2	0	1	0
Distant metastases	M1	39	0	2	0	1	1	0	1	0
TNM stage groupings	I	356	23	10	22	3	3	10	0	1
	II	63	7	5	14	2	1	0	0	0
	III	301	7	9	6	14	3	0	1	0
	IV	54	0	4	0	2	3	0	3	0

tumor necrosis in the grade 1 group, 28 in the grade 2 group, 65 in the grade 3 group, and 124 in the grade 4 group.

Papillary RCC

A combination of features of both histologic subtypes was present in 5 samples and these were assigned according to the predominant histological pattern. Type 1 carcinomas were essentially of low-grade; while type 2 carcinomas were mostly of high-grade

Chromophobe RCC

In 5 cases with predominantly eosinophilic cells, the possibility of oncocytoma was excluded by the diffuse membranous CD117 and diffuse cytoplasmic CK7 reactivity of the tumor cells, along with the positivity of the Hale colloidal iron staining.

Xp11 Translocation RCC

The labeling for TFE3 protein was diffuse in 8 samples, and focal in 2 samples. The FISH assay confirmed *TFE3* gene fusion in every case.

Clear Cell Papillary RCC

All of the tumors were in stage pT1. The FISH assay supported the histopathological diagnosis in each case.

Collecting Duct RCC

All of the tumors were in an advanced stage, the main part of the tumor being centered in the medulla. The *Ulex europaeus* staining revealed diffuse positivity in 2 cases and focal positivity in 1 case.
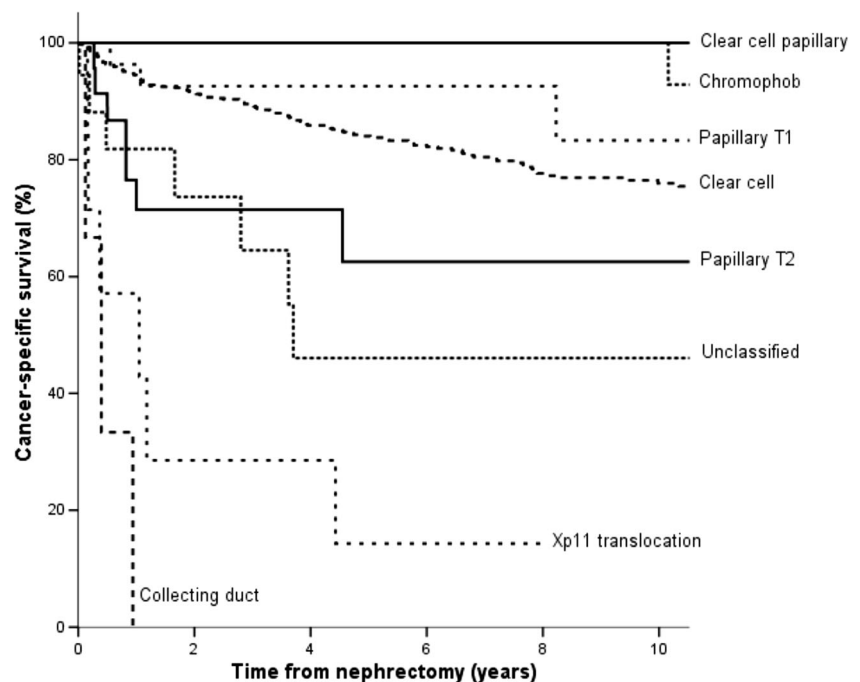
Mucinous Tubular and Spindle RCC

The patient did not have any evidence of disease recurrence or metastatic dissemination during the 15 month follow-up period.

Unclassified RCC

The majority of cases proved to be high-grade carcinomas.

Correlation between the Morphotype and CSS

Follow-up data sets were accessible for 804 patients (763 non-metastatic and 41 metastatic diseases at the time of surgery). 131 patients with clear cell RCC, 3 patients with type 1 papillary RCC, 7 patients with type 2 papillary RCC, 7 patients with unclassified RCC, 6 patients with Xp11 translocation RCC, and 3 patients with collecting duct RCC had died from an RCC-related cause. The median follow-up of these patients was 29 months (range 1–254 months), whereas the median follow-up for all survivors was 68 months (range 2–313 months). The CSS rates of histological types are shown in Fig. 1. The 5-year CSS was significantly different between patients with clear cell RCC and with chromophobe RCC ($p = 0.021$) or with unclassified RCC ($p < 0.001$) or with

Fig. 1 Cancer-specific survival rates of 763 non-metastatic patients with RCC based on histologic subtype. A 100% 5-year survival rate was observed for clear cell papillary RCC and chromophobe RCC. Clear cell RCCs had an 83.4%, papillary RCCs an 81%, unclassified RCCs a 46%, Xp11 translocation RCCs a 20%, and collecting duct RCCs a 0% 5-year survival rate

Xp11 translocation RCC ($p < 0.001$), but not between patients with clear cell RCC and those with papillary RCC ($p = 0.39$). Although the statistical significance in survival rates could not be calculated between clear cell RCC and clear cell papillary RCC or collecting duct RCC because of the limited number of cases in the latter entities, the Kaplan Meyer curves leave no doubt that these entities represent a quite different outcome.

Among the 90 patients with non-metastatic clear cell RCC at the time of nephrectomy and who died from an RCC-related cause, 18 patients received tyrosine-kinase inhibitors. Although the average survival time was longer in the treated group (5.9 years vs 4.5 years), this did not affect CSS significantly ($p = 0.271$); hence, the treatment of metastatic disease did not conflict with what the survival data tell us in Fig. 1.

Grade and Microscopic Tumor Necrosis in Clear Cell RCC

CSS rates according to the four-tiered ISUP grade and the two-tiered grade assessment are shown in Fig. 2. A higher TNM stage predicted a significantly poorer prognosis (see Table 2). When CSS according to the presence or absence of microscopic tumor necrosis was analyzed, the necrotic tumors exhibited a significantly poorer outcome than the non-necrotic tumors ($p < 0.001$; not shown). When the presence or absence of tumor necrosis was tested in patients with low-grade tumors vs high-grade tumors (Fig. 3), necrosis was associated with a significantly poorer outcome only in high-grade tumors. In

univariate Cox proportional hazard analysis, the ISUP grade, TNM stage, tumor necrosis, giant tumor cells, rhabdoid/sarcomatoid morphology and positive surgical margins all proved to be negative predictors of CSS. In multivariate Cox proportional hazards analysis, however, only the ISUP grade, TNM stage and positive surgical margin turned out to be independent prognostic factors (Table 2).

Subtypes and Grade in Papillary RCC

The 5-year CSS rates in type 1 and type 2 subtypes are shown in Fig. 4. When the 5-year CSS was calculated according to the ISUP grade, 100% was observed for grade 1, 94% for grade 2, 74% for grade 3 and 33% for grade 4 samples, respectively. The 5-year survival rate was significantly better for patients with grade 2 tumors than for those with grade 3 tumors ($p = 0.011$). The sample size in grade 1 tumors did not allow a comparison of survival rates between those with grade 1 and grade 3 tumors. However, there was no significant difference in survival rates between cases with grade 1 vs grade 2 ($p = 0.696$), and grade 3 vs grade 4 ($p = 0.445$); and, therefore, samples with grades 1 and 2, and grades 3 and 4 were merged to low-grade and high-grade categories. The 5-year CSS rates according to the two-tiered grading system exhibited a significant difference; namely 95% for low-grade tumors and 59% for high-grade tumors (Fig. 4). In a Cox proportional hazard analysis, the ISUP grade and TNM stage, but not the
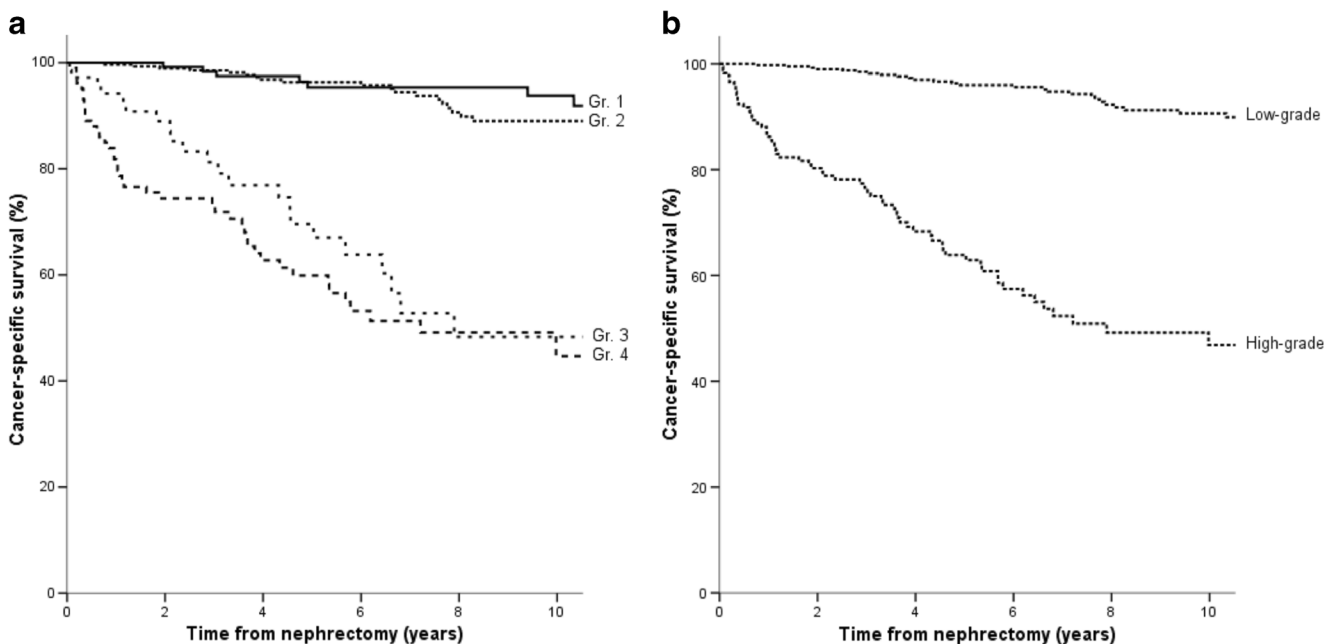
Fig. 2 Cancer-specific survival in clear cell RCC according to the ISUP grading system. **a** The Kaplan-Meier estimation did not reveal any difference in biological behavior between grade 1 vs grade 2 tumors ($p = 0.550$), and grade 3 vs 4 tumors ($p = 0.226$). Grade 1 or grade 2 tumors displayed a significantly better survival rate among patients than grade 3 tumors ($p < 0.0001$). **b** When the grade 1 and 2 tumors were lumped together into low-grade carcinomas, and grade 3 and 4 tumors into high-grade carcinomas, the survival analysis revealed a significant difference between the low-grade and high-grade groups ($p < 0.0001$)

Table 2 Cox regression analysis for cancer-specific survival rates in non-metastatic clear cell RCC

Characteristic	Hazard ratio	CI 95%	p value
Univariate			
ISUP grade	7.50	5.01–11.21	<0.001
TNM stage	2.54	2.04–3.15	<0.001
Surgical margin status	2.95	1.57–5.53	<0.001
Microscopic tumor necrosis	6.74	4.53–10.07	<0.001
Rhabdoid/sarcomatoid change	5.14	3.39–7.78	<0.001
Giant tumor cells	3.93	2.51–6.15	<0.001
Multivariate			
ISUP grade	4.33	2.36–7.95	<0.001
TNM stage	1.86	1.49–2.33	<0.001
Surgical margin status	2.61	1.39–5.2	0.003
Microscopic tumor necrosis	1.69	0.93–3.05	0.081
Rhabdoid/sarcomatoid change	0.96	0.57–1.61	0.896
Giant tumor cells	0.67	0.4–1.13	0.139

morphotype, exerted a significant effect on the patient outcome (see Table 3).

Discussion

Distribution of RCC Morphotypes in Hungary

The incidence of RCC morphotypes is markedly influenced by geographic location and race [12, 13]. In our study, the incidence of entities reflects the situation in white people from Central Eastern Europe, a fact which should be kept in mind when tumor prevalences from countries populated with different races are compared with those populated exclusively by Caucasians. Our study provided three new observations which complement or contradict the corresponding epidemiologic data of the 2016 WHO "blue book".

First, our series was characterized by a a relatively low incidence of papillary RCC (6.9%). A literature survey on the incidence of RCC in European countries reveals a uniform occurrence rate of approximately 80% for clear cell RCC and a geographical variation for the occurrence of papillary RCC. In the series of 2333 RCCs from Austria, 82.8% were clear cell, 10.9% papillary, 3% chromophobe, 0.3% collecting duct, and 3% unclassified [14]. In the study of 2197 small RCCs (≤ 4 cm) from Germany, the occurrence of clear cell, papillary, chromophobe and unclassified histology was 84.4%, 10.3%, 4.5% and 0.8%, respectively [15]. Also, a papillary RCC occurrence rate of 11% was observed in both Italy and Switzerland [16, 17]. In a recent publication from Denmark that focused on incidental renal neoplasms, 16% of the cases were diagnosed with papillary RCC [18]. The reason for the relative low prevalence of papillary RCC in the Carpathian Basin remains unclear at present.

Second, as regards the occurrence of the uncommon subtypes, clear cell papillary and Xp11 translocation RCC had a similar (1.1%) prevalence. Our observation disagrees with those obtained in a much smaller series from the USA, claiming that clear cell papillary RCC should be the fourth most common (4.1%) RCC morphotype [19]. Regrettably,

Fig. 3 Kaplan Meier estimates in clear cell RCC according to low-grade (ISUP grade 1 and 2) and high-grade (ISUP grade 3 and 4) assessment, and the presence or absence of microscopic tumor necrosis. The survival rates tended to be worse when tumor necrosis was present. However, the difference attained a level of significance only in the high-grade subtypes ($p = 0.02$)
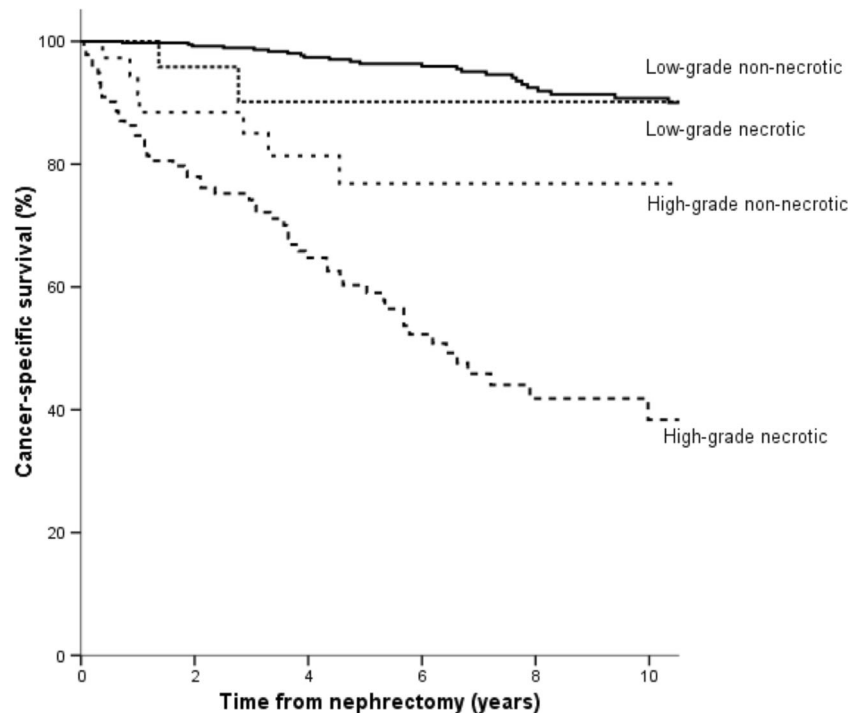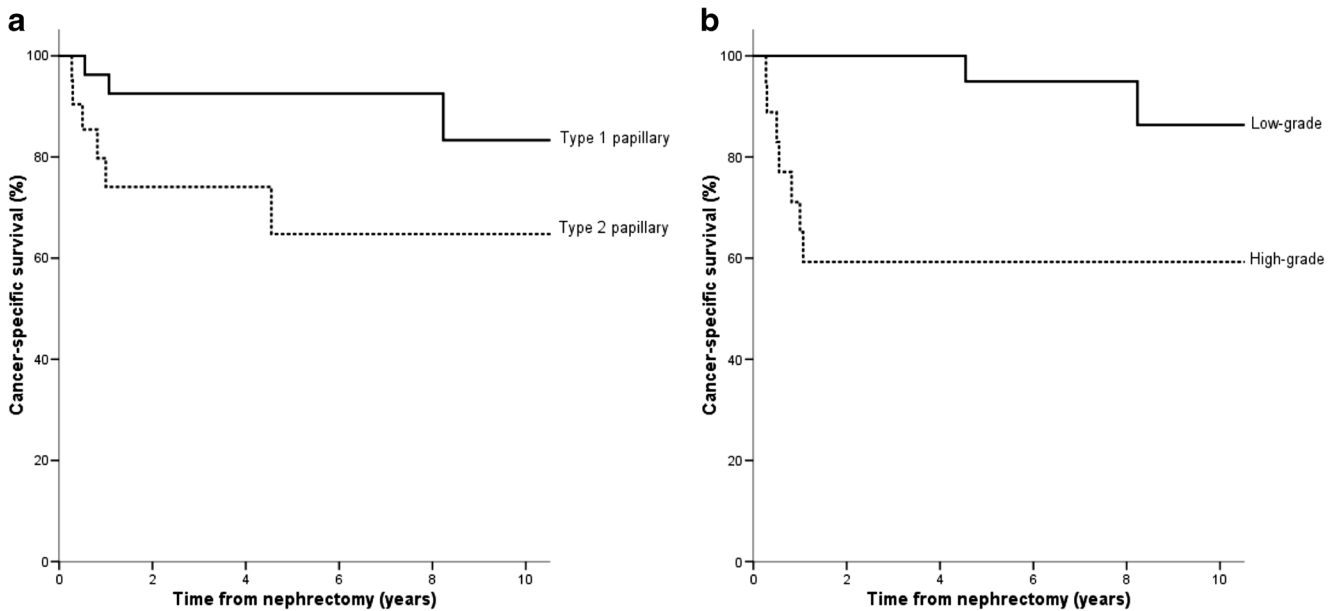
Fig. 4 Kaplan Meier estimates in papillary RCC. **a** The 5-year CSS rates in type 1 and type 2 subtypes were 92% and 65%, respectively ($p = 0.039$). **b** A significant difference was seen in survival rates between the low-grade (ISUP grade 1 + grade 2) and the high-grade (ISUP grade 3 + grade 4) subtypes ($p < 0.001$)

that study did not investigate the race of their patients, and hence a possible racial difference in the occurrence rate of clear cell papillary RCC should not be concluded. Collecting duct RCC or mucinous tubular and spindle cell RCC are very rare subtypes worldwide, and accordingly, these were the rarest in the present series. Our series comprised 28 extensively cystic carcinomas, and the vast majority of cases turned out to be cystic clear cell RCC [10, 20]. Tubulocystic RCC did not occur in our cohort.

Table 3 Cox regression analysis for cancer-specific survival rates in non-metastatic papillary RCC

Characteristic	Hazard ratio	CI 95%	*p* value
Univariate			
ISUP grade	4.12	1.75–9.69	0.001
TNM stage	2.8	1.36–5.78	0.005
WHO type	3.64	0.9–14.7	0.039
Surgical margin status	2.97	0.36–24.1	0.30
Microscopic tumor necrosis	1.89	0.5–7.15	0.34
Rhabdoid/sarcomatoid change	3.18	0.63–16.1	0.16
Giant tumor cells	2.38	0.29–19.4	0.41
Multivariate			
ISUP grade	2.77	1.01–7.53	0.046
TNM stage	2.33	103.5.28	0.042
WHO type	3.15	0.55–17.85	0.19
Surgical margin status	2.54	0.02–247.3	0.68
Microscopic tumor necrosis	1.74	0.33–9.16	0.51
Rhabdoid/sarcomatoid change	5.11	0.25–102.3	0.28
Giant tumor cells	0.36	0.003–49.1	0.68

Third, a surprising finding was the lack of ACKD-associated RCC, which was said to be the most common RCC subtype in end-stage kidneys [21]. In our series, the most frequent subtype was clear cell RCC. In the evaluation of 43 RCCs in the native kidneys of patients who received kidney transplants in Budapest, Hungary, the predominant histological type was clear cell RCC [22]. In a multi-institutional study from Italy and Spain that analyzed the outcomes of RCC in patients with end-stage renal disease, clear cell RCC was similarly the most frequent subtype; and ACKD-associated RCC was not identified at all [23]. In a recent study of 181 patients with end-stage renal disease and RCC from South Korea, tumor histologic type was clear cell in 63%, papillary in 17%, chromophobe in 5%, clear cell papillary in 2.8% and ACKD-related in 6.1% of the cases [24]. Taken together, these findings do not support at all the statement that ACKD-associated RCC is the most common RCC subtype in end-stage renal disease [1, 23].

Prognostic Value of Histologic Subtypes of RCC

Previous large sample sized-studies focusing on the prognostic impact of clear cell, papillary and chromophobe RCCs provided contradictory results. In the study of Patard et al. [25] on 4063 RCC cases, the 5-year survival rates for localized clear cell, papillary, and chromophobe RCC were around 73.2% (in our cohort 83.4%), 79.4% (in our cohort 81%), and 87.9% (in our cohort 100%), respectively. However, when histologic subtypes, TNM stage, Furhman grade, and Eastern Cooperative Oncology Group performance status were subjected to a multivariate analysis, the histologic subtypes did

not prove to be an independent prognosticator. By contrast, in the study of Leibovich et al. on 3062 RCCs, clear cell RCC subtype remained a significant predictor of cancer specific death after adjustment for tumor size, stage and grade [26]. Capitanio et al. assessed the magnitude of the effect of histologic subtype on cancer-specific mortality in 11,618 nephrectomies because of RCC [27]. In a multivariate model predicting cancer-specific mortality, histologic subtype remained an independent predictor. In the study of 5339 Italian patients, the histologic subtype was shown to be a predictive variable for cancer-specific mortality in a multivariate analysis [16].

In the present study, the Kaplan Meier curves explored three, prognostically different groups.

The first group, associated with an excellent prognosis, was formed by chromophobe RCC and clear cell papillary RCC. Chromophobe RCC has been described as usually a low-grade neoplasm with little tendency to progress and metastasize; and the reported 5-year survival rates range from 78% to 100% [28, 29]. Predictors of progression include the microscopic tumor necrosis, sarcomatoid change and stage of the tumor [28, 30]. Although chromophobe RCCs should not be graded at the moment, all our cases lacked high-grade features, and only 3 out of 42 displayed microscopic tumor necrosis; and the majority of cases were limited to the kidney, features which help explain the observed excellent survival rate. Regarding clear cell papillary RCC, all our cases were kidney-limited and low-grade tumors, with no evidence of recurrence or metastatic disease in the follow-up period. Similar features have been reported with this subtype all over the world. Because of the excellent outcome data, this entity was recently suggested to be renamed as clear cell papillary neoplasm of low malignant potential [31].

The second prognostic group, displaying a fair outcome (5-year survival rate around 80%), comprised papillary RCC and clear cell RCC. In a recent study investigating correlations between tumor grade and histologic characteristics with clinical outcome in 154 cases of papillary RCC, the histologic subclassification was of relative prognostic significance [32]. Our findings turned out to be quite similar. Type 1 tumors exhibited a pretty good, 92% 5-year survival rate; morphologically these cancers were usually manifested with ISUP grade 1 or grade 2 atypia and were usually presented with kidney-limited disease. In contrast, in type 2 tumors the 5-year survival rate was just 65%; morphologically these cancers were predominantly present with ISUP grade 3 or grade 4 atypia and almost half of the tumor cases had grown outside the kidney at the time of the surgical removal. In Cox proportional hazard analysis, the ISUP grade and TNM stage, but not the morphotype, had an effect on the patient outcome. In an Austrian study on 88 type 1 and 89 type 2

papillary RCCs, the presence and extent (>20%) of histological tumor necrosis were demonstrated to be negative prognostic factors in type 1, but not in type 2 carcinoma [33, 34]. Since the sample size in our series was much smaller, we could not investigate microscopic tumor necrosis in isolation.

The third group, displaying a bad prognosis, was observed with cases of unclassified RCCs, Xp11 translocation RCCs and collecting duct RCCs. More than half of our cases with unclassified RCC exhibited rhabdoid or sarcomatoid change or giant tumor cells, and the majority spread beyond the kidney; these features are predictors of a dismal prognosis. Xp11 translocation RCC and collecting duct RCC have reportedly the worst prognosis, and the corresponding survival data in our series was in complete accordance with this finding.

Grade and Microscopic Tumor Necrosis as Prognostic Parameters in Clear Cell RCC

The survival analysis according to the ISUP grade provided two, statistically different subgroups, namely ISUP 1 plus 2 tumors, characterized by an excellent 5-year survival rate (96%), and ISUP 3 plus 4 tumors, characterized by a much worse survival rate (63%). Delahunt et al. recently regraded 3017 clear cell RCCs from the Mayo Clinic according to the ISUP grades [6]. The difference in the survival rate between the grade 1 and grade 2 groups did not attain a level of significance, and a similar situation was observed in our series. In contrast to our results, however, the survival rates of grade 3 vs grade 4 cancers were significantly different. The reason for the different survival rates in the Szeged and the Mayo series appears to be the difference in the rates of grades: 21.5% and 9% for grade 1, 48.5% and 42% for grade 2, 12.2% and 40% for grade 3, and 17.6% and 9% for grade 4, respectively. The differences in the cases of the grade 1 and grade 3 cancers are significant, with many more grade 1 tumors in Szeged, and many more grade 3 tumors in Rochester. In our cohort, there was no significant difference in the survival rates between cases with grade 1 vs grade 2, and grade 3 vs grade 4 atypia and, therefore, samples with grades 1 and 2, and grades 3 and 4 could be merged to low-grade and high-grade categories. This is an important finding.

Treating microscopic tumor necrosis as a prognostic parameter multivariate analyses yielded contradictory results [6, 35, 36]. In our study, the multivariate Cox model excluded microscopic tumor necrosis as an independent predictor of survival. Nevertheless, we do not rule out the possibility that a larger sample size might lead to a different result because when Delahunt et al. incorporated microscopic tumor necrosis into the ISUP grading system, a significant difference in survival between each of the grades for clear cell RCC was observed [6].

Morphotype and Grade as Prognostic Parameters in Papillary RCC

Papillary RCC is a heterogeneous disease with two histologic subtypes and variations in patient outcomes. Genetically, type 1 tumors are usually associated with alterations in the *MET* pathway, while type 2 tumors have at least three different pathways, among which *CDKN2A* loss or fumarate hydratase gene mutation are associated with a low survival rate [37]. Unfortunately, any correlation between the main driver genetic events and the grade of the tumor was not sought in that study.

In our series, type 1 tumors exhibited a pretty good, 92% 5-year survival rate. By contrast, the 5-year survival rate in type 2 tumors was only 65%. In a Cox proportional hazard analysis, however, the ISUP grade and TNM stage, but not the morphotype, had an effect on patient outcome. Similar results were obtained in a recent publication investigating correlations between tumor grade and histologic characteristics with clinical outcome in 154 cases of papillary RCC [33]. In the present study, no significant difference was found in survival rates between cases with grade 1 vs grade 2, and grade 3 vs grade 4 atypia, while the 5-year CSS rates outcome in terms of the to the two-tiered grading system revealed a significant difference between the low-grade (95%) and high-grade cases (59%).

Two-Tiered Grading for Clear Cell and Papillary RCCs

Since in clear cell RCC and papillary RCC there were no difference in survival in ISUP grade 1 and grade 2, and ISUP grade 3 and grade 4 tumors, we have decided to start reporting these subsets as either "low-grade" (ISUP 1 or 2) or "high-grade" (ISUP 3 or 4). We think that this simplification helps the urologists and oncologists to better understand the pathology report. Our findings are supported by a recent report published by urologists, who simplified the four-tiered Fuhrman grading system into a low-grade/high-grade scheme and the prognostic accuracy of the two schemes agreed perfectly in 2415 cases with clear cell RCC [38].

Morphological Prognosticators and Postoperative Management

The updated assessment of tumor grade, TNM stage, and histological subtype is mandatory since these variables can serve as selection criteria for clinical trials investigating perioperative management of localized kidney cancer [39]. In the ARISER study on organ confined clear cell RCC, for example, high-risk patients were defined on the basis of TNM stage and nuclear grade, and these patients received adjuvant girentuximab immunotherapy postoperatively, unfortunately without clinical benefit [40].

Summary and Conclusions

The distribution and prognostic features of RCC subtypes in 928 Hungarian Caucasian patients were analyzed after a revision of cases according to the 2016 WHO Renal Tumor Classification. A relatively low incidence of papillary RCC was observed. Also, Xp11 translocation RCC and clear cell papillary RCC exhibited incidences of 1.1% and 1.1%, respectively. ACKD-associated RCC did not occur in a cohort of 16 end-stage kidney disease with RCC. In clear cell RCC and papillary RCCs, low-grade (ISUP grade 1 plus 2) and high-grade groups (ISUP grade 3 and 4) were assigned, and these groups were associated with statistically different survival rates. Lastly, among the pathological prognostic factors in clear cell RCC, microscopic tumor necrosis did not prove to be an independent predictor of outcome.

References

1. Moch H, Humphrey PA, Ulbright TM, Reuter VE (2016) WHO classification Tumours of the urinary system and male genital organs. International Agency for Research on Cancer, Lyon

2. Srigley JR, Delahunt B, Eble JN et al (2013) The International Society of Urological Pathology (ISUP) Vancouver classification of renal neoplasia. Am J Surg Pathol 37:1469–1489

3. Delahunt B, Cheville JC, Martignoni G et al (2013) The International Society of Urological Pathology (ISUP) grading system for renal cell carcinoma and other prognostic parameters. Am J Surg Pathol 37:1490–1504

4. Reuter VE, Argani P, Zhou M, Delahunt B, Members of the ISUP Immunohistochemistry in Diagnostic Urologic Pathology Group (2014) Best practices recommendations in the application of immunohistochemistry in the kidney tumors: report from the International Society of Urologic Pathology consensus conference. Am J Surg Pathol 38:e35–e49

5. Steffens S, Janssen M, Ross FC et al (2014) The Fuhrman grading system has no prognostic value in patients with nonsarcomatoid chromophobe renal cell carcinoma. Hum Pathol 45:2411–2416

6. Delahunt B, McKenney JK, Lohse CM, Leibovich BC, Thompson RH, Boorjian SA, Cheville JC (2013) A novel grading system for clear cell renal cell carcinoma incorporating tumor necrosis. Am J Surg Pathol 37:311–322

7. Tan PH, Cheng L, Rioux-Leclercq N et al (2013) Renal tumors: diagnostic and prognostic biomarkers. Am J Surg Pathol 37:1518–1531

8. Genega EM, Ghebremichael M, Najarian R et al (2010) Carbonic anhydrase IX expression in renal neoplasms: correlation with tumor type and grade. Am J Clin Pathol 134:873–879

9. Gupta R, Billis A, Shah RB et al (2012) Carcinoma of the collecting ducts of Bellini and renal medullary carcinoma: clinicopathologic analysis of 52 cases of rare aggressive subtypes of renal cell carcinoma with a focus on their interrelationship. Am J Surg Pathol 36:1265–1278

10. Williamson SR, Cheng L (2016) Clear cell renal cell tumors: not all that is "clear" is cancer. Urol Oncol 34:292.e17–292.e22

11. Sobin LH, Gospodarowicz MK, Wittekind C (2009) TNM classification of malignant tumors, 7th edn. Wiley-Blackwell, Oxford

12. Tarabeia J, Kaluski DN, Barchana M, Dichtiar R, Green MS (2010) Renal cell cancer in Israel: sex and ethnic differences in incidence and mortality, 1980-2004. Cancer Epidemiol 34:226–231

13. Lipworth L, Morgans AK, Edwards TL et al (2016) Renal cell cancer histologic subtype distribution differs by race and sex. BJU Int 117:260–265

14. Pichler M, Hutterer GC, Chromecki TF, Jesche J, Kampel-Kettner K, Pummer K, Zigeuner R (2012) Renal cell carcinoma stage migration in a single European Centre over 25 years: effects on 5- and 10-year metastasis-free survival. Int Urol Nephrol 44:997–1004

15. Steffens S, Junker K, Roos FC et al (2014) Small renal cell carcinomas–how dangerous are they really? Results of a large multicenter study. Eur J Cancer 50:739–745

16. Novara G, Ficarra V, Antonelli A et al (2010) Validation of the 2009 TNM version in a large multi-institutional cohort of patients treated for renal cell carcinoma: are further improvements needed? Eur Urol 58:588–595

17. Moch H, Gasser T, Amin MB, Torhorst J, Sauter G, Mihatsch MJ (2000) Prognostic utility of the recently recommended histologic classification and revised TNM staging system of renal cell carcinoma: a Swiss experience with 588 tumors. Cancer 89:604–614

18. Rabjerg M, Mikkelsen MN, Walter S, Marcussen N (2014) Incidental renal neoplasms: is there a need for routine screening? A Danish single-center epidemiological study. APMIS 122:708–714

19. Zhou H, Zheng S, Truong LD, Ro JY, Ayala AG, Shen SS (2014) Clear cell papillary renal cell carcinoma is the fourth most common histologic type of renal cell carcinoma in 290 consecutive nephrectomies for renal cell carcinoma. Hum Pathol 45:59–64

20. Dhakal HP, McKenney JK, Khor LY, Reynolds JP, Magi-Galluzzi C, Przybycin CG (2016) Renal neoplasms with overlapping features of clear cell renal cell carcinoma and clear cell papillary renal cell carcinoma: a clinicopathologic study of 37 cases from a single institution. Am J Surg Pathol 40:141–154

21. Tickoo SK, dePeralta-Venturina MN, Harik LR et al (2006) Spectrum of epithelial neoplasms in end-stage renal disease: an experience from 66 tumor-bearing kidneys with emphasis on histologic patterns distinct from those in sporadic adult renal neoplasia. Am J Surg Pathol 30:141–153

22. Végső G, Toronyi E, Hajdu M et al (2011) Renal cell carcinoma of the native kidney: a frequent tumor after kidney transplantation with favorable prognosis in case of early diagnosis. Transplant Proc 43:1261–1264

23. Breda A, Luccarelli G, Rodriguez-Faba O et al (2015) Clinical and pathological outcomes of renal cell carcinoma (RCC) in native kidneys of patients with end-stage renal disease: a long-term comparative retrospective study with RCC diagnosed in the general population. World J Urol 33:1–7

24. Song C, Hong SH, Chung JS, Byun SS, Kwak C, Jeong CW, Seo SI, Jeon HG, Seo IY (2016) Renal cell carcinoma in end-stage disease: multi-institutional comparative analysis of survival. Int J Urol 23:465–471

25. Patard JJ, Leray E, Rioux-Leclercq N, Cindolo L et al (2005) Prognostic value of histologic subtypes in renal cell carcinoma: a multicenter experience. J Clin Oncol 23:2763–2771

26. Leibovich BC, Lohse CM, Crispen PL, Boorjian SA, Thompson RH, Blute ML, Cheville JC (2010) Histological subtype is an independent predictor of outcome for patients with renal cell carcinoma. J Urol 183:1309–1315

27. Capitanio U, Cloutier V, Zini L et al (2009) A critical assessment of the prognostic value of clear cell, papillary and chromophobe histological subtypes in renal cell carcinoma: a population-based study. BJUI 103:1496–1500

28. Volpe A, Novara G, Antonelli A et al (2012) Chromophobe renal cell carcinoma (RCC): oncological outcomes and prognostic factors in a large multicentre series. BJU Int 110:76–83

29. Frees S, Kamal MM, Knoechlein L et al (2016) Differences in overall and cancer-specific survival of patients presenting with chromophobe versus clear cell renal cell carcinoma: a propensity score matched analysis. Urology. doi:10.1016/j.urology.2016.05.048

30. Amin MB, Paner GP, Alvarado-Cabrero I, Young AN, Stricker HJ, Lyles RH, Moch H (2008) Chromophobe renal cell carcinoma: histomorphologic characteristics and evaluation of conventional pathologic prognostic parameters in 145 cases. Am J Surg Pathol 32:1822–1834

31. Diolombi ML, Cheng L, Argani P, Epstein JI (2015) Do clear cell papillary renal cell carcinomas have malignant potential? Am J Surg Pathol 39:1621–1634

32. Cornejo KM, Dong F, Zhou AG et al (2015) Papillary renal cell carcinoma: correlation of tumor grade and histologic characteristics with clinical outcome. Hum Pathol 46:1411–1417

33. Warrick JI, Tsodikov A, Kunju LP et al (2012) Papillary renal cell carcinoma revisited: a comprehensive histomorphologic study with outcome correlations. Hum Pathol 45:1139–1146

34. Pichler M, Hutterer GC, Chromecki TF, Pummer K, Mannweiler S, Zigeuner R (2013) Presence and extent of histological tumour necrosis is an adverse prognostic factor in papillary type 1 but not in papillary type 2 renal cell carcinoma. Histopathology 62:219–228

35. Frank I, Blute ML, Cheville JC, Lohse CM, Weaver AL, Zincke H (2002) An outcome prediction model for patients with clear cell renal cell carcinoma treated with radical nephrectomy based on tumor stage, size, grade and necrosis: the SSIGN score. J Urol 168:2395–2400

36. Lam JS, Shvarts O, Said JW et al (2005) Clinicopathologic and molecular correlations of necrosis in the primary tumor of patients with renal cell carcinoma. Cancer 103:2517–2525

37. The Cancer Genom Atlas Network (2016) Comprehensive molecular characterization of papillary renal-cell carcinoma. N Engl J Med 374:135–145

38. Becker A, Hickmann D, Hansen J et al (2016) Critical analysis of a simplified Fuhrman grading scheme for prediction of cancer specific mortality in patients with clear cell renal cell carcinoma–impact on prognosis. Eur J Surg Oncol 42:419–425

39. Pierorazio PM, Johnson MH, Patel HD et al (2016) Management of Renal Masses and Localized Renal Cancer: systematic review and meta-analysis. J Urol. doi:10.1016/j.juro.2016.04.081

40. Chamie K, Donin NM, Klöpfer P et al (2016) Adjuvant weekly girentuximab following nephrectomy for high-risk renal cell carcinoma: the ARISER randomized clinical trial. JAMA Oncol. doi:10.1001/jamaoncol.2016.4419

ORIGINAL ARTICLE

Renal Cell Carcinoma with Clear Cell Papillary Features: Perspectives of a Differential Diagnosis

Áron Somorácz[1] · Levente Kuthi[2] · Tamás Micsik[3] · Alex Jenei[2] · Adrienn Hajdu[2] · Brigitta Vrabély[3] ·
Erzsébet Rásó[1] · Zoltán Sápi[3] · Zoltán Bajory[4] · Janina Kulka[1] · Béla Iványi[2]

Abstract
Thirty-one cases of low-grade renal cell carcinoma (RCC) with clear cells and tubulopapillary/papillary architecture were analyzed retrospectively with immunohistochemical and genetic markers to gain more experience with the differential diagnosis of such cases. All samples coexpressed CK7 and CA9; the TFE3 or TFEB reactions were negative; the CD10 and the AMACR stainings were negative in 27 cases and 30 cases, respectively. The FISH assays for papillary RCC, available in 27 cases, and deletion of chromosome 3p, available in 29 cases, gave negative results. The results for 3p deletion, *VHL* gene mutation or *VHL* gene promoter region hypermethylation testing, along with the diffuse CD10-positivity in 2 cases confirmed 21 cases as clear cell papillary RCC (CCPRCC; CK7+, CA9+; no 3p loss, no *VHL* abnormality) and 10 cases as clear cell RCC (CCRCC; CK7+, CA9+; no 3p loss, *VHL* abnormality mutation/hypermethylation present). In CCPRCCs, the representative growth pattern was branching tubulo-acinar, commonly accompanied by cyst formation. The linear nuclear arrangement or cup-shaped staining of CA9 did not necessarily indicate CCPRCC, and the absence of these did not exclude the diagnosis of CCPPRC. One tumor infiltrated the renal sinus; the others exhibited pT1 stage; and metastatic outcome was not recorded. The CCRCC cases were in pT1 stage; 6 exhibited cup-shaped staining of CA9, and 1 displayed lymph node metastasis at the time of surgery. Distant metastatic disease was not observed. In summary, the *VHL* abnormalities distinguished the subset of CCRCC with diffuse CK7-positivity and no 3p loss from cases of CCPRCC.

Keywords Clear cell carcinoma · Clear cell papillary carcinoma · Cytokeratin 7-positivity · Differential diagnosis · *VHL* gene

Introduction

Clear cell papillary renal cell carcinoma (CCPRCC) is an infrequent subset of RCC [1, 2]. Although CCPRCC shares

---

Áron Somorácz and Levente Kuthi contributed equally.

Electronic supplementary material The online version of this article (https://doi.org/10.1007/s12253-019-00757-3) contains supplementary material, which is available to authorized users.

✉ Áron Somorácz
somoracz14@gmail.com

1   2nd Department of Pathology, Semmelweis University, Üllői út 93, Budapest H-1091, Hungary

2   Department of Pathology, University of Szeged, Szeged, Hungary

3   1st Department of Pathology and Experimental Cancer Research, Semmelweis University, Budapest, Hungary

4   Department of Urology, University of Szeged, Szeged, Hungary

histopathogical features with clear cell RCC (CCRCC), papillary RCC and Xp11.2 translocation RCC, its immunohistochemical coexpression of cytokeratin 7 (CK7) and carbonic anhydrase 9 (CA9), and negativity for CD10, alpha-methyl-CoA racemase (AMACR), and TFE3 usually clarifies the diagnosis [3–7]. The renal angiomyoadenomatous tumor (RAT) is now regarded as being in the spectrum of CCPRCC [8–10]. Genetically, CCPRCCs lack chromosome 3p deletion or *VHL* gene mutation or *VHL* promoter hypermethylation, the hallmarks of CCRCC, and have no loss of chromosome Y or gain of chromosome 7 and 17, the hallmarks of papillary RCC [2–4, 11–13].

In surgical pathology practice, the separation of CCPRCCs from CCRCCs can pose certain difficulties. The distinction is crucial, because CCPRCCs have a very limited potential for metastasis (fatal outcome has been reported only in two patients out of 400 [14]), whereas in low-grade CCRCCs distant metastases can occur several years after nephrectomy. To learn more about the differential diagnosis of low-grade RCCs with

CCPRCC features, a series of such tumors were subjected to a retrospective immunohistochemical analysis, applying CK7, CA9, CD10, AMACR, TFEB and TFE3 immunostainings, and the immunophenotypes were correlated with the results of genetic markers for CCRCC or papillary RCC.

Materials and Methods

Case Selection and Review Process

This study was conducted with the permission of the Medical Research Council (17489-4/2017/EKU). The hematoxylin and eosin-stained slides of 2326 consecutive RCC samples were reexamined for clear cell papillary RCC-like tumors, including low-grade nuclei, the presence of any degree of tubulopapillary growth pattern of tumor cells with clear cytoplasm, linear arrangement of nuclei away from the basal membrane, along with the presence of a leiomyomatous stroma. Demographical and clinical data were collected from the database management systems of Semmelweis University and University of Szeged.

Tissue Microarray and Immunohistochemical Reactions

Tissue microarray blocks were prepared for immunohistochemistry with TMA Master (3DHISTECH) applying a 2 mm core diameter. One to four representative cores were then punched out from the donor blocks. Immunohistochemical staining for CA9, CK7, CD10, AMACR, TFEB and TFE3 were performed (see the dilutions and sources in Supplementary Table 1). The epitope retrieval was performed for each antibody according to the manufacturer's recommendations. The reactions were conducted using Autostainer (Dako). Afterwards, slides were evaluated microscopically by estimating the proportion (%) of immunopositive cells. Staining in over 50% of the tumor cells, in 10 to 50% of tumor cells, or in less than 10% of the tumor cells, was interpreted as diffusely or focally positive or negative, respectively.

Fluorescent in Situ Hybridization (FISH)

FISH assays were carried out to detect either the loss of chromosome 3p and chromosome Y or gain of chromosome 7 and 17. Tissue sections were cut from the TMA blocks and deparaffinized. The assays were done using a VHL/cen3 probe (ZytoLight® SPEC VHL/CEN3 Dual Color Probe, Zytovision,) and centromeric probes for chromosome 7, 17 and Y (Cytocell) according to the manufacturer's instructions. Slides were digitalized by using a Pannoramic Midi slide scanner (3DHISTECH), and reactions were evaluated using

a Pannoramic Viewer (3DHISTECH) in the following way. Fifty tumor cells from each case were examined and were compared with the same number of cells of the peritumoral tissue, which served as an internal control. The cutoff values of chromosomal gain and/or loss were set at the mean ±3SD of the corresponding control values, as done in previous studies [5]. The analysis of 3p deletion was also performed based on a published method [15].

VHL Gene Sequence Analysis and VHL Gene Promoter Hypermethylation

A PCR-based amplification method was used for VHL gene mutation analysis as earlier described [16]. The VHL exons were amplified via specific primer pairs (Supplementary Table 2). In the case of pathological mutation, the apparently tumor-free renal tissue was analyzed as well. A GenomeLAB DTCS - Quick Start Kit (Beckman Coulter) was used for DNA sequencing. The latter was carried out according to the manufacturer's instructions using the GenomeLab GeXP Genetic Analysis System (Beckman Coulter). The methylation status of VHL gene promoter region was determined using the methylation-specific PCR method. The extracted genomic DNA was modified using the EpiJET Bisulfite Conversion Kit (ThermoFischer Scientific), and followed by PCR-based amplification with methylation-specific primer pairs (Supplementary Table 3). The methylation status (nonmethylated, methylated) was determined by gel electrophoresis of the PCR products, as reported previously [17].

Criteria for Diagnosing a Tumor as CCPRCC

The diagnosis of CCPRCC was made if the above-mentioned morphology together with characteristic immunophenotype (CK7- and CA9-positivity, negative CD10 or at most focal CD10-positivity, negative TFE3 and TFEB stainings), along with the lack of genetic alterations indicating CCRCC (3p deletion, VHL mutation, VHL promoter hypermethylation), and PRCC (7 and 17 trisomy, loss of Y) were detected. Tumors with the same morphology, CK7 and CA9 coexpression, but with diffuse CD10-positivity or with altered VHL status were classed as CCRCC.

Results

Using the inclusion criteria, we retrieved 31 samples. All tumors coexpressed CK7 and CA9. The TFE3 and TFEB reactions were uniformly negative; and the CD10 and the AMACR reactions were negative in 27 and 30 cases, respectively. The FISH assays for papillary RCC, available in 27 cases, and deletion of chromosome 3p, available in 29 cases, yielded negative results. The histomorphology, the results for

VHL mutation and *VHL* methylation testing, and the immunophenotype confirmed 21 cases as CCPRCC and 10 cases as CCRCC. The principal characteristics of the two subsets are summarized in Tables 1 and 2.

Features of CCPRCCs

Here, 21 tumors were examined, and the specimens were obtained from 12 females and 9 males. The mean age was 60 years (with range 28 to 84 years). Partial nephrectomy was performed in 4 patients and radical nephrectomy in 17 patients; and one tumor developed in a transplanted kidney. Twenty cases were incidental findings of imaging performed for non-urological symptoms.

Gross Findings

All the tumors were solitary, and the mean size was 23 mm (with range 6 to 65 mm). Cystic change was present in 12 samples; and multilocular cystic mass existed in cases 7 and 15. The tumorous parenchyma was grey-white to yellow-brown, occasionally with small hemorrhagic foci.

Microscopic Findings

Each tumor was circumscribed, and at least one thin fibrous, or fibromuscular capsule was present, except in one case. The capsule was thick (400-800 μm) and contained smooth muscle in 13 tumors. A minimal infiltration of renal sinus fat was observed in Case 3 (Fig. 1a, b). Vascular invasion was not detected in any of the cases examined. The dominant growth pattern was tubulo-acinar (15 tumors), with cyst formation in a continuum from microscopic to macroscopic cystic spaces in 12 samples. Also, a papillary architecture was observed in 14 tumors and was detected mainly focally, except in one case where it was predominantly seen. Solid areas with compact cell nests and trabeculae were seen in 11 samples, and it was mostly made up of a small proportion of the tumorous parenchyma. Foamy macrophages, psammoma bodies and necrosis were absent. Although the clear cell phenotype was a distinctive feature, the tumor cells displayed various cytological characteristics. Most of them were cuboidal or columnar, but flattened forms in cysts, as well as elongated cells arranged focally in a fascicular pattern in solid areas were also encountered. Some tumor cells – especially in solid areas – had eosinophilic cytoplasm. Prominent nucleoli were not present. The linear arrangement of nuclei together with its orientation away from the basement membrane was observed in 16 tumors (from a minimal to an extensive presence). Mitotic figures were occasionally seen. Stromal smooth muscle was found in 18 cases including two samples with abundant myomatous stroma (cases 1 and 7).

Immunohistochemical and Molecular Profile

All tumors exhibited a strong and diffuse CK7 expression. Immunoreaction for CA9 resulted in diffuse staining in 17 tumor samples, and focal staining in 4 tumor samples. The "cup-shaped" pattern was detected in 17 cases, visible mainly in the tubular and cystic areas. Focal CD10-positivity was found in 2 samples. Weak granular, diffuse AMACR-positivity was noted in Case 14.

The mutation status of the *VHL* gene was investigated in 11 samples, and in Case 12, single nucleotide polymorphism (SNP) in untranslated region (UTR) was found. The *VHL* gene promoter hypermethylation status was analyzed in 16 samples; and none of these harbored promoter region hypermethylation.

Follow-up

The median time was 52.5 months (with range 1 to 184 months). Three patients did not have a follow-up, and two patients died in non-cancer-related causes. No evidence of tumor progression and recurrence was documented in the data of the 18 surviving patients.

Features of CCRCCs Mimicking CCPRCC

In this group, we analyzed 10 cases, and the mean age was 51 years (with range 37 to 69 years) with 5 female and 5 male patients. Half of the cases were treated via partial nephrectomy. Tumor-related symptoms were registered in two patients. In Case 23, a CCRCC (CA9 and CD10: diffusely positive; CK7 negative) was resected from the contralateral kidney two months after the first surgery. And in Case 24, a metastatic perihilar lymph node was removed together with the tumorous kidney (Fig. 1c-f).

Gross Findings

The mean size of the tumors was 29 mm (with range 15 to 50 mm). Cystic change was noticed almost in all cases (9/10). The cut surface was indistinguishable from those seen in CCPRCC.

Microscopic Findings

A capsule containing smooth muscle was present in 6 cases. The predominant growth pattern was tubulo-acinar (5/10), followed by cystic (2/10), papillary (1/10) and solid (1/10). In Case 29, the distribution of tubulo-acinar, papillary and cystic pattern was the same. The tumors were composed of clear cytoplasm cells with focal eosinophilic granulations. Also, an apical linear nuclear arrangement was noted in 6 cases, and 2 cases contained a smooth muscle rich stroma. The infiltration of the renal vein, renal sinus and perinephric fat tissue was not observed.

Table 1 Clinicopathological features of the cases examined

Patient	Sex	Age (y)	ESRD	Tumor-related symptoms	Size (mm)	AJCC Stage	ISUP Grade	Follow-up period (months)*	Progression§	Comment
Clear cell papillary RCC										
1	M	68	No	No	21	T1aNxMx	1	31	No	
2	M	57	No	No	20	T1aNxMx	2	35	No	
3	M	64	No	No	30	T3aNxMx	2	NA	ND	Sinus fat tissue infiltration
4	F	68	No	No	30	T1aNxMx	1	12	No	
5	M	84	ESRD	No	10	T1aNxMx	1	1	No	
6	F	63	No	No	8	T1aNxMx	2	46	No	Ipsilateral oncocytoma
7	F	81	No	No	25	T1aNxMx	1	113	No	
8	F	78	No	No	20	T1aNxMx	1	184	No	
9	M	56	ACKD	No	10	T1aNxMx	1	85	No	
10	M	66	No	No	11	T1aNxMx	1	3	No	
11	F	49	No	No	38	T1aNxMx	1	10	No	
12	M	75	No	No	65	T1bNxMx	2	80	No	
13	F	52	No	No	25	T1aNxMx	2	158	No	
14	M	32	No	No	8	T1aNxMx	1	101	No	
15	F	57	No	No	6	T1aNxMx	1	NA	ND	
16	F	30	ESRD	No	8	T1aNxMx	1	86	No	
17	F	60	No	Abdominal pain	22	T1aNxMx	1	3	No	
18	M	76	No	No	10	T1aN0Mx	1	62	No	Ipsilateral angiomyolipoma and papillary adenomas
19	F	69	No	No	13	T1aNxMx	1	8	No	
20	F	28	ESRD	No	20	T1aNxMx	2	59	No	Tumor in a graft kidney
21	F	56	No	No	30	T1aNxMx	1	NA	ND	
Clear cell RCC										
22	F	41	No	No	20	T1aNxMx	1	26	No	
23	F	44	No	No	50	T1bN1Mx	1	36	No	Lymph node metastasis
24	M	37	No	Hematuria	37	T1aNxMx	1	67	No	Contralateral clear cell RCC two months later
25	M	47	ACKD	No	19	T1aNxMx	1	12	No	
26	F	53	No	No	30	T1aNxMx	1	19	No	
27	F	69	No	No	24	T1aNxMx	2	37	No	
28	M	69	No	Lumbar pain	15	T1aNxMx	1	100	No	Ipsilateral papillary adenoma
29	M	40	No	No	30	T1aNxMx	1	10	No	
30	F	51	No	No	40	T1aNxMx	1	3	No	
31	M	61	No	No	25	T1aNxMx	2	6	No	

*Follow-up, determined from the surgery to the last follow-up; §Progression, assessed by radiological and/or autopsy data

M male; *F* female; *ESRD* end-stage renal disease; *ACKD* acquired cystic kidney disease; *NA* not available; *ND* no data

Immunohistochemical and Molecular Profile

There was a coexpression of CK7 in a diffuse fashion and CA9 in a diffuse (8 cases) or focal fashion (2 cases). The cup-shaped distribution of CA9 was present in 6 cases. Diffuse CD10-positivity was observed in cases 23 and 24.

The *VHL* gene mutation status was analyzed in 9 samples, and in cases 22, 23 and 31 a pathogenic mutation was identified that was not present in the tumor-free renal parenchyma (Fig. 2). The sequencing revealed an SNP without any clinical significance in Case 24. The remaining 5 tumors analyzed harbored no genetic change. Also, the *VHL* gene promoter hypermethylation was tested in 8 cases, and 7 of them possessed promoter region hypermethylation.

Follow-up

All the cases had follow-up data with a median of 31.6 months (with range 3 to 100 months). None of them experienced any recurrence and cancer-related death.

Table 2 Morphological, immunohistochemical, and molecular characteristics of the cases examined.

Patient	Architecture of tumor volume (%)					Immune profile (%)					Molecular characteristics					
	Tubular	Papillary	Cystic	Solid	LiN	CK7	CA9	CA9 cup-shaped	CD10	AMACR	+7	+17	-Y	-3p	VHL mut	VHL met
Clear cell papillary RCC																
1	90	-	-	10	No	Diff	Diff	Yes	Neg	Neg	-	-	-	-	wt	ua
2	88	2	-	10	Yes	Diff	Diff	Yes	Foc	Neg	-	-	-	-	wt	-
3	95	-	-	5	Yes	Diff	Diff	Yes	Neg	Neg	nd	nd	nd	nd	nd	nd
4	59	1	20	20	Yes	Diff	Diff	Yes	Neg	Neg	-	-		-	wt	-
5	100	-	-	-	Yes	Diff	Diff	Yes	Neg	Neg	-	nd	-	-	nd	nd
6	95	5	-	-	Yes	Diff	Diff	Yes	Foc	Neg	-	-		-	wt	-
7	44	5	50	1	No	Diff	Diff	Yes	Neg	Neg	-	-		-	wt	-
8	50	50	-	-	Yes	Diff	Diff	Yes	Neg	Neg	-	-		-	ua	-
9	80	10	-	10	No	Diff	Diff	Yes	Neg	Neg	-	-	-	-	wt	-
10	95	5	-	-	Yes	Diff	Diff	Yes	Neg	Neg	-	-		-	wt	-
11	50	40	10	-	Yes	Diff	Diff	Yes	Neg	Neg	-	-		-	wt	-
12	50	-	50	-	Yes	Diff	Diff	Yes	Neg	Neg	-	-		-	5'UTR SNP[#]	-
13	-	80	20	-	No	Diff	Diff	Yes	Neg	Neg	-	-		-	ua	-
14	80	10	10	-	Yes	Diff	Diff	Yes	Neg	Poz[§]	-	-	-	-	wt	-
15	-	20	80	-	Yes	Diff	Diff	No	Neg	Neg	-	-		-	ua	nd
16	95	-	-	5	Yes	Diff	Diff	No	Neg	Neg	-	-			ua	nd
17	50	20	30	-	No	Diff	Diff	No	Neg	Neg	-	-		-	wt	-
18	90	-	5	5	Yes	Diff	Foc	Yes	Neg	Neg	nd	nd	nd	nd	nd	-
19	45	1	50	4	Yes	Diff	Foc	Yes	Neg	Neg	-	-		-	nd	-
20	89	-	1	10	Yes	Diff	Foc	Yes	Neg	Neg	-	-		-	ua	-
21	85	1	5	10	Yes	Diff	Foc	No	Neg	Neg	-	-		-	ua	-
Clear cell RCC																
22	50	5	35	10	Yes	Diff	Diff	Yes	Neg	Neg	-	-		-	mut[a]	+
23	50	20	30	-	Yes	Diff	Diff	Yes	Diff	Neg	nd	nd		-	mut[b]	nd
24	10	50	20	20	No	Diff	Diff	No	Diff	Neg	-	-	-	-	5'UTR SNP[¶]	-
25	80	10	10	-	No	Diff	Diff	Yes	Neg	Neg	-	-		-	wt	+
26	95	1	-	4	Yes	Diff	Diff	Yes	Neg	Neg	-	-		-	wt	+
27	20	10	70	-	Yes	Diff	Diff	Yes	Neg	Neg	-	-		-	wt	+
28	40	-	60	-	Yes	Diff	Diff	Yes	Neg	Neg	-	-	-	-	ua	+
29	20	40	40	-	Yes	Diff	Diff	No	Neg	Neg	-	-	-	-	wt	+
30	30	-	20	50	No	Diff	Foc	No	Neg	Neg	-	-		-	wt	+
31	90	-	-	10	Yes	Diff	Foc	No	Neg	Neg	-	-	-	-	mut[c]	nd

LiN linear nuclear arrangement from basement membrane; *+7 and +17* trisomy of chromosome 7 and 17, respectively; *-Y* deletion of chromosome Y; *-3p* deletion of chromosome 3p; *VHL* mut, von Hippel-Lindau gene mutation status; *VHL* met, von Hippel-Lindau gene methylation status; *nd* not determined; *wt* wild type; *ua* unsuccessful analysis; *5'UTR SNP* single nucleotide polymorphism in 5' untranslated region; *diff* diffuse; *foc* focal; *neg* negative (less than or equal to 10%)

[§] weak granular positivity; [#] exon 3 could not be amplified; [¶] exon1b could not be amplified; [a] c.221T>A/p.V74N; [b] c.625C>T/p.G209*; [c] c.354_361delCTTCAGAGinsT

Discussion

The WHO classification of RCCs defines the subsets via a synthesis of histopathological, immunohistochemical, and genetic data [1]. In the current study, we focused on the discrimination of CCPRCC from other tumor types by applying the well-known immunohistochemical markers supplemented with a molecular analysis that seeks to find chromosomal abberations and *VHL* abnormalities (including mutations as well as methylation analysis). We made a formal diagnosis of CCPRCC when both the immunohistochemical and the genetic tests were in complete accordance with the histology.

All the RCC subtypes with clear cell phenotype (i.e. *TFE3* or *TFEB* translocation RCCs, *TCEB1*-mutated RCC [18],
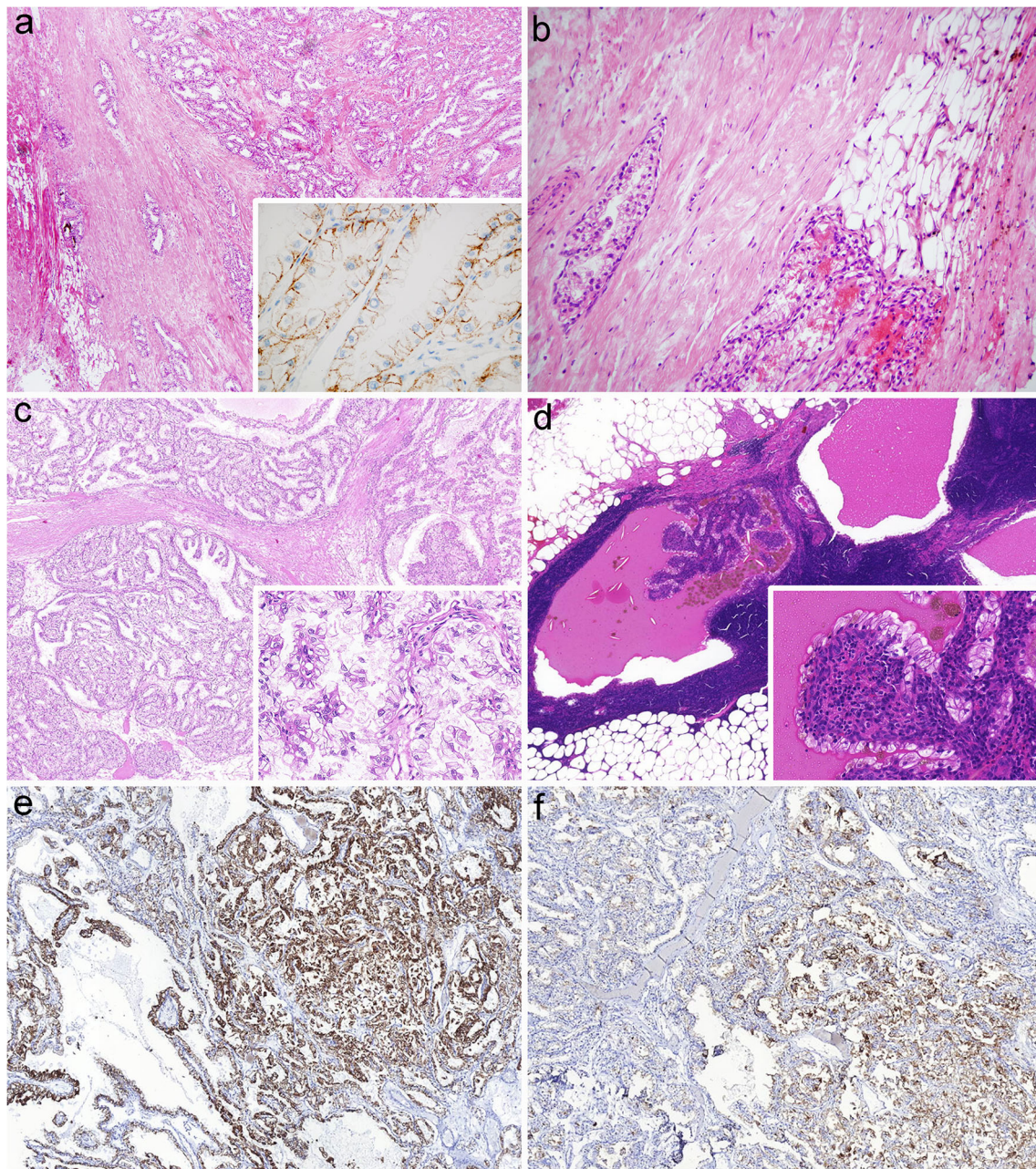
Fig. 1 **a-b Case 3 with sinus fat invasion** The tumor showed a branching tubular pattern and an immunophenotype characteristic for CCPRCC (basolateral CA9 reaction in the insert) (**a**). Superficial infiltration of sinus fat was seen (**b**). **Figure 1 c-f Case 23 with lymph node metastasis** The tumor displayed the morphological features of CCPRCC, partly with papillary architecture (**c**). The lymph node metastasis was mainly cystic; with some papillary infoldings (insert in figure d) (**d**). The tumor exhibited a diffuse CK7 positivity (**e**), but extensive CD10 staining was also observed (**f**). The latter, together with the *VHL* gene mutation detected in this tumor were not consistent with the diagnosis of CCPRCC

RCC with 8p monosomy [19], RCC with prominent smooth muscle stroma (RCCSMS) [20–25] and RCC associated with von Hippel-Lindau syndrome) can exhibit a CCPRCC-like histomorphology [26, 27], but CCRCC cases pose the biggest difficulty because this tumor type is the most common and it also has some morphological similarities. CCRCCs are viewed as tumors that are CA9+ and CD10+, and display no more than a focal CK7 positivity. In contrast, the immunophenotype of CCPRCCs is CK7+, CA9+, and CD10-. Perhaps diffuse and strong CK7 positivity is considered the most important and an obligatory diagnostic criterion for CCPRCC. Nevertheless, the lack of a widespread CD10 reaction is also required.

We performed our case selection based on histological features suggestive of CCPRCC, and all the tumors displayed diffuse CK7 staining. In two of them, however,
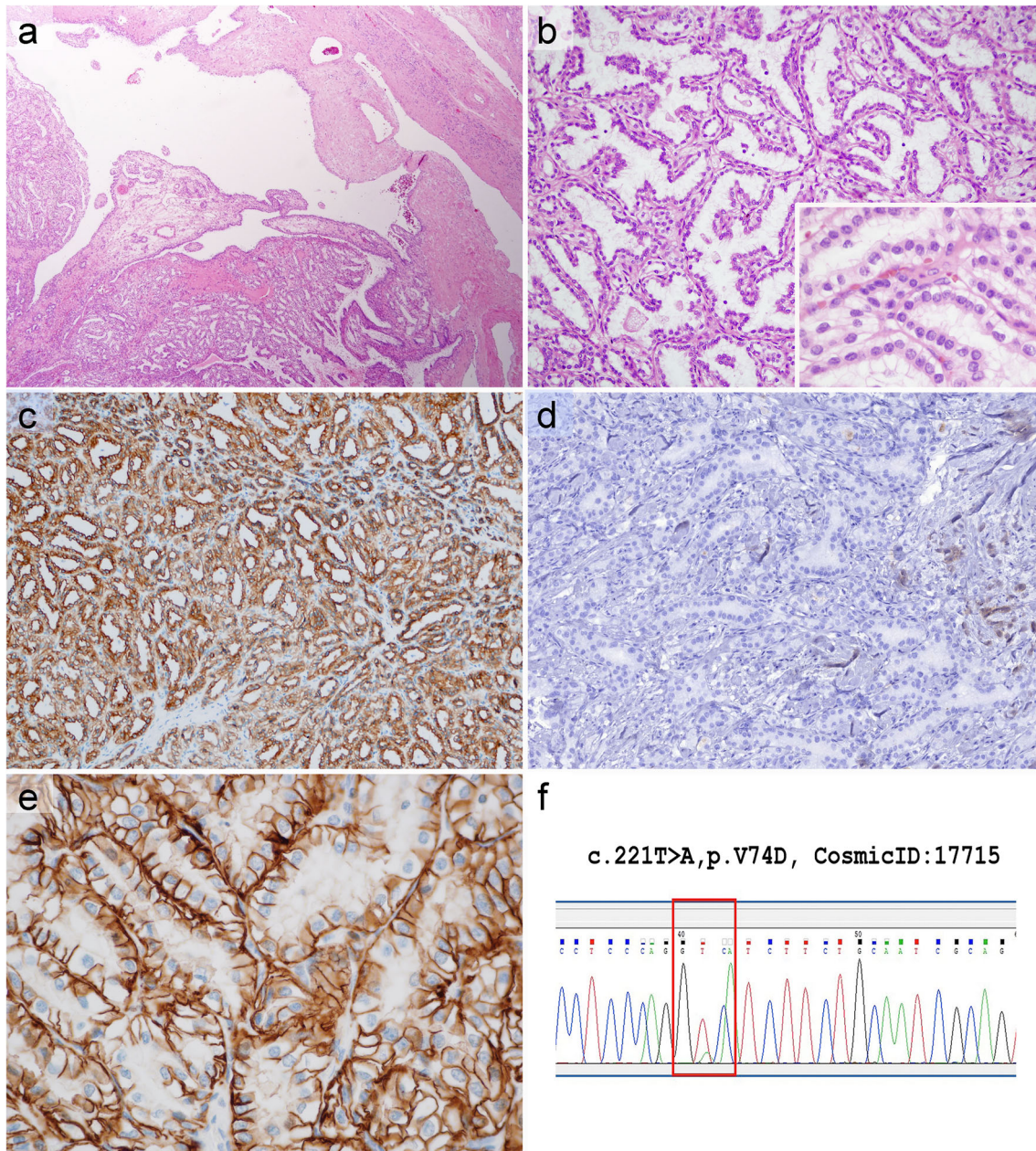
Fig. 2 Case 22 exhibiting morphology and immunophenotype completely consistent with CCPRCC, but containing a *VHL* gene mutation. The tumor had a thick fibromyomatous capsule and it was composed of both solid and cystic areas (**a**). Branching tubular architectural pattern was the most characteristic (**b**). The tumor cells were diffusely positive for CK7 (**c**); and negative for CD10 (**d**). CA9 immunoreaction also resulted in a diffuse staining with a basolateral pattern (**e**). *VHL* gene mutation was detected by direct sequencing (**f**)

CD10 positivity was also diffuse, which supported our diagnosis of CCRCC. In another subset of our cases, the morphology and immunophenotype wholly favoured the diagnosis of CCPRCC; however, either *VHL* mutation (3 cases) or *VHL* promoter hypermethylation (7 cases) was present. We accepted the view of Hes et al. who recommended not classifying cases with any *VHL* gene abnormality as CCPRCC [28]. Based on their approach, our tumors with altered *VHL* status were classified as CCRCC.

After performing an immunohistochemical and molecular analysis, our selected cases with histology of CCPRCCs were subdivided into two groups. These are CCPRCCs (21 cases), and CCRCCs with diffuse CK7 positivity (10 cases).

Features of CCPRCC Cases

The characteristic pattern of these tumors was branching tubulo-acinar that was commonly accompanied by cyst formation. Papillary areas, however, were detected as a minor

component except in three cases. As similar findings on the extent of papillarity were obtained by Aydin et al. [5] and by Williamson et al. [29], we conclude that CCPRCC with predominant papillarity probably occurs quite rarely. Therefore, the WHO designation of this entity seems inaccurate, and the appellation "tubulopapillary" would perhaps be more apt, as was suggested by Aydin et al [5].

Linear nuclear arrangement away from the basement membrane is regarded as characteristic for CCPRCC [30]. Actually, 16/21 of CCPRCCs and 7/10 CCRCCs with diffuse CK7-positivity harbored this phenomenon (from a minimal to extensive presence). Dhakal et al. examined 37 tumors with a morphologic overlap between CCPRCC and CCRCC features, and linear nuclear arrangement was not the exclusive feature of cases classified as CCPRCC [31]. In another series of CCPRCC, Williamson at al. noticed linear nuclear arrangement only in 24/55 cases [32]. These findings suggest that linear nuclear arrangement is an overemphasized phenomenon, since its absence does not exclude the possible diagnosis of CCPRCC, and its presence does not necessarily support the diagnosis of CCPRCC.

The cup-shaped expression of CA9 was not uniformly present in our series. A diffuse cup-shaped expression was observed in 17/21 samples, while a dominant box-shaped staining with a focal cup-shaped expression was noted in 4/21 samples. Upon reviewing the literature, a cup-shaped expression involving 50% of tumor cells was reported by Rohan et al. in 3 out of their 9 cases [6]; and Dhakal et al. noted a cup-like expression of CA9 in 74% of their cases [31]; and Aydin et al. did not mention this feature at all in their 36 cases [5]. Since in our experience the cup-shaped staining pattern cannot be discerned unambiguously in solid areas, the absence of cup-shaped expression should be interpreted with caution when making a concrete diagnosis of CCPRCC for a specific case. A diffuse and weak granular AMACR-positivity was seen in one case. We reviewed the immunoprofile of the published CCPRCC cases and, albeit rarely, AMACR-positivity was reported [5, 6, 11, 29, 32–34]; hence if it is present, it does not necessarily contradict the diagnosis of CCPRCC. Focal CD10-positivity was encountered in two, otherwise completely typical CCPRCC, and VHL gene abnormalities were not present in these samples. The focal extent of CD10 expression

may indicate the possibility of RAT, because a lack of a cystic component viewed microscopically, and the triple coexpression of CK7, CA9 and a certain degree of CD10 were noted in a series of RCC cases classified as RAT [35].

Our CCPRCC group comprised 19 pT1a, 1 pT1b and 1 pT3a cases, respectively. To our knowledge, ours is the first reported case with infiltration outside of the kidney parenchyma. Also, in Case 20 the tumor developed in a transplanted kidney. In a recently published review, Dhakal at al. [36] summarized the findings of 24 articles that reported tumors in transplanted kidneys, but among the 48 tumors described, not one was CCPRCC. Coexisting benign tumors and CCPRCC were observed in two cases. Actually, in Case 6 the oncocytoma had been detected clinically, and during the grossing CCPRCC was discovered. All of our CCPRCC cases had an excellent clinical outcome, reinforcing the view that the carcinoma designation might be exaggerated [14, 37, 38].

Features of CCRCCs with Diffuse CK7-Positivity

A series of CCRCC with diffuse CK7-posivity was published a decade ago by Mai et al [39]. Similar to our experiences, these samples were small-sized, and a non-metastatic course was recorded over a mean of a 3-year follow-up; and diffuse CK7-positivity was viewed as the indicator of indolent behaviour [40].

Our results provide further clinicopathologic data on this rare subset of CCRCC. Accordingly, neither 3p deletion, nor other chromosomal anomalies were present. The VHL gene sequence analysis revealed pathologic mutations in cases 22, 23 and 31. Since VHL mutations were not identified in the non-tumorous renal tissue, the possibility of VHL-disease-associated CCRCC was excluded.

In seven samples, the histological and immunphenotypic data favoured the diagnosis of CCPRCC; however, the presence of the VHL gene promoter hypermethylation abnormality leads us to place these samples into the CCRCC group. In the study of Herman et al. on silecing of the VHL gene by DNA methylation, the hypermethylation of a CpG island in the 5' region was noted in 5 samples out of 26 CCRCCs [16]. Four of these had lost one copy of VHL, while one retained two heavily methylated alleles. The latter observation indicated

Table 3 Overlapping and discriminating features of CCRCCs and CCPRCCs. As we accepted the view of Hes et al. [18] that VHL gene alteration is not compatible with the diagnosis of CCPRCC, altered VHL status was found as the most reliable discriminating feature between CCRCCs and CCPRCCs in our cohort

	Tubulopapillary architecture	Subnuclear vacuolization	Stromal SM	Diffuse CK7+	Diffuse CD10+	CA9 cup-shaped	- 3p	VHL mut	VHL met
CCCRCC	+/-	+/-	+/-	+/-	+/-	+/-	+/-	+/-	+/-
CCCPRCC	+	+/-	+/-	+	-	+/-	-	-	-

SM smooth muscle; mut mutation; met hypermethylaiton

that hypermethylation may inactivate the *VHL* gene even when both wild-type alleles are retained [16]. In our analysis, hypermethylation was noted in seven cases; moreover coexisting *VHL* gene mutation and methylation was seen in Case 22. After a search for methylation data, only 2 tumors analyzed were found in the literature out of 400 or so CCPRCCs [5, 14]. Methylation analyses performed by others in the future may validate our assumption that a *VHL* promoter hypermethylation is definitely not compatible with the diagnosis of CCPRCC. In Case 24 (and in Case 12 in the CCPRCC group) an SNP was observed in the 5' UTR region, a finding treated as insignificant, because the nucleotide change did not induce any amino acid change as well. Interestingly, in 8 cases the histological and immunphenotypic data were entirely consistent with the histopathological diagnosis of CCPRCC, but the presence of *VHL* abnormalities led us to place these samples into the group of low-grade CCRCC with CK7 immunoreactivity and no 3p loss. Every case was in the pT1 stage, and there was no progression or recurrence.

In summary, in our study the immunophenotype and the genetic profile of 31 RCCs composed of clear cells, low-grade nuclei and a tubulopapillary architecture were investigated retrospectively. Twenty-one cases were classified as CCPRCC (CK7+, CA9+; -3p absent, *VHL* abnormality not present) and 10 as CCRCC with diffuse CK7-positivity (CK7+, CA9+; -3p absent, *VHL* abnormality present). Based on our findings, the following conclusions can be drawn. First, CCPRCCs rarely exhibit a predominant papillary architecture, hence their name is misleading. Second, a linear nuclear arrangement away from the basement membrane and cup-like CA9 positivity are not obligatory features. Third, the evidence for their malignant potential is still subject of debate. Fourth, RCCs with CCPRCC morphology, diffuse CK7 positivtiy, and with an altered *VHL* status (mutation, or promoter hypermethylation) do exist; and these tumors can be interpreted as CCRCC with diffuse CK7 positivity, and they can be definitely differentiated from CCPRCCs only by carrying out molecular tests for the *VHL* status. And last but, not least the biological behavior of both CCPRCCs and CCRCCs with diffuse CK7 positivity seems to be indolent with a favorable clinical outcome. Overlapping and discriminating features of CCPRCCs and CCRCCs are summarized in Table 3.

Compliance with Ethical Standards

Conflict of interest The authors declare that they have no conflict of interest.

Ethical approval The study was ethically approved by the Medical Research Council of Hungary (174894/2017/EKU). The renal carcinoma cases were retrospectively selected from the archives of the pathological institutions and informed consent was not obtained.

References

1. Srigley JR, Delahunt B, Eble JN et al (2013) The International Society of Urological Pathology (ISUP) Vancouver Classification of Renal Neoplasia. Am J Surg Pathol 37:1469–1489
2. Moch H, Humphrey PA, Ulbright TM, Reuter VE (2016) WHO Classification of Tumours of the Urinary System and Male Genital Organs. International Agency for Research on Cancer
3. Tickoo SK, dePeralta-Venturina MN, Harik LR et al (2006) Spectrum of epithelial neoplasms in end-stage renal disease: an experience from 66 tumor-bearing kidneys with emphasis on histologic patterns distinct from those in sporadic adult renal neoplasia. Am J Surg Pathol 30:141–153
4. Gobbo S, Eble JN, Grignon DJ et al (2008) Clear cell papillary renal cell carcinoma: a distinct histopathologic and molecular genetic entity. Am J Surg Pathol 32:1239–1245
5. Aydin H, Chen L, Cheng L et al (2010) Clear cell tubulopapillary renal cell carcinoma: a study of 36 distinctive low-grade epithelial tumors of the kidney. Am J Surg Pathol 34:1608–1621
6. Rohan SM, Xiao Y, Liang Y et al (2011) Clear-cell papillary renal cell carcinoma: molecular and immunohistochemical analysis with emphasis on the von Hippel-Lindau gene and hypoxia-inducible factor pathway-related proteins. Mod Pathol 24:1207–1220
7. Ross H, Martignoni G, Argani P (2012) Renal cell carcinoma with clear cell and papillary features. Arch Pathol Lab Med 136:391–399
8. Michal M, Hes O, Havlicek F (2000) Benign renal angiomyoadenomatous tumor: a previously unreported renal tumor. Ann Diagn Pathol 4:311–315
9. Michal M, Hes O, Kuroda N et al (2009) Difference between RAT and clear cell papillary renal cell carcinoma/clear renal cell carcinoma. Virchows Arch. https://doi.org/10.1007/s00428-009-0788-9
10. Deml KF, Schildhaus HU, Compérat E et al (2015) Clear cell papillary renal cell carcinoma and renal angiomyoadenomatous tumor: two variants of a morphologic, immunohistochemical, and genetic distinct entity of renal cell carcinoma. Am J Surg Pathol 39:889–901
11. Tickoo SK, Reuter VE (2011) Differential diagnosis of renal tumors with papillary architecture. Adv Anat Pathol 18:120–132
12. Kuroda N, Ohe C, Kawakami F et al (2014) Clear cell papillary renal cell carcinoma: a review. Int J Clin Exp Pathol 7:7312–7318
13. Gobbo S, Eble JN, Maclennan GT et al (2008) Renal cell carcinomas with papillary architecture and clear cell components: the utility of immunohistochemical and cytogenetical analyses in differential diagnosis. Am J Surg Pathol 32:1780–1786
14. Diolombi ML, Cheng L, Argani P et al (2015) Do Clear Cell Papillary Renal Cell Carcinomas Have Malignant Potential? Am J Surg Pathol 39:1621–1634
15. Fallon KB, Palmer CA, Roth KA et al (2004) Prognostic value of 1p, 19q, 9p, 10q, and EGFR-FISH analyses in recurrent oligodendrogliomas. J Neuropathol Exp Neurol 63:314–322

16. Akanni OE, Ferrari M (2006) Sequencing of Von Hippel-Lindau (VHL) Gene from Genomic DNA for Mutation Detection in Italian Patients. EJIFCC 17:12–16

17. Herman JG, Graff JR, Myohanen S et al (1996) Methylation-specific PCR: a novel PCR assay for methylation status of CpG islands. Proc Natl Acad Sci USA 93:9821–9826

18. Hakimi AA, Tickoo SK, Jacobsen A et al (2015) TCEB1-mutated renal cell carcinoma: a distinct genomic and morphological subtype. Mod Pathol 28:845–853

19. Lan TT, Keller-Ramey J, Fitzpatrick C et al (2016) Unclassified renal cell carcinoma with tubulopapillary architecture, clear cell phenotype, and chromosome 8 monosomy: a new kid on the block. Virchows Arch 469:81–91

20. Canzonieri V, Volpe R, Gloghini A et al (1993) Mixed renal tumor with carcinomatous and fibroleiomyomatous components, associated with angiomyolipoma in the same kidney. Pathol Res Pract 189:951–956

21. Martignoni G, Brunelli M, Segala D et al (2014) Renal cell carcinoma with smooth muscle stroma lacks chromosome 3p and VHL alterations. Mod Pathol 27:765–774

22. Petersson F, Branzovsky J, Martinek P et al (2014) The leiomyomatous stroma in renal cell carcinomas is polyclonal and not part of the neoplastic process. Virchows Arch 465:89–96

23. Kuhn E, De Anda J, Manoni S et al (2006) Renal cell carcinoma associated with prominent angioleiomyoma-like proliferation: Report of 5 cases and review of the literature. Am J Surg Pathol 30:1372–1381

24. Shannon BA, Cohen RJ, Segal A et al (2009) Clear cell renal cell carcinoma with smooth muscle stroma. Hum Pathol 40:425–429

25. Petersson F, Martinek P, Vanecek T et al (2018) Renal Cell Carcinoma With Leiomyomatous Stroma: A Group of Tumors With Indistinguishable Histopathologic Features, But 2 Distinct Genetic Profiles: Next-Generation Sequencing Analysis of 6 Cases Negative for Aberrations Related to the VHL gene. Appl Immunohistochem Mol Morphol 26:192–197

26. Williamson SR, Zhang S, Eble JN et al (2013) Clear cell papillary renal cell carcinoma–like tumors in patients with von Hippel-Lindau disease are unrelated to sporadic clear cell papillary renal cell carcinoma. Am J Surg Pathol 37:1131–1139

27. Rao P, Monzon F, Jonasch E et al (2014) Clear cell papillary renal cell carcinoma in patients with von Hippel-Lindau syndrome–clinicopathological features and comparative genomic analysis of 3 cases. Hum Pathol 45:1966–1972

28. Hes O, Compérat EM, Rioux-Leclercq N (2016) Clear cell papillary renal cell carcinoma, renal angiomyoadenomatous tumor, and renal cell carcinoma with leiomyomatous stroma relationship of 3 types of renal tumors: a review. Ann Diagn Pathol 21:59–64

29. Williamson SR, Eble JN, Cheng L et al (2013) Clear cell papillary renal cell carcinoma: differential diagnosis and extended immunohistochemical profile. Mod Pathol 26:697–708

30. Zhou H, Zheng S, Truong LD et al (2014) Clear cell papillary renal cell carcinoma is the fourth most common histologic type of renal cell carcinoma in 290 consecutive nephrectomies for renal cell carcinoma. Hum Pathol 45:59–64

31. Dhakal HP, McKenney JK, Khor LY et al (2016) Renal Neoplasms With Overlapping Features of Clear Cell Renal Cell Carcinoma and Clear Cell Papillary Renal Cell Carcinoma: A Clinicopathologic Study of 37 Cases From a Single Institution. Am J Surg Pathol 40:141–154

32. Williamson SR, Gupta NS, Eble JN et al (2015) Clear Cell Renal Cell Carcinoma With Borderline Features of Clear Cell Papillary Renal Cell Carcinoma: Combined Morphologic, Immunohistochemical, and Cytogenetic Analysis. Am J Surg Pathol 39:1502–1510

33. Aron M, Chang E, Herrera L et al (2015) Clear Cell-Papillary Renal Cell Carcinoma of the Kidney Not Associated With End-stage Renal Disease Clinicopathologic Correlation With Expanded Immunophenotypic and Molecular Characterization of a Large Cohort With Emphasis on Relationship With Renal Angiomyoadenomatous Tumor. Am J Surg Pathol 39:873–888

34. Alexiev BA, Drachenberg CB (2014) Clear cell papillary renal cell carcinoma: Incidence, morphological features, immunohistochemical profile, and biologic behavior: A single institution study. Pathol Res and Pract 210:234–241

35. Petersson F, Grossmann P, Hora M et al (2013) Renal cell carcinoma with areas mimicking renal angiomyoadenomatous tumor/clear cell papillary renal cell carcinoma. Hum Pathol 44:1412–1420

36. Dhakal P, Giri S, Siwakoti K et al (2017) Renal Cancer in Recipients of Kidney Transplant. Rare Tumors 9:6550

37. Adam J, Couturier J, Molinié V et al (2011) Clear-cell papillary renal cell carcinoma: 24 cases of a distinct low-grade renal tumour and a comparative genomic hybridization array study of seven cases. Histopathology 58:1064–1071

38. Massari F, Ciccarese C, Hes O et al (2018) The Tumor Entity Denominated "clear cell-papillary renal cell carcinoma" According to the WHO 2016 new Classification, have the Clinical Characters of a Renal Cell Adenoma as does Harbor a Benign Outcome. Pathol Oncol Res 24:447–456

39. Mai KT, Kohler DM, Belanger EC et al (2008) Sporadic clear cell renal cell carcinoma with diffuse cytokeratin 7 immunoreactivity. Pathology 40:481–486

40. Mertz KD, Demichelis F, Sboner A et al (2008) Association of cytokeratin 7 and 19 expression with genomic stability and favorable prognosis in clear cell renal cell cancer. Int J Cancer 123:569–576

ORIGINAL ARTICLE

Clinicopathological Findings on 28 Cases with XP11.2 Renal Cell Carcinoma

Levente Kuthi[1] · Áron Somorácz[2] · Tamás Micsik[3] · Alex Jenei[1] · Adrienn Hajdu[1] · István Sejben[4] · Dániel Imre[5] · Boglárka Pósfai[6] · Katalin Kóczián[7] · Dávid Semjén[8] · Zoltán Bajory[9] · Janina Kulka[2] · Béla Iványi[1]

Abstract

Xp11.2 translocation carcinoma is a distinct subtype of renal cell carcinoma characterized by translocations involving the *TFE3* gene. Our study included the morphological, immunohistochemical and clinicopathological examination of 28 Xp11.2 RCCs. The immunophenotype has been assessed by using CA9, CK7, CD10, AMACR, MelanA, HMB45, Cathepsin K and TFE3 immunostainings. The diagnosis was confirmed by *TFE3* break-apart FISH in 25 cases. The ages of 13 male and 15 female patients, without underlying renal disease or having undergone chemotherapy ranged from 8 to 72. The mean size of the tumors was 78.5 mm. Forty-three percent of patients were diagnosed in the pT3/pT4 stage with distant metastasis in 6 cases. Histological appearance was branching-papillary composed of clear cells with voluminous cytoplasm in 13 and variable in 15 cases, including one tumor with anaplastic carcinoma and another with rhabdoid morphology. Three tumors were labeled with CA9, while CK7 was negative in all cases. Diffuse CD10 reaction was observed in 17 tumors and diffuse AMACR positivity was described in 14 tumors. The expression of melanocytic markers and Cathepsin K were seen only in 7 and 6 cases, respectively. TFE3 immunohistochemistry displayed a positive reaction in 26/28 samples. *TFE3* rearrangement was detected in all the analyzed cases (25/25), including one with the loss of the entire labeled break-point region. The follow-up time ranged from 2 to 300 months, with 7 cancer-related deaths. In summary, Xp11.2 carcinoma is an uncommon form of renal cell carcinoma with a variable histomorphology and rather aggressive clinical course.

Keywords Translocation renal cell carcinoma · Xp11.2 · Immunohistochemistry · *TFE3* gene · Fluorescence in situ hybridization (FISH)

Introduction

In the current classification scheme there are 13 distinct types of renal cell carcinoma (RCC), and one of them is the Xp11.2 translocation RCC. It is a rare subtype and is characterized by different translocations involving the transcription factor 3 gene (*TFE3*), that leads to a new fusion gene encoding an aberrant transcription factor [1]. Five common partner genes

---

Levente Kuthi and Áron Somorácz contributed equally to this work.

✉ Levente Kuthi
  kuthi.levente@med.u-szeged.hu

1 Department of Pathology, University of Szeged, 1 Állomás Street, Szeged H-6725, Hungary

2 2nd Department of Pathology, Semmelweis University, Budapest, Hungary

3 1st Department of Pathology and Experimental Cancer Research, Semmelweis University, Budapest, Hungary

4 Department of Pathology, Bács-Kiskun County Teaching Hospital, Kecskemét, Hungary

5 Department of Pathology, Hetényi Géza County Hospital, Szolnok, Hungary

6 Department of Oncotherapy, University of Szeged, Szeged, Hungary

7 Surgical and Molecular Tumor Pathology Centre, National Institute of Oncology, Budapest, Hungary

8 Department of Pathology, Clinical Center and Medical School, University of Pécs, Pécs, Hungary

9 Department of Urology, University of Szeged, Szeged, Hungary

were identified including *ASPL-TFE3*: t(X;17)(p11.2;q25), *PSF-TFE3*: t(X;1)(p11.2;p34), *PRCC-TFE3*: t(X;1)(p11.2;q21), *CLTC-TFE3*: t(X;17)(p11.2;q23) and *NonO-TFE3*: t(X)(p11.2q12) so far in the literature [2–5]. Although Xp11.2 RCC was described as a malignancy among children and adolescents, cases from adults and elders were also reported [6, 7]. The prognosis is controversial, since Xp11.2 RCC has an indolent behavior in children, however, new reports on an aggressive clinical course in adults has been reported as well [6, 8]. Tumor cells usually have blank cytoplasm that mimics clear cell RCC, although the growth pattern is frequently papillary, with psammoma bodies often present [9]. Xp11.2 RCC displays negativity with carbonic anhydrase 9 (CA9) and CK7 [10, 11], while CD10 is often positive and the expression of the melanocytic markers (MelanA and HMB45) are frequent, although they are not expressed in other subsets of RCC [6]. Cathepsin K is a novel marker for Xp11.2 RCC and its positivity indicates the presence of fusion gene *PRCC-TFE3* [12]. The result of translocations involving the *TFE3* gene is the overexpression of the TFE3 protein that can be detected by immunohistochemistry [13]. Although nuclear positivity of the TFE3 protein is a useful diagnostic marker, false negativity and positivity may occur, therefore the identification of the *TFE3* gene rearrangement by fluorescent in situ hybridization (FISH) is needed to confirm the diagnosis [13]. The prognosis of Xp11.2 RCC is still unclear because of the low appearance of series including a great number of patients and the short follow-up period [6]. The three main aims of this retrospective study were: (1) to determine the frequency of Xp11.2 RCC in a large set of surgically treated renal tumors; (2) to provide detailed survival data; and (3) to analyze the morphological features with immunohistochemical and genetic profile to help pathologists establish an accurate histological diagnosis.

Material and Methods

Case Selection

A retrospective study was performed that included morphological, immunohistochemical and molecular pathological analysis. The cases were collected from the Department of Pathology, University of Szeged (1512 own and 64 consultation cases), the 2nd Department of Pathology, Semmelweis University (818 cases), and the 1st Department of Pathology and Experimental Cancer Research, Semmelweis University (404 cases). The diagnostic criteria for Xp11.2 RCC were the typical morphological pattern or moderate-to-strong nuclear positivity with *TFE3* immunohistochemistry or a positive *TFE3* break-apart FISH analysis. A total of 28 cases of Xp11.2 RCC were diagnosed from 2804 tumors in the three centers. All tumors were selected for further

immunohistochemical analysis. The main clinical data included age, sex and symptoms at the time of the diagnosis. Follow-up data were collected from the general practitioners, patient records as well as the patient database of the University of Szeged and Semmelweis University. Tumor size and AJCC TNM stage were obtained from the original histopathological report, however, the TNM stage was amended according to the eighth edition of AJCC TNM staging. All the hematoxylin-eosin stained slides were reviewed by three pathologists (LK, ÁS, TM) to reevaluate the grade according to the ISUP criteria, the histological pattern (generally papillary or solid pattern) and to estimate the percentage of the cellular morphology (predominantly clear or eosinophilic cells). The presence of foamy cells, intracellular pigment, cholesterol clefts, necrosis and psammoma bodies were also recorded, though the extent of necrosis was not scored.

Immunohistochemistry (IHC) and Tissue Microarray (TMA)

The IHC reactions were carried out on TMA. The recipient TMA block was constructed by using a TMA Master (3DHISTECH Ltd., Budapest, Hungary). Stated briefly, from the most representative paraffin blocks of the tumors, two cylindrical cores of 2 mm in diameter were punched out manually. For IHC labeling a panel of antibodies listed in Table 1 was used. Only membrane labeling for CA9, and nuclear labeling for TFE3 was treated as positive. The scoring was performed in a semiquantitative manner and the cases were classified into three categories, namely negative (no staining or less than 5% of positive cells), focally positive (5–75% of positive cells) and diffusely positive (76–100% of positive cells).

TFE3 Break-Apart FISH Analysis

Fluorescent in situ hybridization assays were carried out to detect *TFE3* gene rearrangement. Four μm thick sections were cut from the TMA blocks. The sections were deparaffinized and the reaction was carried out by using Zyto*Light*® SPEC *TFE3* dual color break-apart FISH probe (ZytoVision GMBH, Bremerhaven, Germany) according to the manufacturer's instructions. The slides were counterstained with 4′, 6-diamidino-2-phenylindole (DAPI, Abbott Laboratories, Abbott Park, IL, USA) and scanned with a Pannoramic Midi slide scanner (3DHISTECH Ltd., Budapest, Hungary). The evaluation was performed by using Pannoramic Viewer (3DHISTECH Ltd., Budapest, Hungary). One hundred nuclei were counted and FISH reaction was considered positive when over 10% of the neoplastic nuclei displayed *TFE3* rearrangement.

Table 1 List of the antibodies used in the study

Antibody	Clonality/Source/Clone	Concentration
CA9	rabbit polyclonal, Novus Biologicals	1/2000
CK7	mouse monoclonal, Cell Marque, OV-TL 12/30	1/100
CD10	mouse monoclonal, Biocare Medical, CM129	1/50
AMACR	rabbit polyclonal, Abcam	1/100
MelanA	mouse monoclonal, Labvision, A103	1/200
HMB45	mouse monoclonal, Cell Marque, hmb-45	1/200
TFE3	rabbit monoclonal, Cell Marque, mrq-37	1/100
Cathepsin K	mouse monoclonal, Abcam, 3f9	1/100

Results

Twenty-eight tumors proved to be Xp11.2 RCC among 2804 nephrectomies reviewed by the three pathology departments (0.99%). The diagnosis was suspected mainly because of the histological appearance. The diagnosis was later confirmed by IHC in each case and by FISH analysis except for *patient #11, #12* and *#24*.

Clinical Data and Follow-Up

The clinicopathological findings are summarized in Table 2. Thirteen male and fifteen female patients were included in our cohort. The median age was 60 years (with range from 8 to 72). Three tumors occurred in children and Wilms' tumor was suspected in all cases. The tumor produced symptoms in 9 patients; in *patient #22* a severe pain was provoked by distant bone metastasis. The tumor was an incidental finding in 7 patients. There were no underlying renal disorders in any patients in the affected kidney, but in *patient #12* contralateral kidney agenesis was present. None of the examined patients had received chemotherapy or had had previous malignant tumors, although pharyngeal carcinoma developed in *patient #2* after the nephrectomy.

Radical nephrectomy was performed in each case except three patients, who were treated with nephron-sparing nephrectomy (tumor resection) because of the relatively small tumors (*patient #7* and *#8*) or the absence of the contralateral kidney (*patient #12*).

Follow-up information was accessible in 21/28 patients and the mean follow-up time was 51 months (with range from 2 to 321 months). Regional lymph node or distant metastasis developed in 13 patients (9 had been discovered before surgery; 6 distant and 3 regional lymph node metastases). Seven patients died from cancer-related causes and one patient died from a non-cancer-related cause. In *patient #15* a regional lymph node metastasis developed after 12 months so she was treated with retroperitoneal lymphadenectomy and at the last follow-up there were no signs of the disease. However, 60 months after the nephrectomy, *patient #14* had multiple pulmonary, hepatic and bone metastases. He received tyrosine kinase and mTOR inhibitors until treatment failure. In *patient #27* multifocal vertebral metastases developed. She is currently receiving tyrosine kinase therapy and stable. The remaining 11 patients were alive with no evidence of disease.

Morphological Aspects

All the examined tumors were unilateral and unifocal. The largest diameter of the tumors ranged from 15 mm to 160 mm and the average was 78.5 mm. In two cases the actual size of the tumor was unknown. Macroscopically the cut surface was usually solid and cystic with sulfur yellow color, as seen in clear cell RCC. Foci of necrosis or hemorrhage were occasionally noted as well. The invasion of the renal vein, sinus and adipose capsule was observed in 7, 8, 6 cases respectively. The predominant architectural appearance was solid pattern (13/28), followed by papillary pattern (11/28), while both solid and papillary patterns were seen in a small proportion of cases (4/28). Tumors were composed mostly of clear cells in 19 cases, mostly of eosinophilic cells in 7 cases and mixed clear cell and eosinophilic morphology was seen in 2 cases. Twenty-two cases had typical architecture with voluminous clear cytoplasm, nested or papillary growth. The remaining 6 cases had diverse architecture, mostly mimicking clear cell RCC, except for *patient #5*, whose tumor resembled rhabdoid morphology and *patient #6*, whose tumor had anaplastic carcinoma appearance. The presence of foamy cells, intracytoplasmic pigment, cholesterol clefts, psammoma bodies and necrosis were observed in 7, 4, 1, 11 and 17 cases respectively. Most of the tumors had high-grade nuclear features (19/28). Detailed summary of the microscopic findings can be found in Table 3. Figures 1 and 2 include representative images of the morphological features.

IHC Findings

Results of immunohistochemistry are summarized in Table 4 and representative pictures are presented on Fig. 3. Three cases displayed positivity with CA9, although two of these were necrotic tumors. All the examined cases were negative with CK7, while CD10 was strongly positive in 17 cases.

Table 2 Clinicopathological features of the patients

	Age (y)	Sex	Symptoms†	Side	Size (mm)	pT Stage	Node Status§	Metastasis or recurrence*	Follow-up (mo)	Status
1	52	M	–	L	70	4	–	–	–	LTF
2	69	M	Incidental finding on CT	L	50	1b	–	–	–	LTF
3	47	M	Hematuria, flank pain	R	100	3b	Neg	Lung, Liver	2	DOD
4	69	F	Hematuria	R	80	3a	–	Bone-U, Local R	53	DOD
5	59	M	Flank pain	L	140	4	Pos	–	–	LTF
6	67	M	Fatigue, subcostal pain	L	160	4	Pos	Liver, LN	2	DOD
7	40	M	–	L	25	1a	–	None	127	NED
8	15	F	Palpable ventral mass	L	55	1b	–	Lung, Vertebral column	14	DOD
9	46	M	Incidental finding	L	100	2a	Neg	Local R	13	DOD
10	72	F	Flank pain	L	140	3a	–	–	4	DOD
11	21	F	–	R	–	3a	–	–	–	LTF
12	14	M	–	L	–	1a	–	None	12	NCRD
13	31	M	Incidental finding on US	L	55	1b	–	None	87	NED
14	57	M	–	L	100	3a	Neg	Lung, Liver, Vertebral column	81	DOD
15	40	F	–	R	110	3a	–	LN	65	NED
16	50	F	–	R	45	1b	–	None	31	NED
17	32	M	Incidental finding	B	15	1a	–	None	24	NED
18	60	F	Incidental finding	–	16	1a	–	–	–	LTF
19	66	F	–	R	60	1b	Pos	Adrenal gland	–	LTF
20	32	M	–	R	20	1a	Pos	Liver	–	LTF
21	17	F	–	R	35	1a	–	None	175	NED
22	36	F	Shoulder pain	R	120	3b	–	Scapula	13	AWD
23	40	F	Incidental finding	R	41	1b	–	None	24	NED
24	8	F	Palpable ventral mass	L	100	2b	–	–	321	NED
25	54	F	–	R	120	3a	Neg	None	10	NED
26	66	M	Abdominal pain	L	110	2b	–	None	4	NED
27	51	F	–	R	65	1b	–	Vertebral column	3	AWD
28	46	F	Incidental finding	L	110	3a	Pos	None	7	NED

†Symptoms: including any tumor-related symptoms; incidental finding indicates a symptomless tumor; −, no data. pT Stage: classification by AJCC 2016 TNM Staging System. §Node Status: nodal status at time of surgery; −, no lymph node was removed; Neg, negative; Pos, positive. A lymph node metastasis that developed during the follow-up period is listed in the" Metastasis" column. *Metastasis: either found earlier or at the same time with the primary renal tumor, or during the follow-up period; Bone-U, bone, exact location is unknown; −, no data; R, recurrence; LN, lymph node. ¶Status: DOD, died of disease; LTF, patient is deceased, but lost to follow-up; NED, no evidence of disease; NCRD, not a cancer-related death; AWD, alive with disease; −, no data

AMACR was negative in 14 tumors and a diffuse-to-focal positivity was seen in the remaining 14 cases. The diagnostic *TFE3* reaction strongly labeled the nuclei in 26/28 cases, however, Cathepsin K displayed positivity only in 6 tumors. MelanA was positive in four cases and HMB45 showed a weak-to-diffuse positivity in three patients.

FISH Findings

FISH reaction was performed in 25 cases, because in *patient #11*, *#12* and *#24*, the quality of tumor tissue was not appropriate for proper molecular analysis. For the above-mentioned three cases, FISH was repeated using the original paraffin blocks, although the test remained unsuccessful. In 21 tumors typical split signals were seen (Fig. 4 A), while in *patient #9* and *#10* truncated signal pattern was mostly observed (Fig. 4 B). In *patient #14*, signals were separated, even though they were unusually close to each other (Fig. 4 C). In *patient #23* (a female) an entire break-point region was completely absent (Fig. 4 D). Hence in this case only one signal pair was detected in the nuclei of the tumor cells, while in the surrounding renal parenchyma two unaffected signal pairs were present. The immunophenotype and histomorphology led us to classify the case as Xp11.2 RCC. No other abnormalities were seen by using FISH in any cases.

Table 3 Histological findings of the investigated tumors

	PP (%)	SP (%)	CCs (%)	ECs (%)	Foamy cells	IP	ChC	PB	Necrosis	ISUP grade
1	5	95	50	50	−	−	−	−	+	4
2	40	60	30	70	+	+	−	−	−	2
3	1	99	20	80	−	−	−	−	+	4
4	50	50	90	10	−	−	−	−	+	2
5	−	100	10	90	−	−	−	−	+	4
6	−	100	5	95	−	−	−	−	+	4
7	−	100	100	−	−	−	−	−	−	1
8	90	10	80	20	−	−	−	−	−	2
9	50	50	70	30	−	−	−	−	+	4
10	80	20	75	25	−	−	−	−	+	4
11	95	5	90	10	+	−	−	−	−	3
12	50	50	80	20	−	−	−	+	+	3
13	100	−	100	−	+	−	+	+	+	2
14	10	90	60	40	−	+	−	+	−	2
15	80	20	70	30	−	+	−	−	+	3
16	90	10	75	25	+	−	−	+	−	3
17	100	−	100	−	−	−	−	+	−	2
18	5	95	30	70	+	−	−	+	−	3
19	10	90	80	20	−	−	−	+	+	2
20	−	100	95	5	−	−	−	+	+	4
21	−	100	30	70	−	−	−	+	−	2
22	50	50	90	10	−	−	−	−	+	3
23	−	100	80	20	+	−	−	−	+	3
24	−	100	60	40	−	−	−	−	−	3
25	80	20	30	70	+	−	−	+	+	3
26	95	5	90	10	−	+	−	−	+	3
27	100	−	50	50	−	−	−	+	−	3
28	90	10	80	20	−	−	−	−	+	3

PP, indicates papillary pattern; SP, solid pattern; CCs, clear cells; ECs, eosinophilic cells; IP, intracytoplasmic pigment; ChC, cholesterol clefts; PB, psammoma bodies; +, present; −, absent

Discussion

Clinicopathological Findings of Xp11.2 RCC

We reviewed 2804 nephrectomy cases and identified 28 Xp11.2 translocation RCCs. In our cohort its frequency was lower, compared to literature data (0.99 vs. 1–4%) [22]. That is due to the relatively large number of patients included in our study, the analysis may roughly represent the ratio of Xp11.2 RCC in Hungary. In these neoplasms the characteristic cytogenetic change is the translocation involving the MIT family transcription factor *TFE3* gene [1]. These tumors were once regarded as childhood malignancies, though because of the significant overlapping features with clear cell and papillary RCC and the limited cytogenetic data, some authors suggested that the exact frequency in adults is underestimated [14]. In our cohort 12 tumors occurred in patients who were less than 40 years old, only four tumors affected children, and the oldest

patient examined was 72 years old. Nine patients were symptomatic and tumor-related pain was the most common symptom. Only seven tumors did not produce any noticeable signs. A link between previous use of chemotherapy and translocation RCC was reported [15], but in our study there was no patient with a prior history of malignancy. Discriminating Xp11.2 RCC from other subtypes of RCC is crucial for prognostic and predictive reasons. It was suggested recently, that patients with Xp11.2 RCC may benefit from mTOR inhibitors and VEGF-targeted agents [16, 17]. The diagnosis relies on morphological features, immunohistochemical findings and molecular pathological analysis. Xp11.2 RCC has no specific macroscopic appearance; in fact most tumors resemble clear cell RCC with a sulfur yellow cut surface along with foci of hemorrhage and/or necrosis [9]. Xp11.2 RCC is usually diagnosed as a sizeable mass in the kidney. The mean size of our tumors (78.5 mm) was larger than in the earlier reported series [2, 14, 18]. In our previous analysis, only unclassified RCC

Fig. 1 Representative images of typical morphological features of Xp11.2 renal cell carcinomas. (A) Solid-nested pattern with admixture of eosinophilic and clear cells. (B) Alveolar pattern populated by eosinophilic cells. Psammoma bodies are also present. (C) Papillary pattern with voluminous clear cells and psammoma bodies. D Occasionally the nuclei are near the apical surface of the cells and they mimic clear cell papillary renal cell carcinoma. The arrows indicate the psammoma bodies. All images have a magnification factor of 200x
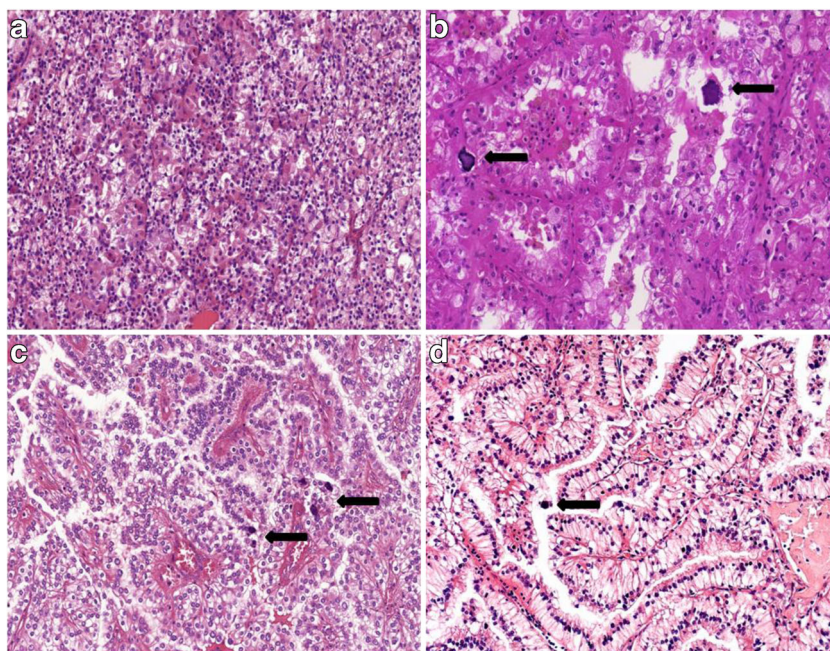
and collecting duct carcinoma were larger than Xp11.2 RCC [19]. An invasion of the renal vein and/or the sinus is quite frequent; at least one of these was noticed in 12 patients. Metastatic spread to the regional lymph nodes or distant organs was observed in 32% of the cases; six patients had nephrectomy at the pM1 stage. Our observations on the rate of pT3/pT4 stage and the occurrence of metastasis are in accordance with the literature data [14]. This late stage discovery might partly explain the generally poor outcome in Xp11.2 RCC.

Microscopic Features of Xp11.2 RCC

Microscopically the predominant growth patterns are papillary, tubular, nested and mixed. A striking histological finding is the presence of psammoma bodies [2, 18]. A different distribution was observed in our cohort, as a result of solid pattern observed as most frequent, followed by papillary and mixed architecture. Tumors were composed of mainly clear cells in 19 and of eosinophilic cells in 7 cases. Additionally the simultaneous presence of both cell types was noted in two

Fig. 2 Representative images of Xp11.2 renal cell carcinomas with unusual morphological features. (A) Tubular pattern resembling low-grade clear cell carcinoma. (B) Solid pattern with foci of comedo-like necrosis. (C) Rhabdoid tumor-like pattern. (D) Anaplastic carcinoma appearance. All images have a magnification factor of 200x
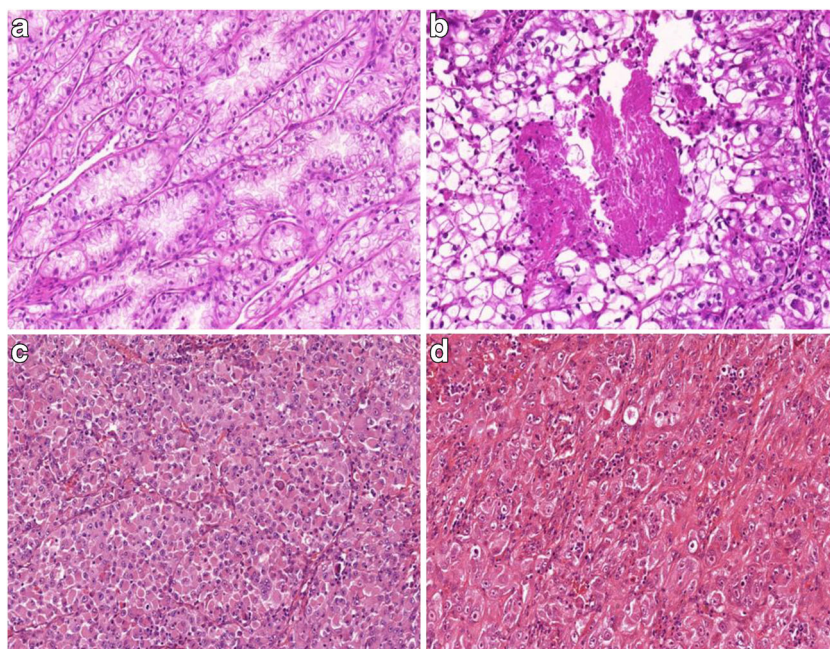
**Table 4** Immunohistochemical results of the analyzed cases

	CA9	CK7	CD10	AMACR	MelanA	HMB45	Cathepsin K	TFE3 IHC	TFE3 FISH
1	N	N	D	N	N	N	N	D	+
2	N	N	D	N	N	N	N	D	+
3	N	N	N	N	N	N	N	D	+
4	N	N	D	D	N	N	D	D	+
5	N	N	D	N	N	N	N	D	+
6	N	N	N	N	N	N	N	D	+
7	N	N	D	F	N	N	N	D	+
8	N	N	D	D	N	N	N	D	+
9	N	N	N	N	N	N	N	D	+
10	N	N	D	N	D	N	N	D	+
11	N	N	D	F	N	N	F	F	NA
12	N	N	D	D	N	N	N	D	NA
13	N	N	D	D	N	D	N	D	+
14	N	N	D	D	N	F	D	D	+
15	N	N	N	N	D	N	N	D	+
16	N	N	D	D	N	N	N	D	+
17	N	N	D	F	N	N	N	D	+
18	N	N	F	D	N	N	N	F	+
19	N	N	F	N	N	N	N	D	+
20	F	N	N	N	N	N	N	N	+
21	N	N	D	N	N	D	D	D	+
22	N	N	F	D	N	N	F	D	+
23	N	N	N	N	N	N	N	D	+
24	N	N	N	N	D	N	N	F	NA
25	N	N	D	D	N	N	N	F	+
26	N	N	D	D	F	N	F	F	+
27	F	N	D	N	N	N	N	N	+
28	F	N	F	F	N	N	N	D	+

N, indicates negative; F, focally positive; D, diffusely positive; NA, data not available

cases. Psammoma bodies were observed in 11 cases. Foamy cells and intracytoplasmic pigment are common features in papillary RCC; hence their extensive presence can cause differential diagnostic problems. However, in our cohort both foamy cells and intracytoplasmic pigment occurred in a small proportion of cases and they did not have a predominant papillary pattern. Microscopic tumor cell necrosis was observed in 60% of tumors. Although the effect of necrosis on the outcome in Xp11.2 RCC is doubtful, in a large set of RCC patients, poor prognostic effect of microscopic tumor necrosis was identified earlier in the three most frequent types of RCC [20]. Cases with atypical architecture can cause serious

Fig. 3 Representative images of the immohistochemical features of the analyzed tumors. (**A**) Tumor cells display diffuse TFE3 nuclear positivity. (**B**) Cathepsin K expression in an Xp11.2 renal cell carcinoma. (**C**) Diffuse cytoplasmic and membranous CD10-positivity is frequently seen in Xp11.2 renal cell carcinomas. (**D**) MelanA expression in Xp11.2 renal cell carcinoma. All images have a magnification factor of 200x
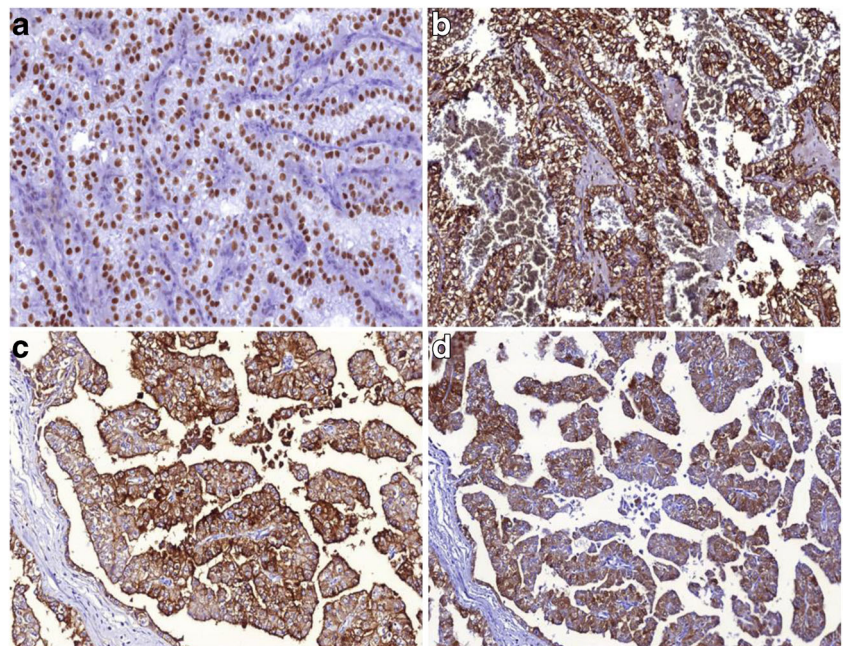
Fig. 4 Representative images of the signal patterns seen in the analyzed tumors. (**A**) Typical split signals (red and green arrows) are present in a male patient (*patient #17*). (**B**) Truncated signal pattern consisting of a pair of fused signals (yellow arrows) and a single red signal was observed in *patient #10*. (**C**) Although signals are separated (red and green arrows), they are unusually close to each other. In lymphocytes normal fused signals (yellow arrows) are present (*patient #14*). (**D**) The loss of an entire break-point region was observed in *patient #23*. The yellow arrow indicates the intact chromosome X
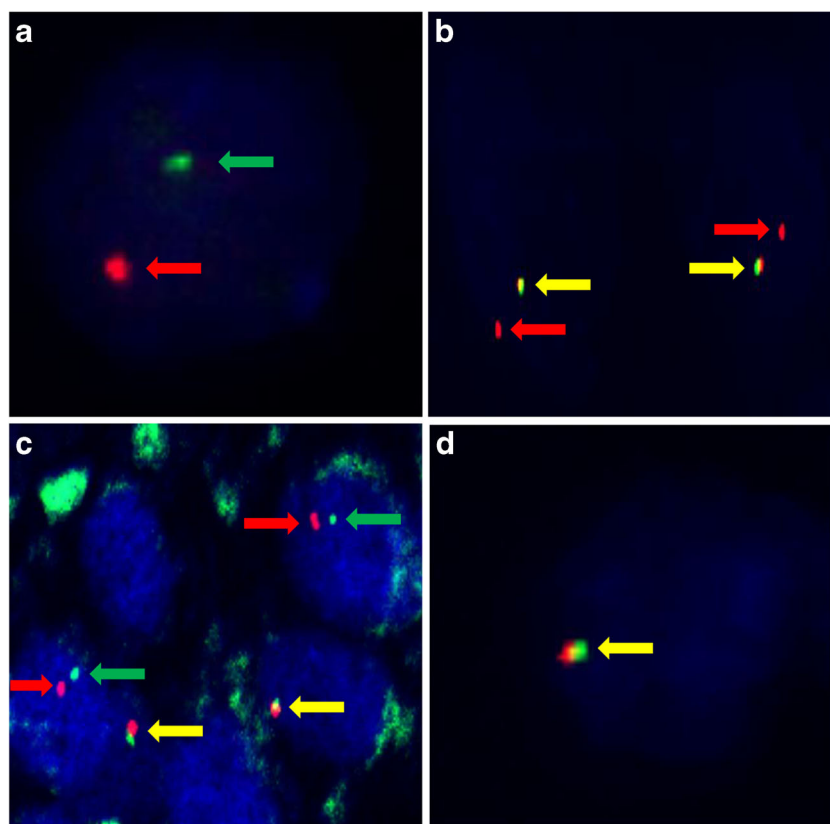
diagnostic difficulties; namely, the morphological spectrum of Xp11.2 RCC is quite broad, furthermore urothelial cell carcinoma mimicking translocation RCC was reported as well [13]. In our cohort, a case mimicking anaplastic carcinoma and another with rhabdoid morphology were observed. Some authors suggested that the specific translocation has an influence on histological appearance [21]. Because of the absence of fusion partner analysis, we cannot argue for or against this statement. The influence on the prognosis of the fusion partner is yet unclear [23].

Immunophenotype of Xp11.2 RCC

Xp11.2 RCC is negative with CA9, CK7 and positive with CD10 and AMACR [10]. In our series, both CA9 and CK7 were completely negative in almost every case, except for CA9 in three samples. However, two of these tumors were extensively necrotic, therefore we concluded that the staining was related to hypoxia of the tumor tissue. Diffuse CD10 labeling was noted in 60% of cases, while AMACR-positivity was observed only in 50% of the tumors. MelanA and HMB45 expression is frequent in *TFEB* translocation RCC, nevertheless is rare in Xp11.2 translocation RCC [5]. Similar proportion was described in our cohort; namely, MelanA and HMB45 were positive in 4 and 3 tumors

respectively. For the diagnosis of Xp11.2 RCC, TFE3 immunostaining is the most frequently used method. The specificity and sensitivity of the immunohistochemistry were found to be 99.6% and 97.5% [24], although in some cases false negativity and false positivity can occur [23, 25]. Argani et al. described that the shorter incubation time with automated detection system made TFE3 IHC more sensitive, while the specificity of the reaction decreased. For the false-negative results, some authors declared that it can be caused by preanalytical factors (e.g. fixation time) or by different analytical methodologies applied (e.g. poor-quality antibodies and inappropriate antigen retrieval) [13, 26]. There were only two tumors (*patient #20* and *#27*) with *TFE3*-negativity and the remaining cases displayed a diffuse and strong nuclear positivity. Therefore, in our analysis the sensitivity of TFE3 immunohistochemistry correlates with data of the earlier reports [24]. Cystine protease Cathepsin K is a novel immunohistochemical marker for Xp11.2 RCC, although the expression depends on the fusion partner of the *TFE3*. This can serve as an explanation of its expression in only approximately 60% of Xp11.2 RCC [12, 27]. Six cases with Cathepsin K-positivity were described, that is slightly under the reported rate in literature [13]. The difference might be related to the different translocation partners.

Genetic Markers of Xp11.2 RCC

Reverse transcription polymerase chain reaction (RT-PCR) is a sensitive method for the identification of different kinds of chimeric mRNA transcripts, though the limited availability of frozen samples generally makes the testing problematic or even impossible [28]. Cytogenetic karotyping is another classic methodology for recognizing structural changes among chromosomes. Nevertheless it requires a special laboratory, technicians and fresh material, hence the use of karotyping in the routine diagnosis of solid tumors is limited. Currently next-generation sequencing can be used to reveal the partner genes and identify new ones, as Pei et al. did [29]. FISH reactions have been performed on FFPE samples with satisfactory for some time now. *TFE3* break-apart FISH assay was introduced in 2011 and since that it has become an indispensable diagnostic tool for Xp11.2 RCC [13, 30]. In our study the diagnosis was supported with *TFE3* break-apart FISH analysis in 25 cases. The classic break-apart pattern was observed in 21 tumors and the truncated signal pattern was noted in 2 cases. For the latter cases, two explanations exist. First of all, truncation effect of cutting the tumor cell nuclei is a well-known problem in FISH assays on FFPE slides [13]. On the other hand, in our cases this was the dominant pattern. In *patient #9* a single red signal was seen in 100% of the positive tumor cells, while in *patient #10* split and a single red signal was observed in 17% and 83% of the positive tumor cells respectively. Therefore it is considered by our team that the labeled part of the *TFE3* was lost due to an atypical break in the gene sequence. Atypical FISH patterns are known for both epitheloid renal neoplasia along with soft tissue sarcomas [30–32]. In *patient #14* the signals were unusually close to each other, and this phenomenon is the indicative of intrachromosomal inversion [4]. In a female patient an entire break-point region was completely missing from the majority of the tumor cells. This was considered to be a result of an atypical translocation. Otherwise, the histomorphology and immunophenotype were concordant with Xp11.2 RCC, so the final diagnosis was made on summary of the above-mentioned results. Such signal pattern was presumed earlier [30], though to our best knowledge, this is the first report of such a signal pattern in Xp11.2 RCC. Optimized *TFE3* break-apart FISH assay is extremely useful in routine diagnosis and pathology consultation [27]. However, FISH analysis has its own limitations as well, whereas poor fixation, inappropriate hybridization, and/or extensive contamination with normal stromal cells can lead to negative results. It must be stated that break-apart FISH test has low sensitivity for intrachromosomal or paracentric inversions like in *RBM10-TFE3* and *NonO-TFE3* RCCs [33]. In these cases, despite the typical microscopic appearance and the characteristic immunophenotype, FISH can provide equivocal or even negative results. In this particular scenario, one must be really cautious about setting the diagnosis as Xp11.2 RCC, and fusion partner analysis (if available) by RT-PCR or RNA sequencing should be considered [33].

Clinical Course of Xp11.2 RCC

Some authors previously reported that Xp11.2 RCC had an indolent course [35–38]. Camparo et al. calculated a mortality rate of 13.6% for Xp11.2 RCC from their analysis and literature data, although the follow-up period was quite short [14]. A fascinating case of Xp11.2 RCC was reported by Mangel et al. [38]. In their report, rapid progression of a stable disease was noted after the patient became pregnant, and the authors considered that the enormous tumor evolution was triggered by cytokines and hormones produced by the placenta, especially human chorionic gonadotropin. In our cohort the median follow-up time was 14 months. In the meantime, 33% of the patients died from a cancer-related cause. This indicates the fact that Xp11.2 RCC has the same mortality rate as the calculated rate for overall RCC patients [39].

The strength of our study is the relatively high number of systematically analyzed cases by descriptive light-microscopy, a panel of immunohistochemistry and FISH analysis. Two tumors with a fairly unusual morphology was included, one with anaplastic carcinoma appearance and another with rhabdoid morphology. Unique FISH pattern with the complete loss of the labeled break-point region was observed. The clinical follow-up was not complete for all patients, however, the mean follow-up period was more than 4 years.

One limitation of this current study is the absence of cytogenetic studies and the data for fusion partner analysis.

In summary, the results of 28 Xp11.2 RCC cases were presented from a large surgically treated series of RCC. Xp11.2 RCC is a rare form of renal cell carcinoma; and it is accounted for 0.99% of all RCC cases in our study. In adults the outcome is rather poor. Cases with an unusual histomorphology may cause differential diagnostic problems, though the use of antibodies in combination can improve the diagnostic performance. Finally, to avoid false negative and false positive cases, the use of *TFE3* break-apart FISH studies and/or fusion partner analysis are strongly recommended.

Compliance with Ethical Standards

Ethical Approval The study was ethically approved by the Medical Research Council of Hungary (174,894/2017/EKU). The renal carcinoma

cases were retrospectively selected from the archives of the pathological institutions and informed consent was not obtained.

Conflict of Interest The authors declare that they have no conflict of interest.

References

1. Argani P, Faria M (2005) Translocation carcinomas of the kidney. Clin Lab Med 25:363–378
2. Argani P, Antonescu CR, Illei PB et al (2001) Primary renal neoplasms with the ASPL-TFE3 gene fusion of alveolar soft part sarcoma: a distinctive tumor entity previously included among renal cell carcinomas of children and adolescents. Am J Pathol 159:179–192
3. Sidhar SK, Clark J, Gill S et al (1996) The t(X;1)(p11.2;q21.2) translocation in papillary renal cell carcinoma fuses a novel gene PRCC to the TFE3 transcription factor gene. Hum Mol Genet 5:1333–1338
4. Clark J, Lu YJ, Sidhar SK et al (1997) Fusion of splicing factor genes PSF and NonO (p54nrb) to the TFE3 gene in papillary renal cell carcinoma. Oncogene 15:2233–2239
5. Argani P, Lui MY, Couturier J et al (2003) A novel CLTC-TFE3 gene fusion in pediatric renal adenocarcinoma with t(X;17)(p11.2;q23). Oncogene 22:5374–5378
6. Argani P, Olgac S, Tickoo SK et al (2007) Xp11 translocation renal cell carcinoma in adults: expanded clinical, pathologic and genetic spectrum. Am J Surg Pathol 31:1149–1160
7. Zhong M, De Angelo P, Osborne L et al (2012) Translocation renal cell carcinomas in adults: a single-institution experience. Am J Surg Pathol 36:654–662
8. Qu Y, Gu C, Wang H et al. (2016) Diagnosis of adults Xp11.2 translocation renal cell carcinoma by immunohistochemistry and FISH assays: clinicopathological data from ethnic Chinese population. Sci rep 6:2167
9. Armah HB, Parwani AV (2010) Xp11.2 translocation renal cell carcinoma. Arch Pathol Lab Med 134:124–129
10. Argani P, Cheville J, Ladanyi M (2016) MiT family translocation renal cell carcinomas. In: Humphrey PA, Ulbright TM, Reuter VE (eds) Moch H. Pathology and Genetics of Tumours of the Urinary System and Male Genital Organs. IARCC Press Lyon, WHO Classification of Tumours, pp 33–34
11. Argani P, Hicks J, De Marzo AM et al (2010) Xp11 translocation renal cell carcinoma (RCC): extended Immunohistochemical profile emphasizing novel RCC markers. Am J Surg Pathol 34:1295–1303
12. Martignoni G, Gobbo S, Camparo P et al (2011) Differential expression of cathepsin K in neoplasms harboring TFE3 gene fusions. Mod Pathol 24:1313–1319
13. Rao Q, Williamson SR, Zhang S et al (2013) TFE3 break-apart FISH has a higher sensitivity for Xp11.2 translocation-associated renal cell carcinoma compared with TFE3 or cathepsin K immunohistochemical staining alone: expanding the morphologic spectrum. Am J Surg Pathol 37:804–815
14. Camparo P, Vasiliu V, Molinie V et al (2008) Renal translocation carcinomas: clinicopathologic, immunohistochemical, and gene expression profiling analysis of 31 cases with a review of the literature. Am J Surg Pathol 32:656–670
15. Argani P, Laé M, Ballard ET et al (2006) Translocation carcinomas of the kidney after chemotherapy in childhood. J Clin Oncol 24:1529–1534
16. Malouf GG, Camparo P, Oudard S et al (2010) Targeted agents in metastatic Xp11 translocation/TFE3 gene fusion renal cell carcinoma (RCC): a report from the juvenile RCC network. Ann Oncol 21:1834–1838
17. Choueiri TK, Lim ZD, Hirsch MS et al (2010) Vascular endothelial growth factor-targeted therapy for the treatment of adult metastatic Xp11.2 translocation renal cell carcinoma. Cancer 116:5219–5225
18. Argani P, Antonescu CR, Couturier J et al (2002) PRCC-TFE3 renal carcinomas: morphologic, immunohistochemical, ultrastructural, and molecular analysis of an entity associated with the t(X;1)(p11.2;q21). Am J Surg Pathol 26:1553–1566
19. Kuthi L, Jenei A, Hajdu A et al (2017) Prognostic factors for renal cell carcinoma subtypes diagnosed according to the 2016 WHO renal tumor classification: a study involving 928 patients. Pathol Oncol Res 23:689–698
20. Delahunt B, McKenney JK, Lohse CM et al (2013) A novel grading system for clear cell renal cell carcinoma incorporating tumor necrosis. Am J Surg Pathol 37:311–322
21. Argani P, Ladanyi M (2005) Translocation carcinomas of the kidney. Clin Lab Med 25:363–378
22. Komai Y, Fujiwara M, Fujii Y et al (2009) Adult Xp11 translocation renal cell carcinoma diagnosed by cytogenetics and immunohistochemistry. Clin Cancer Res 15:1170–1176
23. Ellis CL, Eble JN, Subhawong AP et al (2014) Clinical heterogeneity of Xp11 translocation renal cell carcinoma: impact of fusion subtype, age, and stage. Mod Pathol 27:875–886
24. Argani P, Lal P, Hutchinson B et al (2003) Aberrant nuclear immunoreactivity for TFE3 in neoplasms with TFE3 gene fusions: a sensitive and specific immunohistochemical assay. Am J Surg Pathol 27:750–761
25. Yang B, Duan H, Cao W et al (2019) Xp11 translocation renal cell carcinoma and clear cell renal cell carcinoma with TFE3 strong positive immunostaining: morphology, immunohistochemistry, and FISH analysis. Mod Pathol 32:1521–1535
26. Argani P, Aulmann S, Illei PB et al (2010) A distinctive subset of PEComas harbors TFE3 gene fusions. Am J Surg Pathol 34:1395–1406
27. Martignoni G, Pea M, Gobbo S et al (2009) Cathepsin-K immunoreactivity distinguishes MiTF/TFE family renal translocation carcinomas from other renal carcinomas. Mod Pathol 22:1016–1022
28. Green WM, Yonescu R, Morsberger L et al (2013) Utilization of a TFE3 break-apart FISH assay in a renal tumor consultation service. Am J Surg Pathol 37:1150–1163
29. Pei J, Cooper H, Flieder DB et al (2019) NEAT1-TFE3 and KAT6A-TFE3 renal cell carcinomas, new members of MiT family translocation renal cell carcinoma. Mod Pathol 32:710–716
30. Mosquera JM, Dal Cin P, Mertz KD et al (2011) Validation of a TFE3 break-apart FISH assay for Xp11.2 translocation renal cell carcinomas. Diagn Mol Pathol 20:129–137
31. Argani P, Aulmann S, Karanjawala Z et al (2009) Melanotic Xp11 translocation renal cancers: a distinctive neoplasm with overlapping features of PEComa, carcinoma, and melanoma. Am J Surg Pathol 33:609–619

32. Papp G, Nagy D, Sápi Z (2017) Unusual signal patterns of break-apart FISH probes used in the Diagnosis of Soft Tissue Sarcomas. Pathol Oncol Res 23:863–871

34. Kato I, Furuya M, Baba M et al (2019) RBM10-TFE3 renal cell carcinoma characterised by paracentric inversion with consistent closely split signals in break-apart fluorescence in-situ hybridisation: study of 10 cases and a literature review. Histopathology 75:254–265

35. Argani P, Ladanyi M (2003) Distinctive neoplasms characterised by specific chromosomal translocations comprise a significant proportion of the paediatric renal carcinomas. Pathology 35:492–498

36. Dal Cin P, Stas M, Sciot R et al (1998) Translocation (X;1) reveals metastasis 31 years after renal cell carcinoma. Cancer Genet Cytogenet 101:58–61

37. Perot C, Bougaran J, Boccon-Gibod L et al (1999) Two new cases of papillary renal cell carcinoma with t(X;1)(p11;q21) in females. Cancer Genet Cytogenet 110:54–56

38. Rais-Bahrami S, Drabick JJ, De Marzo AM et al (2007) Xp11 translocation renal cell carcinoma: delayed but massive and lethal metastases of a chemotherapy-associated secondary malignancy. Urology 70:178e3–178e6

39. Mangel L, Bíró K, Battyáni I et al (2015) A case study on the potential angiogenic effect of human chorionic gonadotropin hormone in rapid progression and spontaneous regression of metastatic renal cell carcinoma during pregnancy and after surgical abortion. BMC Cancer 15:1013

40. Patard JJ, Leray E, Rioux-Leclercq N et al (2005) Prognostic value of histologic subtypes in renal cell carcinoma: a multicenter experience. J Clin Oncol 23:2763–2771